THE ROLE OF CELL SURFACE GRP78 IN ATHEROSCLEROSIS

THE ROLE OF CELL SURFACE GRP78 AND ANTI-GRP78 AUTOANTIBODIES IN THE DEVELOPMENT AND PROGRESSION OF ATHEROSCLEROTIC LESIONS

By

ELIZABETH D. CRANE, B.Sc.

A Thesis Submitted to the School of Graduate Studies

In Partial Fulfillment of the Requirements for the Degree

Doctor of Philosophy

DOCTOR OF PHILOSOPHY (PhD) (2016) McMaster University

(Biochemistry & Biomedical Sciences) Hamilton, Ontario, Canada

TITLE: The Role of Surface GRP78 and Anti-GRP78 Autoantibodies in the Development and Progression of Atherosclerotic Lesions

AUTHOR: Elizabeth D. Crane, B.Sc. (Ball State University)

SUPERVISOR: Richard C. Austin, Ph.D.

NUMBER OF PAGES: xv, 113

ABSTRACT

Damage to the endothelium is an important contributor to the initiation and progression of atherosclerosis. GRP78 is an endoplasmic reticulum (ER)-resident molecular chaperone in normal healthy endothelium that functions to assist in the correct folding of newly synthesized proteins and to prevent the aggregation of folding intermediates. In addition, GRP78 is present as a transmembrane protein on the surface of lesion-resident endothelial cells. Surface GRP78 is known to act as a surface signaling receptor in cancer cells and is activated by anti-GRP78 autoantibodies (GRP78a-Abs) isolated from the serum of cancer patients. However, the role of cell surface GRP78 on endothelial cells and the influence of GRP78a-Abs in atherosclerosis is unknown. The objectives of this study were to investigate the effects of GRP78a-Abs on lesion development, examine whether engagement of cell surface GRP78 by GRP78a-Abs modulates endothelial cell function, and determine whether GRP78a-Abs were associated with cardiovascular disease (CVD) in humans. This research showed that ApoE$^{-/-}$ mice with advanced atherosclerotic lesions have elevated serum levels of GRP78a-Abs and ApoE$^{-/-}$ mice immunized against recombinant GRP78 demonstrated a significant increase in GRP78a-Abs titers as well as accelerated lesion growth. Furthermore, this work demonstrated that activation of surface GRP78 on endothelial cells by GRP78a-Abs significantly increases gene expression of adhesion molecules ICAM-1 and VCAM-1 as well as leukocyte

adhesion through the NFκB pathway. Additionally, middle-aged to elderly adults at risk for CVD showed a trend toward elevated circulating GRP78a-Ab levels. Our results suggest that signaling through cell surface GRP78 can activate intracellular pathways that contribute to endothelial cell activation and augment atherosclerotic lesion development. These findings demonstrate a novel role for GRP78a-Abs and surface GRP78 receptor activity in endothelial cell function and the early stages of lesion development, as well as establish an initial framework for future work involving circulating GRP78a-Abs and atherosclerotic disease in humans. Furthermore, this work indicates inhibiting the interaction of GRP78a-Abs with cell surface GRP78 could present a novel therapeutic strategy to modulate lesion growth, thereby reducing the risk for atherosclerosis and cardiovascular disease.

ACKNOWLEDGEMENTS

I would like to thank my supervisor Dr. Richard Austin for his support and guidance during the course of completing my Ph.D. degree. I truly appreciate the opportunities he afforded to me as a member of his lab and research team. I am privileged to have had years of scientific experiences as well as immeasurable personal growth during my time at St. Joseph's Hospital. I would also like to thank my committee members, Dr. Geoff Werstuck and Dr. Bernardo Trigatti for their guidance and discussions throughout this project.

I would like to thank all of the members of the Austin Lab for their assistance and support over the years. I am grateful to Dr. Sarka Lhotak for her training and expertise in immunohistochemistry and histological sectioning. I would like to thank Dr. Edward Lynn for the scientific discussions and generous advice, and am grateful to Ali Al-Hashimi for all of his help as my tangential project partner and fellow graduate student.

I am deeply grateful to Celeste Collins for her friendship, support, and compassionate ear. I would also like to thank my lab bench neighbor Celeste Bouchard for her comradery, sunshine personality, and infallible ability to make me laugh.

I will always be grateful to my parents, Jim and Cindy Lewis, for their love and encouragement towards pursuing my education and scientific curiosity.

And most importantly, I would like to thank my husband, best friend and biggest supporter, Justin. You continually encouraged and believed in me, and your patience and love has been immeasurable throughout this difficult process. Without you I would not have succeeded. I love you.

TABLE OF CONTENTS

LIST OF FIGURES

LIST OF TABLES

LIST OF ABBREVIATIONS

4HNE	4-hydroxynonenal
7KC	7-ketocholesterol
α_2M	alpha 2 macroglobulin
apoE	apolipoprotein E
ATF6	activating transcription factor 6
ATP	adenosine triphosphate
B2M	beta-2-microglobulin
BP	blood pressure
BAPTA	1,2-bis(2-aminophenoxy)ethane-N,N,N',N'-tetraacetic acid
BMI	body mass index
Ca^{2+}	calcium
CP	conformational peptide
CVD	cardiovascular disease
DAPI	4',6-diamidino-2-phenylindole
DMSO	dimethyl sulfoxide
EC	endothelial cell
eIF2α	eukaryotic translation initiation factor 2(α subunit)
ELISA	enzyme linked immuno-sorbent assay
ELBW	extremely low birth weight
ER	endoplasmic reticulum
ERSE-1	ER stress-response element
GADD153	growth arrest and DNA damage gene 153
GRP78	glucose regulated protein 78 kDa
GRP78a-Ab	anti-GRP78 autoantibodies

GT	glucose tolerance
HDL	high-density lipoprotein
ICAM-1	intracellular adhesion molecule 1
IgG	immunoglobulin G
IMT	intimal medial thickness
IRE1	inositol-requiring enzyme-1
KDEL	lysine-aspartate-glutamate-leucine
KLH	keyhole limpet hemocyanin
LDL	low-density lipoprotein
LDLR	low density lipoprotein receptor
mRNA	messenger ribonucleic acid
NBW	normal birth weight
NFκB	nuclear factor kappa B
oxLDL	oxidized low-density lipoprotein
PAGE	polyacrylamide gel electrophoresis
PBS	phosphate-buffered saline
PBST	phosphate-buffered saline with tween
PERK	PKR-like ER kinase
PI3K	phosphoinositide 3-kinase
PKC	protein kinase C
SRB1	scavenger receptor class B type 1
SREBP	sterol regulatory element-binding protein
Tg	thapsigargin
Tm	tunicamycin
TNFα	tumor necrosis factor α
VCAM-1	vascular cell adhesion molecule

Chapter 1 - Introduction

1.1 Atherosclerosis

Atherosclerosis is the underlying cause of cardiovascular disease (CVD) and its complications are key initiators of CVD development(1). Compounding factors such as dietary, genetic, and environmental pressures contribute to the occurrence and pathogenesis of atherosclerosis and its consequences such as myocardial infarction and stroke(2). CVD and its associated diseases, including atherosclerosis, account for the leading cause of death in the world(3). This is not predicted to change based on the continued rise of obesity and diabetes, strong risk factors for atherosclerosis(4), as well as an increasing elderly population(5, 6).

Atherosclerosis is characterized by the accumulation of lipids in the arterial subendothelium, leading to focal areas of inflammation, particularly in regions of disturbed laminar flow, which cause thickening and hardening of the arterial wall(7, 8). This accumulation of lipid increases the binding and transmigration of monocytes into the subendothelium, thereby triggering proliferation and migration of smooth muscle cells, expansion of the extracellular matrix, and a thickening of the arterial wall(9). Early lesions, composed of fatty streaks containing lipid-laden monocyte-derived macrophages, progress into advanced lesions characterized by fibrous plaques. Continued inflammation and lipid accumulation also induces macrophage apoptosis and impaired

efferocytosis, resulting in large regions of necrosis and cholesterol crystal accumulation in advanced lesions(1, 10). These atherosclerotic plaques become thin and destabilize over time, resulting in plaque rupture, acute arterial thrombosis, and occlusion of the artery(11).

1.2 Endothelial Cell Function and Dysfunction

The vascular endothelium acts as the physical barrier between the blood and the vessel wall and is responsible for maintaining vascular homeostasis. Healthy endothelial cells regulate localized inflammation through the transient expression of cell surface factors that recruit monocytes and aid in their trans-endothelial migration(12) The disruption of vascular health and damage to the endothelium is regarded as the important initiating event which renders the vasculature susceptible to atherogenesis (12). Loss of normal endothelial function leads to disruption of vasomotion, loss of vascular integrity, and areas of local inflammation allowing leukocyte infiltration and initiating plaque development(13). One hallmark feature of endothelial dysfunction is the decrease in the bioavailability of nitric oxide (NO) which acts as a vasodilator and is thought to be atheroprotective in the healthy endothelium(14). The loss of NO availability is attributed to the reduction in endothelial nitric oxide synthase (eNOS) activity and an increase in reactive oxygen species generation(15). Atherogenic and inflammatory signals can also trigger endothelial cell activation, characterized by increased expression of surface adhesion molecules ICAM, VCAM, and E-selectin(16). Expression of these surface proteins promotes

leukocyte recruitment and migration into the vessel wall and initiates additional inflammatory stimuli including cytokine and growth factor expression(17). Prolonged endothelial cell activation causes injury to the vessel wall and can result in endothelial cell dysfunction, increased vascular stiffness, dysregulation of leukocyte trafficking, and subsequent formation of atherosclerotic plaques(16).

While multiple cardiovascular risk factors including dysglycemia, hypertension, and hyperlipidemia have been associated with impaired endothelial cell function, haemodynamic shear stress in regions of highly disturbed flow can drive endothelial cells towards a more pathological phenotype independent of other contributing disease states (18-21). Branching vessel geometry creates disturbances in blood flow and causes mechanical strain on the vessel wall. The arterial endothelium can adapt to some extent to local haemodynamic characteristics through continual structural remodeling and adjusting cellular signaling pathways (22). However, these adaptations often result in a malformed endothelium leaving the vessel wall susceptible to atherogenic stimuli. Endothelial cells in regions of disturbed flow found at curvatures, branches, and bifurcations show reduced cell alignment and a polygonal morphology(23). Conditions of disturbed flow elicit disorganization of the F-actin cytoskeleton and a differential regulation of gap junction proteins in cultured endothelial cells, similar to those observed in advanced atheromas of human carotid arteries (24, 25).

Atherosclerotic plaques preferentially develop at specific anatomical locations such as the coronary arteries or lesser curvature of the aortic arch that are characterized by disturbed flow patterns in both humans and animals (26). Endothelial cells adjacent to unidirectional laminar flow maintain a homeostatic, atheroprotective program, whereas endothelial cells exposed to disturbed flow show an increase in expression of many proatherosclerotic genes including proapoptotic and proinflammatory molecules(27). Disturbed flow increases the expression of IL-8, MCP-1 and the receptors for a number of interleukins as well as enhanced the inducible expression of adhesion molecule VCAM-1 in human endothelial cells(24, 27). In a porcine model of atherosclerosis, transcriptional expression of proinflammatory markers such as IL-1α and IL-6 as well as members of the NFκB system were up-regulated in regions of disturbed flow, however no active nuclear NFκB was observed nor any difference in expression of ICAM-1 or VCAM-1, commonly associated with NFκB mediated signaling(28). These *in vivo* observations are consistent with findings from LDLR knockout mice showing endothelial cells located in lesion-prone sites express higher levels of p65 and IκBs, but lack NFκB activation, suggesting that these sites are primed for NFκB activation and that additional systemic proatherosclerotic stimuli contribute to the preferential lesion development seen in these regions(29).

Another common feature associated with athero-susceptible regions of the endothelium is the upregulation of genes associated with the synthesis and

processing of proteins in the endoplasmic reticulum (ER). Cells exposed to adverse conditions that disrupt protein folding and induce ER stress initiate the unfolded protein response (UPR) as a strategy to restore ER homeostasis(30). Work published from our lab and others demonstrates UPR activation during all stages of atherosclerotic lesion development and is a prominent feature in growing lesions(31, 32). Endothelial cells isolated from atheroprone sites of the aortic arch from adult swine show an increased expression of the protein-folding chaperone GRP78 as well as p-ATF6 and p-IRE1α, both transducers of the UPR(33). Similar results were also observed in athero-susceptible sites of ApoE$^{-/-}$ mice and cultured endothelial cells, suggesting that disturbed flow contributes to a chronic altered endothelial phenotype associated with ER stress and activation of the UPR(22, 34, 35). These cellular changes indicate an active attempt by the stressed endothelium to adapt to the adverse conditions of disturbed flow, however this state leaves cells vulnerable to additional challenges from systemic proatherogenic stimuli.

1.3 ER Stress and the Unfolded Protein Response

The ER is a network of interconnected membrane-bound vesicles responsible for processing secretory and cell surface proteins. This organelle provides a unique chemical environment for nascent polypeptide folding, post-translational modifications, and quality control prior to transport to the Golgi apparatus. In the Golgi the correctly folded proteins are further processed, sorted

and packaged. Nascent polypeptides translocate into the ER from ER membrane-bound ribosomes through the Sec61 complex (36). The oxidizing environment of the ER lumen is optimal for Cys-Cys disulfide bond formation (36, 37) . Additionally, the ER is the largest calcium store in the cell, containing a resting Ca^{2+} concentration of 400 μM (38) and Ca^{2+} is an essential cofactor for proper chaperone-nascent polypeptide and chaperone-chaperone interactions (38, 39). The importance of properly maintained Ca^{2+} levels in the ER is highlighted by experiments using Ca^{2+} ionophores, which cause ER Ca^{2+} depletion and inhibition of the secretion of proteins from the ER (40). The post-translational modification of N-linked glycosylation is also catalyzed within the ER lumen. Interestingly, underglycosylated proteins (likely due to protein misfolding) have increased affinity for molecular chaperones which supports their role in post-translational modification (41). Mature, properly folded and modified proteins are transported out of the ER to the Golgi *cis*-face in coatomer protein (COP) II coated vesicles (42). Irrevocably damaged or misfolded proteins are removed through the ER-associated degradation (ERAD) pathway which includes the retro-translocation of misfolded proteins via the Sec61 translocon into the cytosol (43). Following their clearance from the ER, damaged and misfolded proteins are ubiquitinated and targeted for degradation by the proteasome (44).

Perturbations of ER homeostasis can occur through physiological or pathological stimuli that affect its ability to fold polypeptide chains into functional

proteins, thereby leading to accumulation of unfolded proteins in the lumen of the ER(45). An accumulation of unfolded or misfolded proteins in the ER overwhelms the protein folding capacity of the cell, leading to ER stress. Cells have developed a multi-faceted stress response pathway, termed the unfolded protein response (UPR) that is sensitized by ER stress and works toward reestablishing proper protein synthesis and restoring ER homeostasis(46). Three distinct classes of ER stress integral protein transducers have been identified and compose the divergent arms of the UPR pathway including: the inositol-requiring protein-1 (IRE1), activating transcription factor-6 (ATF6), and protein kinase RNA (PKR)-like ER kinase (PERK).

Under normal conditions, IRE1, ATF6, and PERK are bound to the chaperone 78kDa glucose-regulated protein (GRP78), also known as Bip, which retains the three ER stress transducers in an inactive state(47). ER stress promotes binding of GRP78 to accumulated unfolded proteins, resulting in the release of GRP78 from these signaling regulators and the initiation of the UPR(48). Activation of these pathways by GRP78 dissociation ultimately serves to relieve the protein synthesis burden on the ER while simultaneously increasing folding capacity, thereby alleviating ER stress and restoring protein homeostasis (Fig. 1)(49).

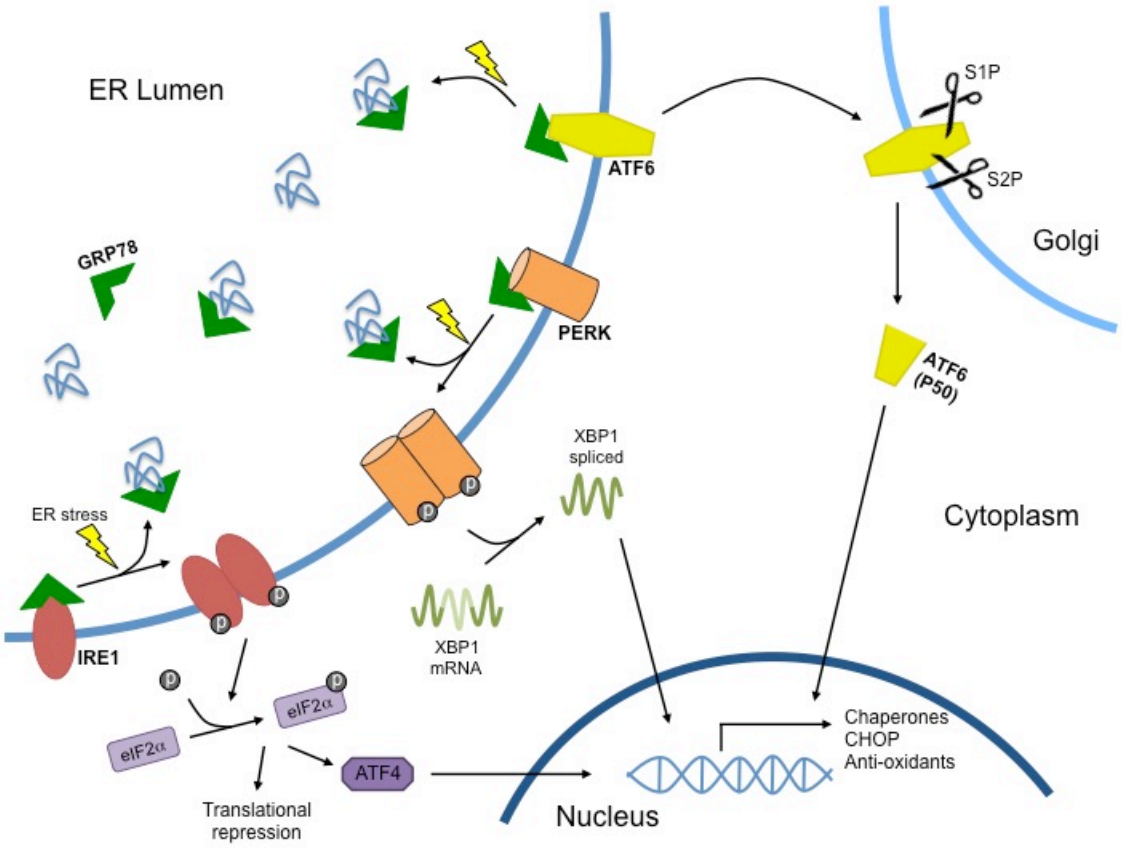

Figure 1. ER stress triggers the UPR signaling network. In response to ER stress, GRP78 dissociates from the UPR stress sensors IRE1, PERK, and ATF6, leading to their activation. UPR signaling leads to suppression of general protein translation and specific upregulation of molecular chaperones and anti-oxidant response. The purpose of the UPR is to ultimately restore ER homeostasis, however prolonged and unrelieved ER stress culminates in the initiation of apoptosis and resulting cell death.

1.3.1 IRE1 Pathway

Discovered in the early 1990s, the IRE1 pathway was identified in budding yeast *Saccharomyces cerevisiae* using genetic screening for alterations in UPR signaling(50). IRE1 encodes a type I ER-resident transmembrane protein

comprised of a lumenal and a cytoplasmic domain, the latter containing a protein kinase domain(51). In normal cells, the IRE1 protein kinase is maintained in an inactive monomeric form by its binding with GRP78(52). In response to ER stress, IRE1 oligomerizes and autophosphorylates, subsequently activating its RNase activity (46). Currently, there is some debate regarding the mechanism by which IRE1 senses ER stress. Accumulation of misfolded proteins in the ER lumen is known to trigger GRP78 dissociation from IRE1, allowing its oligomerization in the ER membrane(53, 54). However, recent studies contend that IRE1 also binds directly to unfolded proteins as seen with GRP78, causing a conformational change and activating its RNase activity(55, 56).

The RNase activity of IRE1 acts on XBP1 (X-box binding protein-I) mRNA and excises a 26 bp-intron fragment. The 5' and 3' mRNA fragments are then ligated to generate spliced XBP1 mRNA that encodes an activator of UPR target genes (57). Although both the precursor and spliced mRNAs of XBP-1 are translated to protein, the difference in their primary sequences causes them to have contrasting functions. The spliced form of XBP1 is more stable and is a potent activator of UPR target genes while the precursor form acts as a repressor of the UPR target genes(58). Upon resolution of the UPR, the precursor form of XBP1 mRNA continues to accumulate as ER stress is alleviated and IRE1 is inactivated(58).

The functions of IRE1 and XBP1 may not be limited to activation of the UPR; in fact, studies with mice possessing a heterozygous genotype for *XBP1* have demonstrated insulin resistance when fed a high-fat diet(59). Further, this very same pathway was also shown to mediate B-lymphocyte differentiation into plasma cells(60). Thus, while the IRE1/XBP1 pathway may act to relieve ER stress via upregulating the UPR, this pathway might also be required for differentiation of cells producing high levels of protein.

1.3.2 ATF6 Pathway

The discovery of the IRE1 pathway sparked interest in the UPR and further research lead to the discovery of the ATF6 pathway. ATF6 is synthesized in the ER as an inactive precursor that is tethered to the ER membrane and also bound to GRP78(61). Upon conditions of ER stress, GRP78 dissociates from ATF6 and translocates to the lumen of the ER to enhance its protein folding capacity. Subsequently, ATF6 is transported to the Golgi complex where it is cleaved by site-1 (S1P) and site-2 (S2P) proteases that release the cytosolic DNA binding fragment of ATF6 (ATF6f)(61). ATF6f then translocates to the nucleus where it acts as a transcription factor that binds to the ATF/cAMP response element and the ER stress-response element (ERSE-1), activating UPR responsive genes necessary for the enhanced folding capacity of the secretory pathway.

The proteolytic system utilized by ATF6, S1P and S2P is shared with the sterol regulatory element-binding protein (SREBP) family of transcription factors(62). When cholesterol becomes depleted from the cell, the SREBP precursor moves from the ER to the Golgi where it is cleaved by S1P and S2P. After being released from the membrane, the transcriptionally active fragment of cleaved SREBP translocates to the nucleus where it enhances *de novo* lipid synthesis. While ATF6 and the SREBPs require processing in the Golgi, the signals required for their trafficking to the Golgi are completely separate. The SREBPs are translocated to the Golgi upon cholesterol depletion, however, ATF6 translocates to the Golgi in response to a greater burden of unfolded proteins in the ER lumen(63).

Recent studies have now shown that ER stress can also activate the SREBPs, leading to the increased synthesis of cholesterol and triglycerides (64-66). Interestingly, overexpression of GRP78, which is known to alleviate ER stress, was able to prevent SREBP cleavage, decrease the expression of SREBP target genes, and repress hepatic lipid accumulation in obese ob/ob mice(64, 66) . It has also been proposed that GRP78 interacts with the SREBPs in the lumen, as has been reported for PERK, IRE1 and ATF6, to modulate their interaction. Collectively, these studies highlight the crosstalk of the UPR with other physiological processes in the cell.

1.3.3 PERK Pathway

Similar to IRE1, PERK is an ER transmembrane protein containing a lumenal stress (unfolded protein) sensor as well as a cytoplasmic domain possessing protein kinase activity(54). Under conditions of ER stress, PERK oligomerizes and *trans*-autophosphorylates similar to IRE1; however, once activated it further phosphorylates the α-subunit of eukaryotic translation initiation factor-2 (eIF2α) at Ser51(67), which lowers global protein synthesis in the cell. This signal effectively reduces the overall protein folding demand on the ER while specifically stimulating the activation of genes involved in the UPR(47, 68).

Recent studies have proposed conflicting views regarding the effect of eIF2α phosphorylation on cell survival or death. Cells that are PERK-deficient have impaired eIF2α phosphorylation and are more sensitive to ER stress-induced cell death(69), suggesting that eIF2α phosphorylation is a pro-survival strategy that is important for the cell's ability to survive ER stress. However, phosphorylation of eIF2α has also been shown to stimulate translation of activating transcription factor-4 (ATF4), which in turn triggers expression of the transcription factor C/EBP homologous protein (CHOP) that promotes cell death(70, 71) .

The multifaceted consequences of eIF2α phosphorylation on cell viability highlight the need for its strict regulation. Researchers have identified two negative regulators of eIF2α: the growth arrest and DNA-damage inducible

protein-34 (GADD34), and the constitutive repressor of eIF2α phosphorylation (CReP)(72). GADD34 expression is induced by eIF2α phosphorylation and serves as a negative feedback loop(73); conversely, CReP is constitutively expressed and impacts baseline eIF2α de-phosphorylation(74).

1.4 GRP78

GRP78, also known as BiP, is a well characterized molecular chaperone belonging to the HSP70 family and is present in the endoplasmic reticulum (ER) of all cells (75). The peptide sequence of GRP78 is highly homologous across species and is found in most eukaryotic organisms(76). GRP78 is composed of a substrate recognition site and an ATPase activity domain(77). In the ER, GRP78 is involved in protein folding and assembly by binding exposed hydrophobic regions on nascent polypeptides(77). The protein is then released through ATP hydrolysis mediated by the ATPase domain on the N-terminus of GRP78(78). GRP78 goes through repeated cycles of binding and release until no further hydrophobic regions are available for binding on the folded protein(78). Whole body deletion of GRP78 in mice is embryonic lethal due to rapid degeneration of the embryo, highlighting its essential role in cellular function(79).

While classically known as an ER resident chaperone, GRP78 has also been identified in other regions of the cell including the cytosol, mitochondria, and on the cell surface(80). In the cytosol an alternatively spliced isoform of GRP78 has been identified and is thought to be induced under conditions of ER

stress where it enhances cell survival by increasing PERK activation(81). GRP78 is also believed to help maintain mitochondrial homeostasis during ER stress by balancing energy expenditure and buffering Ca^{2+} flux(82, 83) .

1.4.1 Surface GRP78

Of all the known roles for GRP78 outside the ER, the greatest evidence has been obtained for cell-surface GRP78 in its function as a transmembrane cell surface receptor(84). First described in 1997, GRP78 has been identified on the surface of stressed cells where it has been shown to mediate various cellular responses ranging from increased cell proliferation and angiogenesis to induced apoptosis(84, 85). The downstream signaling response stimulated by surface GRP78 appears dependent on its specific ligand and the region of cell-surface GRP78 the ligand recognizes. Work published by our lab demonstrated the ability of surface GRP78 to activate tissue factor procoagulant activity by mediating Ca^{2+} release from the ER through activation of PLC and IP_3 production in bladder carcinoma cells(86). Binding of the active proteinase inhibitor α_2M* to the N-terminal domain of cell-surface GRP78 stimulates cell survival and proliferation in prostate cancer cells by increasing the anti-apoptotic protein Bcl-2 and activating the Akt pathway through the MAPK and PI3K signaling(87). Similarly, a synthetic peptide, RoY, interacted with the N-terminus of surface GRP78 and stimulated endothelial cell proliferation and migration under hypoxic conditions by an unknown mechanism(88). Conversely, antibodies that recognizes the C-terminus of surface GRP78 induced apoptosis by increasing

p53 in prostate and melanoma cancer cells(89). Moreover, peptides derived from kringle 5 of human plasminogen induced cell death in fibrosarcoma cells by interacting with surface GRP78(90). These varied reports highlight the potential for several diverse cellular responses to be mediated by surface GRP78 signaling and emphasize an important role beyond the ER for GRP78 as a surface receptor that could be exploited for therapeutic targeting (Fig. 2).

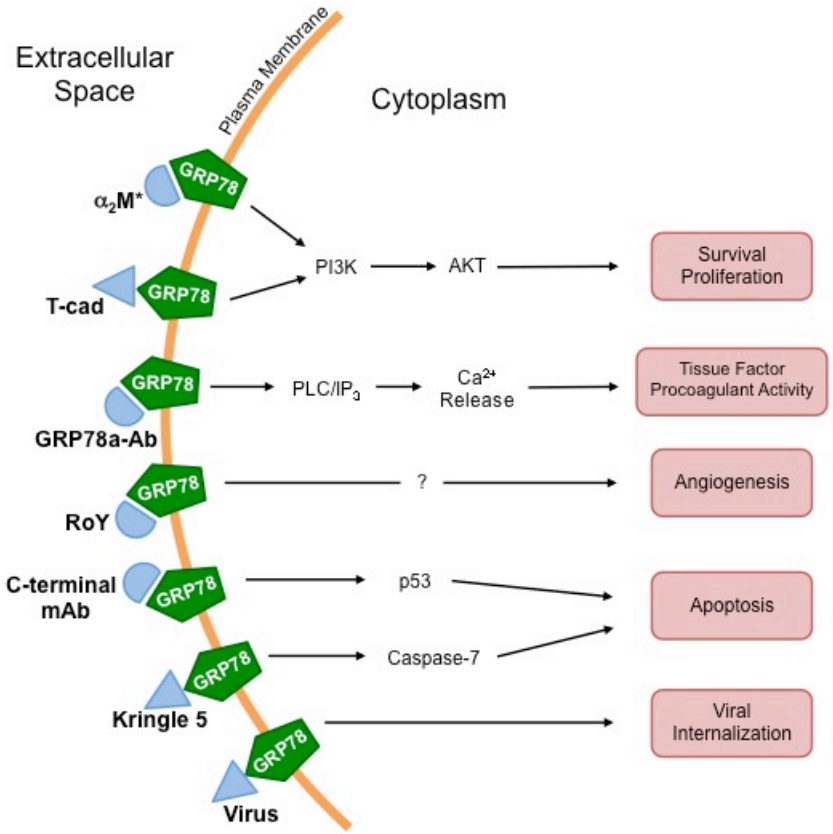

Figure 2. Cell-surface GRP78 acts as a receptor and regulator of cell signaling. Cell-surface GRP78 interacts with a variety of ligands, including activated α_2-macroglobulin (α_2M*) and T-cadherin (T-cad), resulting in cell survival and proliferation signaling. It also promotes tissue factor activity and angiogenesis when bound on the N-terminus by anti-GRP78 autoantibodies (GRP78a-Ab) or RoY respectively. Conversely, surface GRP78 stimulates pro-apoptotic pathways upon interaction with an antibody directed against the C-

terminal domain (C-terminal mAb) or with Kringle 5. Surface GRP78 also facilitates viral entry (e.g. Coxsackie and dengue virus) into host cells.

To characterize vessel surface proteins present during atherosclerosis, Liu et al. performed biopanning of atherosclerotic lesions in ApoE$^{-/-}$ mice using a phage-displayed constrained peptidyl library and identified GRP78 as an endothelial surface protein(91). GRP78 was also confirmed to be present on the surface of lesion-resident endothelial cells in ApoE$^{-/-}$mice as well as on human lesions from iliac artery segments, however it was not present on normal endothelium or in areas that failed to have lesion formation(91). However, in contrast to the known role of GRP78 cell surface signaling activity in cancer, the role of cell-surface GRP78 in atherogenesis remains unclear.

While the precise molecular mechanisms which mediate GRP78 translocation to the cell surface are still unknown, an important study had shown that induction of endoplasmic reticulum (ER) stress stimulates relocalization of GRP78 to the cell surface(92). ER stress is a known hallmark of atherosclerotic lesion progression, suggesting a link between ER stress induced endothelial cell surface GRP78 signaling and atherosclerotic lesion development.

1.4.2 Anti-GRP78 Autoantibodies

The presence of cell surface GRP78 can stimulate the formation of anti-GRP78 autoantibodies (GRP78a-Abs) by the immune system. Autoantibodies to GRP78 have been identified in the serum of patients with a variety of cancers including prostate, melanoma and ovarian(93). Although GRP78a-Abs that recognize both the N- and C-terminal regions of GRP78 have been found, it is important to note that the majority of GRP78a-Abs found in human circulation identify a specific epitope on the N-terminus of surface GRP78 (Leu_{98}-Leu_{115}), indicating the importance of this antigenic region(94). Additionally, high levels of these GRP78a-Abs in cancer patients correlates with advanced disease progression and poorer prognosis(93). Previous work published by our lab demonstrated that binding of anti-GRP78 autoantibodies to surface GRP78 activated tissue factor procoagulant activity by mediating Ca^{2+} release from the ER through activation of PLC and IP_3 production in bladder carcinoma cells (86). However, the effect of GRP78a-Ab mediated activation of cell surface GRP78 on lesion resident endothelial cells and how it might contribute to atherosclerotic lesion development is unknown.

1.5 Autoantibodies in Atherosclerosis

Atherosclerosis is most recently known as a chronic inflammatory disease, emphasizing the role of the immune system in the progression of lesion development. A number of antibodies targeting self-antigens have been associated with atherosclerosis even in the absence of overt immunization or

additional infection, leading to the theory that atherosclerosis could fundamentally be an autoimmune disease(95). The most commonly known autoantigen linked to atherosclerosis is oxidized LDL (oxLDL), and the corresponding autoantibodies present in humans are related to the extent of atherosclerosis(95, 96).

OxLDL is generated by the oxidation of LDL and accumulates in the vascular wall during development of atherosclerotic lesions(97). While the precise mechanism of LDL oxidation *in vivo* is unclear, it is thought that reactive nitrogen species produced in response to several proatherogenic factors contributes to the oxidative modification of LDL(98, 99). OxLDL contributes to atherogenesis through ER stress induced endothelial cell activation leading to adhesion molecule expression in addition to promoting secretion of inflammatory cytokines and chemokines that stimulate monocyte to macrophage differentiation and smooth muscle cell proliferation(100, 101). Additionally, macrophages can take up oxLDL through scavenger receptors, leading to foam-cell formation(102). Autoantibodies against oxLDL were identified circulating in sera as well as in atherosclerotic lesions from both rabbits and humans(103, 104). Increasing levels of autoantibodies to oxLDL corresponded to lesion progression in $LDLR^{-/-}$ mice fed an atherogenic diet, but did not rise in mice fed a normal chow diet, supporting the idea that measurement of autoantibody titers to oxLDL could be a useful tool for assessing plaque oxLDL levels and lesion composition(105). Since high levels of autoantibodies to oxLDL were observed during atherogenesis, it

was thought that perhaps oxLDL autoantibodies somehow promoted lesion progression. On the contrary, however, immunization against oxLDL in mice and rabbits proved to be atheroprotective and reduced lesion size compared to controls irrespective of an increase in antibodies to oxLDL(106). While these results suggest a role for oxLDL autoantibodies in the clearance oxLDL, there was no evidence of increased clearange of oxLDL mediated by its corresponding autoantibodies in ApoE$^{-/-}$ mice(107). Although additional potential roles of oxLDL autoantibodies have been suggested, including blocking the uptake oxLDL by macrophages, the exact function of these autoantibodies and their relevance *in vivo* remains unclear(108).

1.6 Project Rational, Hypothesis and Objectives

Although signaling through surface GRP78 has been described in cancer cells, the functional significance of endothelial cell surface GRP78 and its potential role in atherosclerotic lesion development is unknown. GRP78 is known as a cell-surface signaling receptor on stressed cells and has been identified on the surface of lesion resident endothelial cells, therefore it was hypothesized that signaling through cell-surface GRP78 on endothelial cells promotes endothelial cell activation and encourages atherosclerotic lesion development. The overall objective of this project was to investigate the role of cell surface GRP78 and GRP78a-Abs in the development and progression of atherosclerosis. Specific objectives include (i) assessing the relationship between GRP78a-Abs and the

extent of atherosclerosis (ii) examining the cellular function of surface GRP78 in endothelial cells (iii) investigating the significance of GRP78a-Abs in humans.

In work described here, we identify GRP78a-Abs in murine models of atherosclerosis and show that serum levels correspond to lesion progression with an atherogenic diet. Moreover, high levels of GRP78a-Abs accelerate early atherosclerotic lesion growth in ApoE$^{-/-}$ mice, via a direct interaction and activation of surface GRP78 on lesion resident endothelial cells. Furthermore, we demonstrate that blocking circulating GRP78a-Abs is a viable strategy toward attenuating lesion progression. In addition, we establish that induction of ER stress stimulates surface GRP78 expression in primary human aortic endothelial cells. We show activation of surface GRP78 by GRP78a-Abs exacerbates proinflammatory signaling and adhesion molecule expression through the NFκB pathway in cultured endothelial cells expressing surface GRP78. Finally, we provide groundwork evaluation of the relationship of GRP78a-Abs in human populations at risk for cardiovascular disease. These findings provide a basis for understanding the role of GRP78a-Abs and the activation of surface GRP78 in endothelial cells and atherosclerotic lesion development.

Chapter 2 – The Role of Anti-GRP78 Autoantibodies in Atherosclerotic Lesion Development *In Vivo*

2.1 Introduction

2.1.1 Animal Models of Atherosclerosis

Genetically modified animal models are extremely useful tools for studying the progression of a disease and the contribution of specific genes to cellular processes or pathology. Wild type mice are protected from the development and progression of atherosclerosis, so to develop an animal model of the disease it was necessary to modify the genetics of mice to increase their susceptibility to atherogenesis(109). Gene targeting initially focused on apolipoprotein E (apoE), a glycoprotein and structural component of most lipoproteins(110). ApoE serves as a ligand for receptors that allow uptake of lipoproteins by the liver, an important process in cholesterol metabolism. ApoE-deficient mice were created in 1992 by the Maeda and Breslow groups and have since been an important advancement in understanding the pathology and progression of atherosclerosis(109, 111, 112). Mice lacking this protein are hypercholesterolemic and spontaneously develop atherosclerotic plaques on a chow diet that resemble human lesions(111, 112). This phenotype becomes more severe when challenged with a high cholesterol or high fat diet(112). Therefore, the ApoE$^{-/-}$ strain is the primary mouse model used by our lab to study atherosclerosis and in the experiments described below.

A second useful animal model for atherogenesis involves the ablation of the low density lipoprotein receptor(LDLR) gene in mice, which was developed by Ishibashi and colleagues (113). These animals have a modest increase in plasma cholesterol and LDL levels when fed a chow diet compared to wild-type mice (113). Unlike ApoE$^{-/-}$ mice, LDLR$^{-/-}$ mice do not develop atherosclerotic lesions on a normal chow diet but quickly develop large advanced lesions only when fed a high cholesterol diet, thus enabling temporal control over the initiation of lesion formation(114).

2.1.2 A Small Peptide Mimetic of Surface GRP78

The small peptide CNVSKDSC was originally described as a tool used by Mintz and colleagues during a screen for circulating tumor-associated antibodies in prostate cancer patients(93). Reactivity of patient serum against the peptide CNVSKDSC was significantly higher in cancer patients than healthy controls and positively correlated with the natural progression of the disease(93). This peptide was shown to mimic the tertiary conformation of an epitope on the N-terminal region of cell surface GRP78 and could be recognized by antibodies against GRP78(93). Patient serum was shown to react with recombinant GRP78, and this reactivity could be blocked by the CNVSKDSC peptide, identifying for the first time autoantibodies against GRP78 and their link to human disease(93). Additional studies have utilized this small peptide conjugated to KLH and immobilized on 96-well plates to develop an ELISA assay for detection of

GRP78a-Abs in serum(94). Moreover, the CNVSKDSC peptide was used to purify anti-GRP78 antibodies from human serum by immunoaffinity(94). This peptide has been established as a useful tool for investigating GRP78a-Abs and provides a potential method for sequestering GRP78a-Abs in circulation.

2.1.3 Objective

Cell surface GRP78 in cancer leads to the development of circulating autoantibodies against GRP78 in cancer patients(84). High levels of GRP78a-Abs correlate with accelerated cancer progression and reduced survival in these patients(93). Although cell surface GRP78 has been identified on atherosclerotic lesions in ApoE$^{-/-}$ mice(91), the relevance and influence of GRP78a-Abs in atherosclerosis is unknown. The objective of this work was to assess the relationship between GRP78a-Abs and atherosclerosis *in vivo*. Here we assess GRP78a-Abs in a number of animal models of atherosclerosis. We also employ several strategies to modulate levels of circulating GRP78a-Abs in ApoE$^{-/-}$ mice and examine the resulting effects on atherogenesis.

2.2 Materials & Methods

2.2.1 Animals

Female C57BL/6 and ApoE$^{-/-}$ mice were obtained from Jackson Laboratories and fed a normal chow diet or high-fat diet *ad libitum* (Harlan Tekland; 88137) with free access to water. In experiments described here, blood was collected from

the right ventricle under isofluorane anesthesia. The mice were then euthanized by cervical dislocation and immediately perfused with PBS followed by 4% paraformaldehyde. The heart and aorta were removed and fixed in buffered formalin overnight before further processing. All procedures were approved by the McMaster University Animal Research Ethics Board.

Serum samples from $LDLR^{-/-}$ mice fed a chow or high-fat diet were generously provided by Dr. Geoff Werstuck. Serum samples from C57BL/6, $ApoE^{-/-}$, $LDLR^{-/-}$, and $SRB1^{-/-}$ mice fed a Paigen diet were generously provided by Dr. Bernardo Trigatti.

2.2.2 Production and purification of human recombinant GRP78 protein

His-tagged full length recombinant human GRP78 (rhGRP78) protein was expressed in Rosetta bacteria and purified by nickel affinity chromatography. Briefly, the GRP78-pET-28b vector was inserted into Rosetta cells by heat shock transformation. Transformed cells were grown in LB media containing 50ng/mL kanamycin and 50ng/mL chloramphenicol to an OD_{600} of 0.8-1.0 and subsequently treated with 500nM IPTG for 3-4 hours to induce rhGRP78 expression. Cells were lysed with sonication and rhGRP78 was purified by gravity flow on a Ni-NTA Agarose (Qiagen) column at 4°C. Contaminating endotoxin was removed by running the protein through a Detoxi-Gel pre-packed column (Pierce). Endotoxin removal below 0.05 EU/mL was confirmed using the E-Toxate detection system (Sigma-Aldrich). Purity of the protein was evaluated

by SDS-PAGE. An ATPase Assay Kit (Innova Biosciences) was used to assess the ATPase activity of the purified protein as a measure of its functionality. Purified recombinant GRP78 was aliquoted and stored at -80°C until further use.

2.2.3 Production and purification of GRP-MSAH$_6$ recombinant protein

Recombinant proteins containing residues 98-115 of GRP78 linked to a hexahistidine-tagged mouse serum albumin (GRP-MSAH$_6$) and MSAH$_6$ alone were produced by expressing the proteins in yeast cells using methods previously established (115, 116). Briefly, after the conditioned media was concentrated the proteins were isolated by affinity purification on nickel-chelate affinity columns. After dialysis against PBS, the proteins were characterized by immunoblotting using both anti-MSA and anti-H$_6$ antibodies. Purified proteins were aliquoted and stored at -80°C until further use.

2.2.4 Purification of mouse anti-GRP78 autoantibodies

Anti-GRP78 autoantibodies were isolated from the serum of 24 week old female apoE$^{-/-}$ mice fed a chow diet. The autoantibodies were purified by affinity chromatography on the CNVSKDSC peptide immobilized on Sepharose 4B as previously described (86, 117).

2.2.5 Immunization against GRP78

To stimulate production of antibodies against GRP78, female apoE$^{-/-}$ mice fed a chow diet were injected at 6 weeks of age with 100 μL TiterMax Gold adjuvant

emulsified in a 1:1 mixture with 50 μg endotoxin-free ovalbumin (OVA), or 50 μg recombinant GRP78 in sterile saline. Mice were given 2 booster injections at 10-day intervals. Blood samples were collected at intermediate time points from the facial vein. Mice were sacrificed at 15 weeks of age (early lesion group) or 25 weeks of age (advanced lesion group) using paraformaldehyde infusion as described above.

2.2.6 Quantification of Cholesterol and Triglycerides

Total cholesterol and triglycerides were measured in serum by enzymatic colorimetric assays Cholesterol E and L-Type Triglyceride M, respectively, according to manufacturers guidelines (Wako Diagnostics).

2.2.7 Analysis of Serum Anti-GRP78 Autoantibody Titers

Antibodies against GRP78 in the serum of mice were determined utilizing an ELISA originally described by Gonzalez-Gronow and colleagues that was optimized in our lab for use with mouse serum(94). Briefly, 96-well plates were coated with the CNVSKDSC peptide conjugated to KLH (5 μg/mL), blocked with PBS-Tween containing 3% BSA, and incubated overnight with serum samples at a 1:100 dilution. Plates were incubated with anti-mouse IgG conjugated to alkaline phosphatase and developed by adding an alkaline phosphatase substrate to the plate for 25 minutes, after which the reaction was stopped with 3M NaOH. Absorbance was read at 405 nm. All assays were performed in triplicate and analyzed relative to a common sample.

2.2.8 Quantification of Atherosclerotic Lesion Size and Necrotic Area

The fixed hearts (with the aortic root) were dissected from the aortic arch, cut transversely, and embedded in paraffin blocks. For each samples, one hundred and twenty 4-μm-thick serial sections were cut through the aortic root. Comparable sections were stained with hematoxylin and eosin. Lesion size and necrotic area were measured from 4-5 sections at 80μm intervals using ImageJ as previously described(118). Necrotic area, defined as regions greater than 3,000-μm^2 devoid of nuclei in the intima, was measured and expressed as a percentage of total lesion area as described previously(119).

2.2.9 Immunohistochemistry

Immunohistochemistry was performed on serial paraffin sections of the aortic root. Horseradish peroxidase substrate staining for Mac-3 (Pharmingen; #55322) and CD3 (Dako Cytomation; A0452) was done as described previously(32, 118). Briefly, dried sections were deparaffinized in xylene and endogenous peroxidase was blocked by incubating in 0.5% H_2O_2 for 10 min. Heat-induced epitope retrieval was performed followed by blocking with normal rabbit or goat serum, respectively. Slides were incubated with primary antibodies for 1.5-2 hours at room temperature, washed and incubated with the appropriate biotinylated secondary antibody for 30 min at room temperature. Following additional washes, slides were incubated with HRP-streptavidin (Invitrogen; #50-242Z) for 30 min at room temperature and exposed to prepared Nova Red (Vector Laboratories; #SK-4800) solution for 3-7 minutes. The reaction was quenched with distilled

water. Sections were counterstained with Gills hematoxylin and mounted with Permount (Fisher Scientific).

2.2.10 *En face* Immunofluorescence

Purified mouse anti-GRP78 autoantibodies isolated previously from apoE$^{-/-}$ mice, as well as control mouse IgG (Sigma Aldrich) were biotinylated using EZ-Link Sulfo-NHS-Biotin (Thermo Scientific) according to the manufacturer's instructions. Female apoE$^{-/-}$ mice at 18 wks of age were injected via the tail vein with 10 μg biotinylated GRP78a-Ab or 10 μg biotinylated IgG. Mice were sacrificed after 30 minutes as described above. The aortic arch was dissected and cut open longitudinally. The aortas were blocked with 10% goat serum and incubated with rat anti-CD31 (1:200; BD Pharmingen) overnight followed by PBS washes and anti-rat Alexa 488 (1:200; Life Technologies) and streptavidin conjugated Alexa 594 (1:200; Life Technologies) for 30 min. Nuclei were stained using DAPI (Sigma-Aldrich). The aortas were mounted on slides with ProLong Gold Antifade Mountant (Life Technologies) and viewed with a Zeiss Axioplan fluorescent microscope (Carl Zeiss Canada). Regions with and without lesions were identified based on published anatomical locations relative to the lesser and greater curvature area(29, 120).

2.2.11 Peptide Infusions

Alzet osmotic mini pumps (Model# 1004) containing the CNVSKDSC peptide dissolved in saline (pump rate: 10 mg/kg/d) or saline alone were surgically implanted subcutaneously in the interscapular region of 11 week old female apoE$^{-/-}$ mice fed a chow diet. Mice were allocated to groups in a weight-matched fashion prior to commencement of the experiment. Body weight was measured each week after the procedure to confirm surgical recovery. No sign of health deterioration (i.e. reduced cage movement, hunching or Barbary) or chronic infection was observed in any of the mice. Mice were sacrificed 4 weeks after pump implantation as described above.

2.2.12 Statistical Analysis

Values are expressed as mean±SE. Statistical analysis was performed using an unpaired Student's *t* test or ANOVA. When significance was attained using ANOVA, a Tukey's post hoc test was used to determine specific differences. Significance was defined as $p<0.05$.

2.3 Results

2.3.1 *Anti-GRP78 autoantibody titers increase in mice with atherosclerosis.*

While C57BL/6 mice are resistant to developing atherosclerosis, it is known that ApoE$^{-/-}$ mice aged 25 weeks have advanced lesion development even when fed a chow diet (32). Therefore, in order to determine the influence of atherosclerosis

progression on GRP78a-Abs, we collected serum from mice with little to no lesions (C57BL/6 mice) as well as those with advanced lesions (ApoE$^{-/-}$ mice). Titer levels of GRP78a-Abs in serum were measured in 26 week old female ApoE$^{-/-}$ mice and age-matched female C57BL/6 mice by ELISA. ApoE$^{-/-}$ mice showed significantly higher levels of GRP78a-Abs, compared to C57BL/6 mice (Fig. 3A). Additionally, ApoE$^{-/-}$ mice with advanced lesions (26 weeks of age) had significantly higher GRP78a-Abs levels than ApoE$^{-/-}$ mice with early lesions (12 weeks of age; Fig.3B). This suggests GRP78a-Abs are associated with the occurrence and severity of atherosclerosis.

To investigate in detail how GRP78a-Abs titers might change over time, plasma titer levels were measured repeatedly by ELISA in C57BL/6 and ApoE$^{-/-}$ mice from 8 to 20 weeks of age while on a chow diet. ApoE$^{-/-}$ mice begin to develop early lesions by 10 weeks of age that can be identified by fatty streaks composed of foam cells in the intima of the vessel wall (32). These areas develop into advanced lesions by 25 weeks of age, therefore this window of time represents a significant period of lesion development during growth in ApoE$^{-/-}$ but not C57BL/6 mice. GRP78a-Abs increased with age in ApoE$^{-/-}$ mice fed a chow diet, and were significantly higher than levels in C57BL/6 mice at 20 weeks of age (Fig. 3C). To examine whether accelerated lesion development influenced GRP78a-Abs levels, mice were fed a high fat diet (HFD) which is known to increase the rate at which ApoE$^{-/-}$ mice develop atherosclerotic lesions(121). ApoE$^{-/-}$ mice on a HFD had significantly higher levels of GRP78a-Abs compared

to C57BL/6 mice at 17 weeks of age (Fig. 3D), suggesting a more rapid induction of GRP78a-Abs under more athlerogenic HFD conditions.

To further examine whether the increase in GRP78a-Ab titers observed in ApoE$^{-/-}$ mice is influenced by the development of atherosclerosis rather than simply being an artifact of the genetic strain, GRP78a-Ab titers were also measured by ELISA in 15 week old female LDLR$^{-/-}$ mice that were fed either a regular chow diet or high fat diet (HFD) for 10 weeks. LDLR$^{-/-}$ mice do not develop atherosclerotic lesions unless challenged with a high fat diet, therefore we expected to see higher GRP78a-Ab titers in the mice fed a HFD compared to those remaining on a regular chow diet. Although not significant, the LDLR$^{-/-}$ mice fed a HFD showed a tendency of higher GRP78a-Ab levels compared to the mice on a chow diet (p=0.21; Fig. 3E).

To examine additional models of atherogenesis, four different strains of mice, C57BL/6, ApoE$^{-/-}$, LDLR$^{-/-}$, and SRB1$^{-/-}$ were fed the atherogenic Paigen diet for 20 weeks. There was no significant difference of GRP78a-Ab levels between these groups (Fig. 3F). To reduce variability and because all previous work had been done using single-gender cohorts, the groups were separated into males and females. When the groups were compared across only one gender, the levels of GRP78a-Abs were significantly higher in ApoE$^{-/-}$, LDLR$^{-/-}$, and SRB1$^{-/-}$ male mice compared to C57BL/6 male mice (Fig. 3G). GRP78a-Ab levels were not significantly different in the female mice (Fig. 3H).

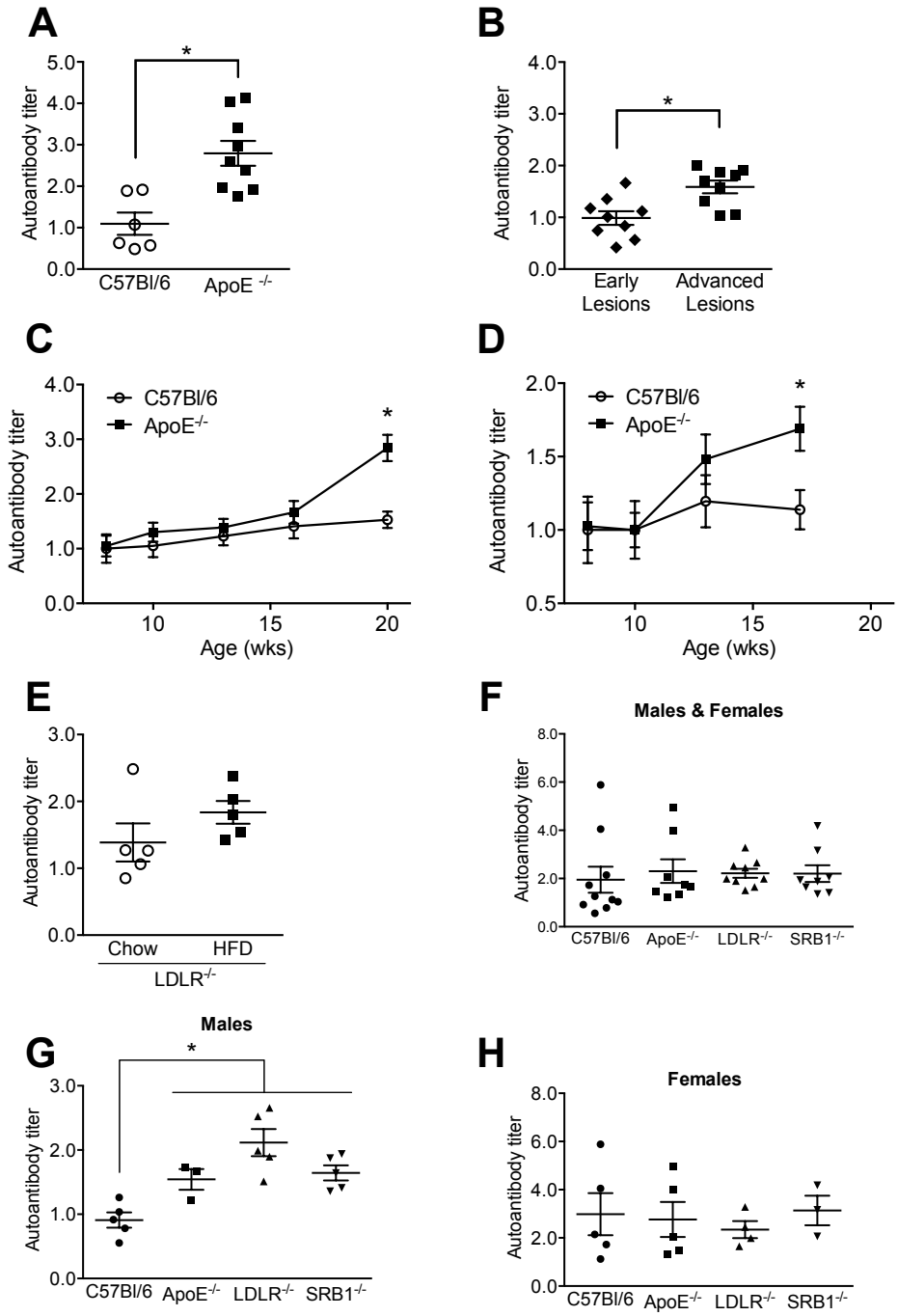

Figure 3. GRP78a-Abs are elevated in mouse models of atherosclerosis. Serum levels of GRP78a-Abs were measured by ELISA from *(A)* female C57BL/6 or ApoE$^{-/-}$ mice at 26 weeks of age fed a chow diet, *(B)* female ApoE$^{-/-}$ mice at 12 weeks of age (early lesion group) or 26 weeks of age (advanced lesion group) fed a chow diet, *(C)* female C57BL/6 or ApoE$^{-/-}$ mice 8-20 weeks of age fed a chow diet, *(D)* female C57BL/6 or ApoE$^{-/-}$ mice 8-17 weeks of age fed a high fat

diet starting at 8 weeks of age, *(E)* 15 week old female LDLR$^{-/-}$ mice on a high fat (HF) or chow diet for 10 weeks (*n*=5 per group).*p<0.05 *versus* age matched C57BL/6 mice. Levels of anti-GRP78 autoantibodies are shown for *(F)* mice fed a Paigen diet and sub-divided by gender into *(G)* male and *(H)* female mice. *P<0.05 *versus* age matched C57BL/6 mice. All data are presented as absorbance units at 405 nm relative to a common sample.

2.3.2 *Production of functional human recombinant GRP78 protein*.

His-tagged full length human recombinant GRP78 (hrGRP78) protein was expressed in Rosetta cells and affinity purified by gravity flow using Ni^{2+} -agarose at 4°C. Contaminating endotoxin was removed by placing the recombinant protein over a Detoxi-Gel pre-packed column. Endotoxin removal below 0.05 EU/mL was confirmed using the E-Toxate detection system (Sigma). The purity of the isolated protein was confirmed with coomassie stain (Fig. 4A). The purified protein was analyzed by western blot and detected by anti-GRP78 and anti-His antibodies(Fig. 4B). Function of hrGRP78 was evaluated by determining ATPase activity with the ATPase assay kit, from Innova Biosciences, which showed that the purified hrGRP78 has 0.022 units/mL of activity (1 unit equals the amount of enzyme that catalyzes the reaction of 1μmol of ATP per minute).

In some instances, the insertion of a His-tag can interfere with the folding or activity of a recombinant protein. Although the recombinant GRP78 included a His-tag, it has been previously shown that this modification does not affect the function or structure of GRP78 and provides a simple method for purification(122). After confirming the activity and purity of rhGRP78, this protein

was used *in vivo* to immunize ApoE$^{-/-}$ mice and stimulate GRP78 autoantibody production.

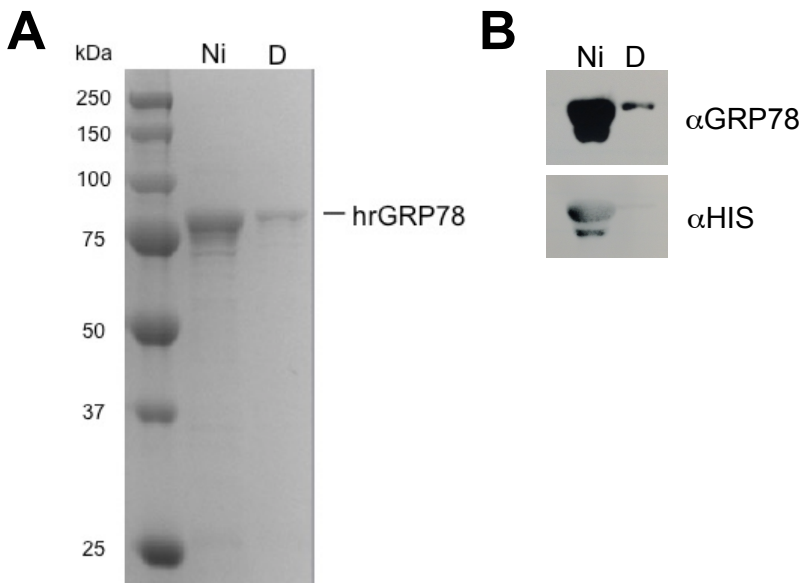

Figure 4. Purification of recombinant human GRP78 protein. Endotoxin was removed from full length recombinant GRP78 expressed in Rosetta cells and purified by nickel affinity gravity-flow chromatography (Ni) by running over a Detoxi-Gel column (D). Samples were separated on an SDS-PAGE gel and stained with *A*. coomassie dye, to visualize proteins and assess purity, or transferred to nitrocellulose and probed for *B*. GRP78 and *C.* HIS.

2.3.3. *ApoE$^{-/-}$ mice with elevated levels of anti-GRP78 autoantibodies have larger and more complex lesions.*

In order to specifically manipulate levels of GRP78a-Abs *in vivo* and determine whether it plays a role in lesion development, ApoE$^{-/-}$ mice were immunized

against rhGRP78 or control ovalbumin. Mice injected with rhGRP78 produced significantly higher levels of GRP78a-Abs at 12, 15 and 25 weeks of age, compared to ApoE$^{-/-}$ mice immunized against ovalbumin (Fig. 5A). At 15 weeks of age, mice with higher levels of GRP78a-Abs had significantly larger lesions, compared to control immunized mice (Fig. 5B-C). There was no significant difference in lesion size in mice at 25 weeks of age (Fig. 5D-E). At 15 weeks of age, fatty streaks were observed in both control and rhGRP78 immunized mice. However areas of more complex lesions were also present in rhGRP78 immunized mice at this time point. Advanced intimal lesions consisting of necrotic area, lipid crystals, and a cellular cap were observed in both treatment groups at 25 weeks of age. Areas of lipid rich necrotic core and cellular debris were observed in mice immunized against GRP78 at both 15 and 25 weeks of age and in control immunized mice with advanced lesions at 25 weeks of age (Fig. 5F). Quantification of the necrotic area in lesions demonstrated a significantly greater amount of necrotic area in mice with higher levels of GRP78a-Abs at 15 weeks of age (Fig. 5G) but not 25 weeks of age (Fig. 5H). This data suggest that the increased GRP78a-Abs exacerbate atherosclerosis formation at early stages of lesion development.

Triglyceride and total cholesterol levels were not significantly different between groups at 15 or 25 weeks of age (Fig. 5I-L). This indicates that any difference in lesion size and characteristics observed between groups is not the result of alterations to triglyceride and total cholesterol levels.

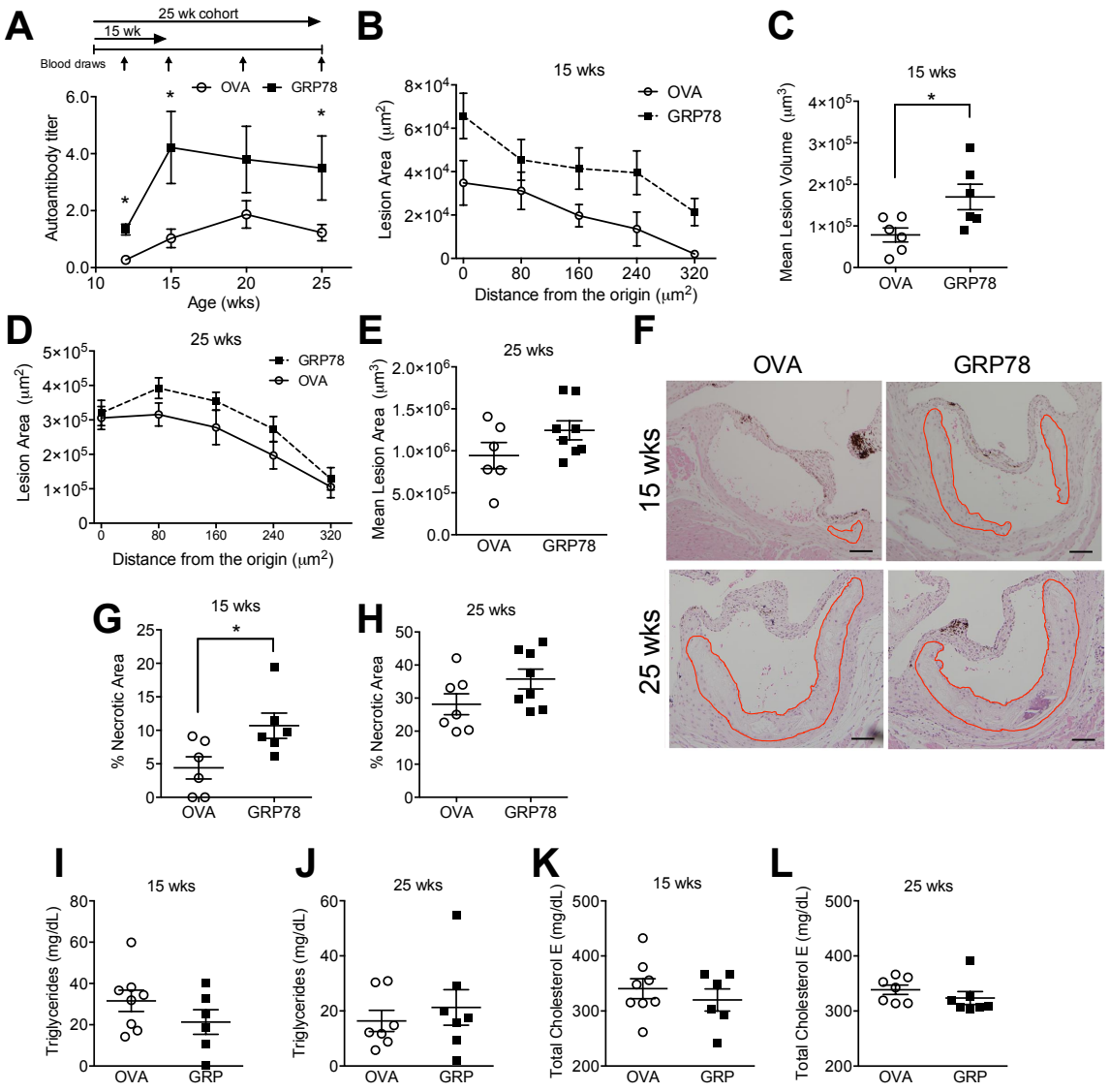

Figure 5. Atherosclerotic lesion growth is accelerated in ApoE$^{-/-}$ mice with elevated GRP78a-Ab titers. *(A)* Serum levels of GRP78a-Abs were measured by ELISA in female ApoE$^{-/-}$ mice fed a chow diet and injected three times at 10 day intervals with 50 μg/ml of ovalbumine (OVA, n=6) (○) or full length recombinant GRP78 (n=6)(■) beginning at 6 weeks of age. Data are presented as absorbance units (AU) at 405 nm relative to a common sample. *p<0.05 *versus* OVA at each time point. *(B-E)* Quantification of atherosclerotic lesion area and volume at the aortic root in 15 and 25 week old mice as indicated. Lesion size was measured in 5-6 sections at 80 nm intervals, *p<0.01 *versus* OVA treated mice. *(F)* Representative cross sections of the aortic root stained with hematoxylin-and-eosin. Lesions are outlined in red. Images were taken at 20X magnification. Bar = 200 mm. *(G-H)* Quantification of necrotic area in lesions at the aortic root. Data are expressed as

percent of total lesion area. *p<0.01 *versus* OVA treated mice. Plasma levels of *(I-J)* triglycerides and *(K-L)* total cholesterol were measured in fed 15 and 25 week old mice as indicated by colorimetric assays. Data are represented as mg/dL.

2.3.4. *Anti-GRP78 autoantibodies bind to lesion resident endothelial cells in ApoE$^{-/-}$ mice.*

GRP78 has previously been identified on the surface of lesion resident endothelial cells in ApoE$^{-/-}$ mice(91). To determine whether GRP78a-Abs interact with endothelium expressing surface GRP78, GRP78a-Abs were isolated from 24 week old female ApoE$^{-/-}$ mice. The purified autoantibodies as well as control mouse IgG were biotinylated for ease of detection. ApoE$^{-/-}$ mice were injected via the tail vein with biotinylated-GRP78a-Abs (b-GRP78a-Abs) or biotinylated-mouse IgG (b-IgG) and sacrificed after 30 min. The ascending aorta and proximal arch were dissected and double stained *en face* for endothelial cells (anti-CD31) as well as binding of biotinylated antibodies (anti-Streptavidin-594). Binding of b-GRP78a-Abs was assessed in regions with high (HP) and low (LP) probabilities for developing lesions as previously identified and described by Iiyama K. and colleagues(120). We observed b-GRP78a-Abs associated with lesion-resident endothelial cells in HP regions, but no detectable b-GRP78a-Abs were observed on endothelial cells in LP regions (Fig. 6). This suggests GRP78a-Abs in mice directly interact with the endothelium and specifically interacts with lesion-resident endothelial cells.

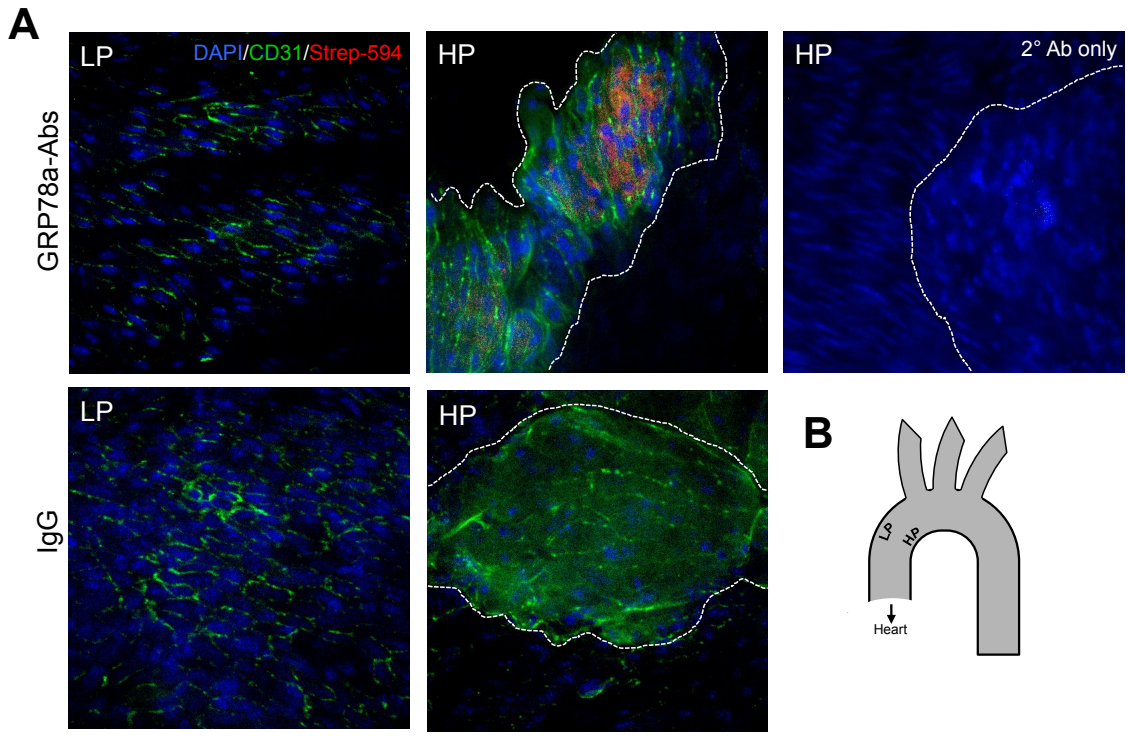

Figure 6. GRP78a-Abs bound to endothelial cells on atherosclerotic lesions. Immunofluorescence images of biotinylated GRP78a-Abs binding lesion resident endothelium in the aortic arch from female apoE$^{-/-}$ mice (18 weeks of age). Mice were injected with 10 µg biotinylated GRP78a-Abs or biotinylated mouse IgG and sacrificed 30 min post injections. *(A)* LP and HP regions were stained *en face*. Dashed lines indicate areas of lesions. Endothelial cells report green with rat anti-mouse CD31 and bound biotinylated antibodies report red with streptavidin-conjugated secondary antibody (Strep-594). Nuclei were counterstained with DAPI (blue). HP regions stained with secondary antibodies only (2° Ab only) served as controls for autofluorescence and non-specific staining. These data indicate that GRP78a-Abs bind to lesion-resident endothelial cells. *(B)* Location of LP and HP regions for atherosclerotic lesion formation on the ascending aorta and proximal arch.

2.3.5. *Production and characterization of a recombinant albumin containing a GRP78 peptide sequence.*

Previous studies have successfully shown that fusion of albumin to small molecules is an effective strategy to extend clearance half-life without inhibiting the effects of the small molecules [116, 123, 124]. Since GRP78a-Abs commonly bind the Leu^{98}-Leu^{115} domain of GRP78, we were interested in linking this sequence to albumin to slow the clearance of the small peptide as a method to bind and neutralize GRP78a-Abs in circulation. To this end, a recombinant protein containing residues 98-115 of GRP78 linked to hexahistidine-tagged mouse serum albumin (GRP-$MSAH_6$) and a control hexahistidine-tagged mouse serum albumin ($MSAH_6$) was generated. Production of the proteins was highest after 72 hours by methanol-induced yeast cells grown in BMMY medium (Fig. 7A). Western blot analysis showed the proteins were detectable by both anti-MSA and anti-HIS antibodies (Fig. 7B).

To test whether this GRP-$MSAH_6$ protein complex was able to bind the GRP78a-Abs, immunoprecipitation assays were performed to measure the degree of protein interaction. In the first experiment, GRP78a-Abs were incubated with GRP-$MSAH_6$ and the resulting complexes were collected with Protein G beads. Although GRP-$MSAH_6$-GRP78a-Ab complex formation was detected with an anti-MSA antibody, GRP-$MSAH_6$ was also detected in the absence of GRP78a-Abs suggesting non-specific binding of GRP-$MSAH_6$ to the

beads. To minimize non-specific column binding, a second experiment utilized the hexahistidine tag on GRP-$MSAH_6$. GRP-$MSAH_6$ was incubated with GRP78a-Abs and pulled down using cobalt beads, which bind specifically to hexahistidine residues. Again, GRP78a-Abs were not detected in complex with GRP-$MSAH_6$ and were only visible in wash fractions (Fig. 7C). Taken together these pull-down assays do not suggest a strong interaction between GRP78a-Abs and the GRP-$MSAH_6$ fusion protein.

To further test the ability of GRP-$MSAH_6$ to interact with GRP78a-Abs, GRP-$MSAH_6$ was incubated with human serum overnight and subjected to ELISA to determine whether the fusion protein could reduce the signal generated by GRP78a-Abs. Serum pre-incubated with GRP-$MSAH_6$ showed a modest reduction in GRP78a-Abs, however this reduction was also seen in serum incubated with $MSAH_6$ (Fig. 7D), therefore it cannot be concluded that the difference was due to specific interactions between GRP78a-Abs and the fusion protein. As the published CNVSKDSC peptide shows a superior ability than GRP-$MSAH_6$ to interact with GRP78a-Abs (Fig. 7D), this peptide was used as the primary strategy for neutralizing GRP78a-Abs in follow-up experiments.

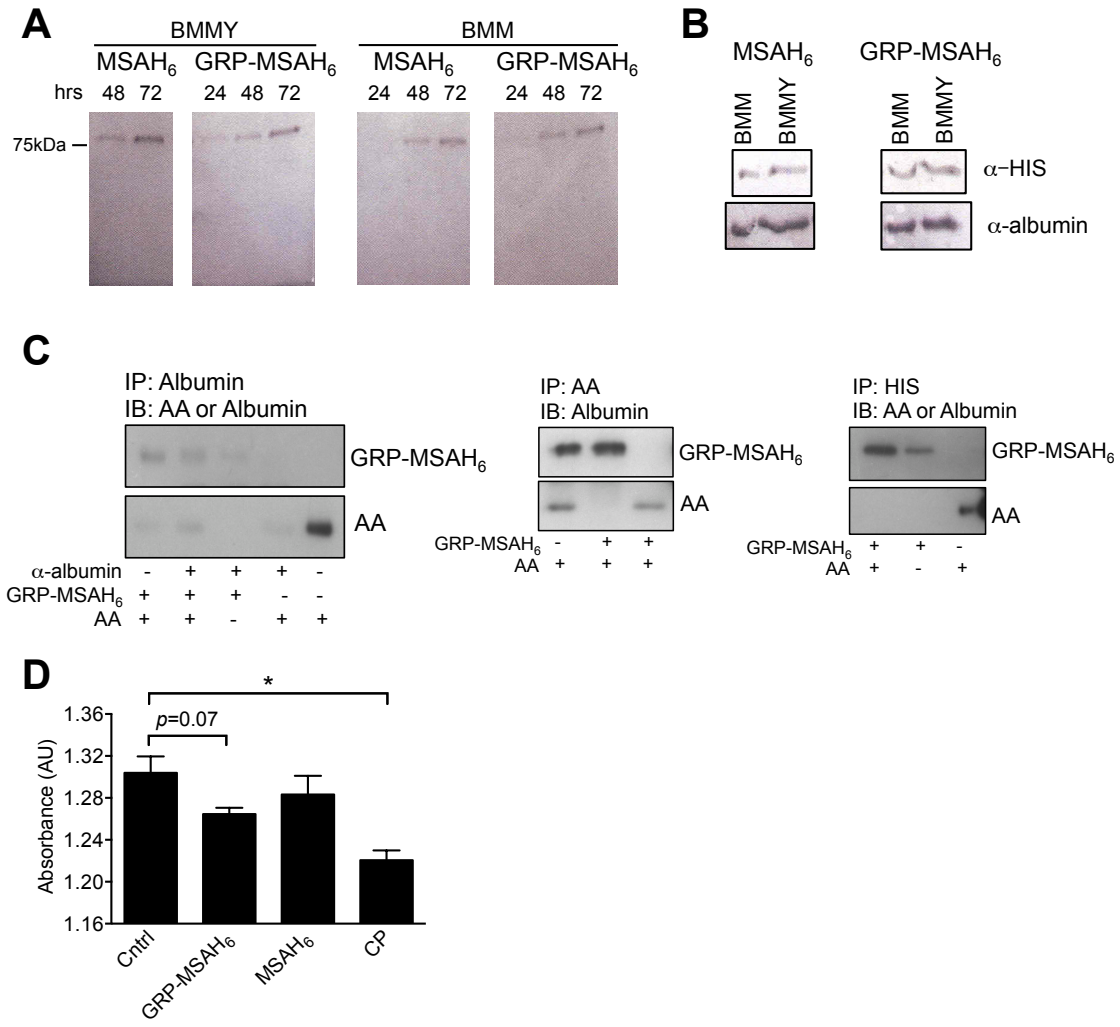

Figure 7. Purification and assessment of recombinant GRP-MSAH$_6$ and MSAH$_6$ proteins. *(A)* Recombinant proteins were optimally expressed in yeast cells grown in BMMY media for 72 hours. Proteins were purified by nickel affinity gravity-flow chromatography and endotoxin was removed by running over a Detoxi-Gel column. *(B)* Samples were separated on an SDS-PAGE gel, transferred to nitrocellulose and detected by albumin and HIS antibodies. *(C)* Immunoprecipitations of GRP-MSAH$_6$ and GRP78a-Abs (AA). Immunoblots visualized with anti-albumin or anti-human antibodies to detect GRP-MSAH$_6$ or GRP78a-Abs respectively. *(D)* Levels of GRP78a-Abs measured by ELISA in serum from prostate cancer patients pre-incubated with GRP-MSAH$_6$, MSAH$_6$, or the CNVSKDSC peptide. Data are presented as absorbance units (AU) at 405 nm. *p<0.05 *versus* control.

2.3.6 *The small peptide CNVSKDSC reduces lesion size in ApoE$^{-/-}$ mice*.

In order to determine whether blocking GRP78a-Abs could attenuate lesion growth, female ApoE$^{-/-}$ mice fed a chow diet were infused with the small peptide CNVSKDSC or saline for 4 weeks using mini-osmotic pumps. Groups were distributed evenly based on starting body weight(Fig. 8A). Body weight did not significantly differ between groups during the course of the experiment (Fig. 8B), suggesting no adverse heath effects due to the procedure. Levels of serum GRP78a-Abs were measured by ELISA and were not significantly different between groups or from baseline (Fig. 8C). Quantification of lesion area and volume in 6 sections at 80μm intervals showed no significant difference between groups (Fig. 8D-F). Although not significant, there was a 20% decrease of lesion volume in CNVSKDSC peptide infused mice compared to saline infused control mice, suggesting that neutralizing circulating GRP78a-Abs could be a valuable strategy toward reducing lesion growth *in vivo*.

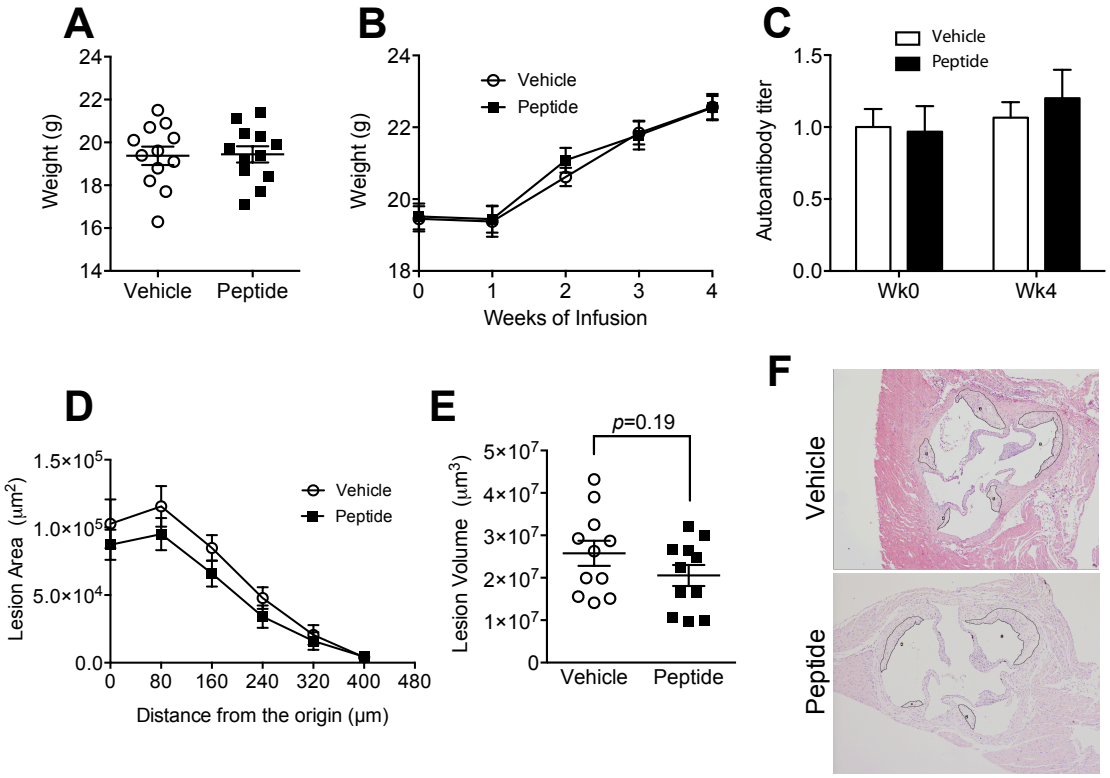

Figure 8. Atherosclerotic lesion size in ApoE$^{-/-}$ mice infused with the peptide CNVSKDSC. ApoE$^{-/-}$ mice at 11 weeks of age fed a chow diet were infused with the CNVSKDSC peptide (10mg/kg/d, n=11, Peptide) or saline control (n=11, Vehicle) for 4 weeks via subcutaneous implantation of an osmotic pump. *(A)* Mouse weights at 11 weeks of age prior to pump implantation. *(B)* Mouse weights monitored weekly after surgical implantation of the pumps. *(C)* Serum levels of anti-GRP78 autoantibodies were measured by ELISA at baseline (wk0) and after 4 weeks (wk4) of infusions. Data are presented as absorbance units at 405 nm relative to the control mice at week 0. *(E)* Lesion areas plotted against the distance along the aortic root and ascending aorta. *(F)* Quantification of atherosclerotic lesion size at the aortic root. Lesion volume was measured in 5-6 sections at 80 nm intervals. *(D)* Cross sections of the aortic root stained with hematoxylin-and-eosin. Representative sections are shown for each treatment group. Lesions are outlined in black. Images were taken at 10X magnification.

2.4 Discussion

The experiments described above suggest a role for GRP78a-Abs in the occurrence and development of atherosclerotic lesions. The correlation between GRP78a-Ab titer levels and the extent of lesion growth as well as detecting an increase in levels of GRP78a-Abs as mice develop more severe atherosclerosis parallels what has been previously observed between levels of GRP78a-Abs and cancer progression. The initial observation that $ApoE^{-/-}$ mice on a chow diet with complex, advanced lesions have higher GRP78a-Ab titers compared to age-matched C57BL/6 mice indicates a possible link between the progression of lesions and the levels of GRP78a-Abs through 20 weeks of age. Similarly, when lesion formation was accelerated by placing mice on a high fat diet, $ApoE^{-/-}$ mice had higher levels of GRP78a-Abs compared to C57BL/6 mice at a younger age than in the chow-fed mice (17 weeks of age). Thus, the accelerated elevation in autoantibodies in parallel to the acceleration of lesion development further supports the idea that levels of GRP78a-Abs correlate with lesion progression.

It is important to note that although C57BL/6 mice are resistant to developing atherosclerosis, they still produce detectable levels of GRP78a-Abs. Before the introduction of the $ApoE^{-/-}$ mouse, C57BL/6 mice were commonly used as a model for studying the mechanisms that contribute to atherosclerosis. C57BL/6 mice do not form large, complex lesions, however small fatty streaks consisting of lipid-rich foam cells can occur at the aortic root. It is possible that

surface GRP78 is present in these areas in low levels in C57BL/6 mice and might therefore contribute to the reported levels of GRP78a-Abs. This is analogous to observations that low levels of GRP78a-Abs are detectable in humans considered to be healthy (93, 94). It has also been speculated that levels of GRP78a-Abs may be related to a general effect on cell death and turnover. For example, basal levels of GRP78a-Abs may reflect plasma levels of GRP78 that are released from dead or dying cells. However, based on work published by Al-Hashimi *et al.*(2010), there may be a threshold level of GRP78a-Abs required to trigger deleterious effects in cells. Perhaps a similar threshold level is required in mice for these autoantibodies to influence lesion development. Alternatively, GRP78a-Abs might be inducing varied effects on lesions depending upon the abundance and availability in circulation.

In order to confirm that GRP78a-Ab production was not simply related to apoE deletion, and to further extend our observations in other established models of atherosclerosis, we measured GRP78a-Abs in $LDLR^{-/-}$ mice. We observed a tendency toward higher GRP78a-Ab levels in $LDLR^{-/-}$ mice on a high fat diet compared to those on a chow diet, however the data is inconclusive as to whether GRP78a-Abs are elevated by lesion development in $LDLR^{-/-}$ mice. The high amount of variability observed between mice compounded by a low *n* (*n*=5 per group) could account for the lack of significance between the groups. Additional experiments assessing GRP78a-Ab levels in larger cohorts of $LDLR^{-/-}$ mice on chow and western diets are needed to determine whether GRP78a-Ab

titers are associated with the incidence of atherogenesis in this model of atherosclerosis.

Additional evidence to indicate a role of GRP78a-Abs in atherosclerosis was shown through the direct binding of biotinylated GRP78a-Abs exclusively to regions of the aortic root containing atherosclerotic lesions. Together with the previously reported observation that GRP78 is expressed on the surface of endothelial cells only on lesions(91), it is likely that the GRP78a-Abs are interacting with surface GRP78 on lesion resident endothelial cells.

To further explore the relationship between GRP78a-Abs and atherogenesis, ApoE$^{-/-}$ mice were immunized against rhGRP78 to see whether specifically manipulating autoantibody levels affected lesion development. Mice immunized against rhGRP78 produced high levels of antibodies that recognized GRP78. At 15 weeks of age mice with high GRP78a-Ab levels had larger lesions, however there was no significant difference at 25 weeks of age. This suggests that GRP78a-Abs might have a greater effect at an earlier time point during initial lesion progression, where the proximity of GRP78a-Abs to the endothelium could contribute to premature endothelial dysfunction. At 25 weeks of age, mice have developed more complex lesions in which many processes are influencing the continued growth of the lesion and deterioration of the vessel wall. Due to the dysregulated and dysfunctional nature of cellular processes within a more advanced lesion, it is possible that the effects of the autoantibodies are not significant enough to stimulate lesion growth to an even greater extent. This may

also reflect that lesion growth during this period of time may be maximal despite conditions or agents that would be expected to increase lesion size. One way to test this theory would be to increase GRP78a-Ab levels in ApoE$^{-/-}$ mice fed a high fat diet as a model of accelerated lesion growth.

Lesion size does not provide a complete picture of lesion composition. Therefore areas of necrosis were measured. Mice with higher levels of GRP78a-Abs also demonstrated a greater amount of necrotic area in lesions at 15 weeks of age. It is uncommon to see large regions of necrotic area in early lesions, which supports the idea that GRP78a-Abs might be affecting the initiation and early lesion progression. Necrotic regions are largely thought to arise from the death of macrophage foam cells in the vessel wall and a lack of phagocytic clearance of cellular debris. One way the GRP78a-Abs might be affecting necrotic area is through promotion of macrophage recruitment via augmentation of adhesion molecule expression on activated endothelial cells. Alternatively, GRP78a-Abs might be acting directly on macrophage foam cells, potentially inducing cell death, thereby contributing to the development of necrotic regions.

Since high levels of GRP78a-Abs in ApoE$^{-/-}$ mice correspond to larger lesions, we wanted to determine whether neutralizing circulating GRP78a-Abs with the CNVSKDSC peptide could attenuate lesion development in ApoE$^{-/-}$ mice. To this end, mice were infused with the small peptide or saline control for 4 weeks. ApoE$^{-/-}$ mice given the CNVSKDSC peptide had a 20% decrease in lesion size compared to controls. This reduction was not statistically significant,

however it suggests that blocking circulating GRP78a-Abs may be a viable approach toward reducing atherosclerotic lesion growth.

Atherosclerotic lesion development is known to be a complex process involving multiple cell types and molecular processes. It is important to consider the possibility that blocking surface GRP78 activation by GRP78a-Abs has only a modest observable effect on overall lesion development *in vivo* due to the variety of factors and mechanisms underlying atherogenesis, requiring a much larger sample size to illicit statistical significance. However, total lesion size is not the only metric to consider when evaluating lesion characteristics and stability. Cholesterol crystal accumulation and growth within the necrotic core can perforate altherosclerotic plaque caps, stimulating aggressive inflammatory and coagulant responses and causing rupture(10). Patients who died from acute myocardial infarction were shown to have cholesterol crystals perforating the intima on ruptured plaques(125). Additionally, proteolytic enzymes and pro-inflammatory cytokines present in atherosclerotic lesions can inhibit collagen fibre formation and illicit collagen breakdown, resulting in unstable, thin fibrous caps prone to rupture(11). Plaque remodeling can improve lesion stability and resistance to plaque rupture. Moreover, a stable atherosclerotic plaque is clinically favored in humans (126). Strategies to reduce vascular inflammation and decrease lipid accumulation are considered the most promising avenues to stabilize plaques and lower susceptibility to rupture (11). Additional work will

need to determine whether blocking GRP78a-Abs alters lesion characteristics or improves plaque stability.

There could also be several reasons for the incongruences in efficacy of the CNVSKDSC peptide between the published *in vitro* and cell free data and the results of the animal experiment described here. Although the peptide has been shown to react with serum in ELISA analysis, the exact binding affinity of the peptide to GRP78a-Abs under the conditions experienced in circulation is unknown. Concepts, strategies and limitations to assess molecular interactions are discussed in length in a recent review(127). To summarize, theoretical modeling and a variety of direct and indirect experimental methods are widely used tools to predict and describe the binding affinity, or the strength of the interaction, between two molecules. However, the authors describe how these strategies have inherent limitations, are generally focused on simple binary interactions, and are incapable of predicting interactions when considering the complex systems involving the biological, chemical, and physical conditions that influence the sensitivity and strength of interactions in a more physiologic situation. Future work should explore the dose dependency of this peptide and alternative delivery methods that may enhance the effectiveness of the blockade of autoantibody formation.

Additionally, the stability of the small peptide CNVSKDSC in plasma is unknown. Many peptides identified with promising pharmacologic activity fail to recapitulate effects when tested *in vivo(128, 129)*. This is generally thought to

occur due to low stability, short plasma half-life time, or unexpected immunogenicity. Short plasma half-life can occur due to enzymatic degradation by enzymes produced from multiple organs and through fast renal clearance. Strategies and methods to prolong plasma half-life times is an area of high interested due to the obvious advantages in therapeutic drug development(129). These strategies include screens to identify specific proteolytic enzymes with the potential to degrade the peptide during systemic circulation followed by targeted modifications based on the exact knowledge of the enzymatic susceptibility of the particular construct.

Chapter 3 – Examining the Cellular Functions of Surface GRP78 in Endothelial Cells

3.1 Introduction

3.1.1 Surface GRP78 Activity *In Vitro*

There are limited studies investigating the function of surface GRP78, often using cancer models, that have demonstrated GRP78 acts as a cell surface signaling receptor (84) and mediates a variety of signaling pathways through complexes with assorted ligands and co-receptors(80). For cancer cells, the expression of GRP78 on the cell surface is part of an adaptive survival response to chronic stress present in the tumor microenvironment(130). Recent evidence has highlighted the role of surface GRP78 as a regulator of cancer cell survival and proliferation. In prostate cancer cells, surface GRP78 promotes cell proliferation upon interaction with α_2-macroglobulin through activation of PI3K/Akt signaling(87). Additionally, binding of α_2-macroglobulin to surface GRP78 activates PAK-2, known to increase cell motility, suggesting surface GRP78 may promote metastasis potential through this pathway (131). Conversely, signaling through surface GRP78 induced apoptosis through suppression of Ras/MAPK when bound by extracellular Par-4 in a different prostate cancer cell line(132). Similarly, binding of surface GRP78 to antibodies recognizing its C-terminal domain stimulated p53 activity and promoted apoptosis in melanoma cells(89).

3.1.2 Surface GRP78 in Endothelial Cells

A handful of studies have examined surface GRP78 function in endothelial cells, however few have been in the context of atherosclerosis. In human umbilical vein cells, surface GRP78 acts as a co-receptor for lipid-anchored T-cadherin (T-cad) and is required for T-cad mediated cell survival under conditions of oxidative stress(133). Surface GRP78 was shown to interact with visceral adipose tissue-derived serine proteinase inhibitor (vaspin), an adipokine shown to promote proliferation and inhibit apoptosis, in human aortic endothelial cells under high glucose conditions. However this group did not demonstrate whether these vaspin-mediated growth and survival signals were dependent on the interaction with surface GRP78(134). Bhattacharjee and colleagues claimed surface GRP78 interacts with tissue factor on the surface of murine endothelial cells and inhibits its procoagulant activity(135), however their experiments only examined this interaction using artificial overexpression of tissue factor in murine cells. Future work is necessary to test whether these effects are present in human cells and tissues.

3.1.3 Objective

These diverse functions of surface GRP78 highlight its various roles as a receptor or target, which depend largely upon the cell type and activating agonist or antibody. For this reason, it is important to examine how surface GRP78 might be acting under specific conditions and in specific cell types in the context

of various disease states. GRP78 was identified on the surface of endothelial cells in atherosclerotic lesions(91), however the role of surface GRP78 activity in these cells and its potential significance in atherosclerotic lesion development is unknown. The objective of this work was to examine the cellular function of surface GRP78 in primary human aortic endothelial cells (HAECs) in response to GRP78a-Abs as a model of the atherogenic endothelium. HAECs are the most relevant *in vitro* model for testing human endothelial cell behavior in the context of atherosclerosis, as they most closely resemble the state of macrovascular ECs *in vivo* compared to alternatives such as EA.hy926 or HMEC-1, and thus are the most likely to provide physiologically relevant results(136). Additionally, although multiple ligands are capable of interacting with surface GRP78, these experiments focused specifically on the activation of surface GRP78 by GRP78a-Abs and the cellular consequences of that interaction in order to more fully elucidate the role of GRP78a-Abs and surface GRP78 signaling in endothelial cell function and atherogenesis.

3.2 Materials & Methods

3.2.1 Cell Culture

Primary human aortic endothelial cells (HAECs) and human umbilical vein endothelial cells (HUVECs) were purchased from Clonetics and grown in endothelial growth medium-2 (EGM-2) supplemented with 1%FBS and growth factors (EGM Bullet Kit, Lonza). All experiments were performed using cells

between passages 4 and 8. Cells were incubated at 37°C with 5% CO_2. Experiments were performed with 300 nM thapsigargin (Tg; Sigma-Aldrich), 2.5 μg/ml tunicamycin (Tm; Sigma-Aldrich), 100 ng/ml TNFα (R&D Systems), 30 nM NF-κB Activation Inhibitor II (JSH-23; Santa-Cruz), 60 μg/ml human anti-GRP78 autoantibodies (GRP78a-Abs, collected and purified by affinity chromatography as described previously(86)), 60 μg/ml human IgG (Sigma-Aldrich), or the CNVSKDSC peptide (CanPeptide, Québec).

3.2.2 Transfections

HAECs were transfected with a pcDNA plasmid containing full length GRP78 (pcDNA-GRP) and a GRP78 mutant replacing the KDEL sequence on the C-terminus with a FLAG tag (pcDNA-ΔKDEL-FLAG). Transfections were performed for 48 hrs with increasing ratios of the transfection reagent XtremeGeneHP (Roche) to plasmid DNA. HUVECs were treated with 1-10 MOI of AdGRP78 or control adenovirus (AdDL) to optimize GRP78 expression. Whole cell lysates were collected from transfected cells and analyzed by western blotting as described below to determine optimum transfection conditions.

3.2.3 Western Blotting

After treatments, HAECs were washed with cold PBS and total lysates were collected in SDS-lysis buffer (60 mM Tris-Cl, pH 6.8, 12.8% glycerol, and 2.05% SDS) containing protease inhibitors (Roche). Cell lysates were disrupted by repeated passes through a 21-gauge needle and syringe, sonication, or repeated freeze-thaw cycles. Protein concentrations were measured using the colorimetric

DC Protein Assay (Bio-Rad Laboratories) in duplicate. Total lysates and surface fractions (see isolation protocol below) were separated on 10% SDS-PAGE mini gels and transferred to nitrocellulose membranes. The membranes were incubated overnight at 4°C with the following antibodies: GRP78 (BD Transduction), CD31 (Cell Signaling), IRE-1α (Cell Signaling), β-actin (Sigma-Aldrich). The membranes were then incubated with the appropriate secondary antibodies (BD Biosciences) conjugated with horseradish peroxidase and visualized with Western Lighting Chemiluminescence Reagent (Perkin Elmer) and Kodak X-OMAT Blue XB-1 film.

3.2.4. Cell Surface Protein Isolation

Cell surface proteins were biotinylated and isolated with the Pierce Cell Surface Protein Isolation Kit (Thermo Scientific) following the manufacturer's instructions. Cells were grown to 80-90% confluence in four T75 flasks. Flasks were washed twice with ice-cold PBS and 10 mLs of ice-cold sulfo-NHS-SS-biotin (0.25 mg/mL in PBS) was added to each flask. Flasks were rocked at 4°C for 30 min and 500 μL Quenching Solution was added to each flask. Cells were gently scraped into solution and combined from all four flasks. Cells were collected by spinning at 500 x *g* for 3min and washed once with TBS. Cells were lysed in 500 μL Lysis Buffer on ice for 30 min with repeated vortexing and sonicated twice on ice using five 1-second bursts. Total lysate aliquots were taken and the remaining lysate was rotated with Immobilized NeutrAvidin Gel for 60 min at room temperature. Columns were washed three times with Wash Buffer and proteins were eluted by

incubating with 50 mM DTT for 60 min. Samples were analyzed by Western blot as described above.

3.2.5 mRNA Quantification by RT-PCR

Total RNA was isolated from HAECs with the RNeasy mini kit (Qiagen) and reverse transcribed using the High-Capacity cDNA Reverse Transcription kit (Applied Biosystems). Quantitative real-time PCR was performed in triplicate with Fast SYBR Green Master Mix (Applied Biosystems) under standard conditions. The primer sequences used are listed in Table 1.

Table 1.
Quantitative RT-PCR primers

Gene	Forward Primer	Reverse primer
ICAM-1	TATGGCAACGACTCCTTCT	CATTCAGCGTCACCTTGG
VCAM-1	CCAGGTGGAGCTCTACTCATTCCC	GCCGGTCAAGGGGGTACACG
B2M	ACTTGTCTTTCAGCAAGGACT	TTCACACGGCAGGCATAC

3.2.6 Cell Adhesion Assay

HAECs were seeded into 24-well fluorescence plates and allowed to adhere overnight. Cells were treated without or with Tm (2.5 μg/mL, 24 hours) followed by the indicated conditions. U937 cells (ATCC) were washed and resuspended at $1x10^6$ cells/mL in HBSS containing HEPES with BCECF-AM (4 μM, Sigma-Aldrich) for 30 minutes at room temperature. Cells were washed with growth media to remove excess fluorophore and resuspended at $1x10^6$ cells/mL with RPMI lacking phenol red (Cat# 11835; Life Technologies). Treated HAECs were washed with PBS and 500 μL BCECF-AM loaded U937 cells were added to each well. Fluorescence was measured at 439 nm excitation to determine the

maximum signal for each well. After 30 min of incubation at 37°C, 3 washes were performed to remove non-adherent cells. Fluorescence was measured a second time as described above. Adhesion was determined for each well as a percentage relative to the maximum fluorescence detected prior to washing. All assays were performed in triplicate.

3.2.7. Statistical Analysis

Values are expressed as mean±SE. Statistical analysis was performed using an unpaired Student's *t* test or ANOVA. When significance was attained using ANOVA, a Tukey's post hoc test was used to determine specific differences. Significance was defined as $p<0.05$.

3.3 Results

3.3.1 *ER stress causes increased GRP78 expression on the surface of endothelial cells.*

Previous reports have shown induction of ER stress is sufficient to cause increased cell surface localization of GRP78 in cancer cell lines (92, 137). Consistent with these findings, primary human aortic endothelial cells (HAECs) treated with 300 nM thapsigargin (Tg) or 2.5 μg/ml tunicamycin (Tm) for 16, 24, or 32 hours expressed increased levels of GRP78 in surface fractions (s-GRP78). This increase was highest at 24 hours post induction of ER stress (Fig. 9A-B). To investigate whether more physiologically relevant factors known to induce ER

stress and contribute to atherogenisis could also stimulate surface GRP78 expression in endothelial cells, HAECs were exposed to lipid oxidation products 7-ketocholesterol and 4-HNE, as well as known inducers of oxidative stress: Sin-1 and peroxynitrite. Increased surface GRP78 expression was also observed under all of these conditions (Fig. 9C).

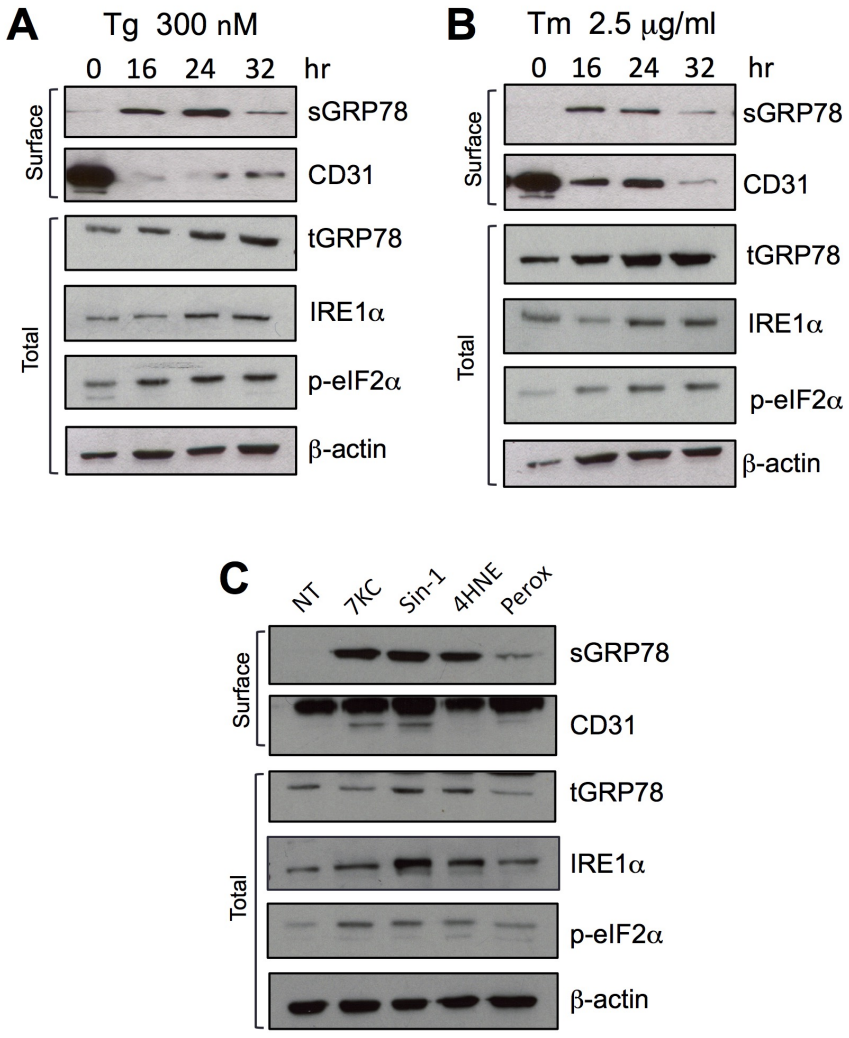

Figure 9. ER stress causes increased GRP78 expression on the surface of endothelial cells. Human aortic endothelial cells were treated with *(A)* 300 nM thapsigargin (Tg) and (*B*) 2.5 μg/mL tunicamycin (Tm) for the indicated time, or with *(C)* 7-ketocholesterol (7KC), Sin-1, 4-hydroxynonenal (4HNE), and peroxynitrite (Peroxy) for 8 hours after which surface proteins were biotinylated and separated from total cell lysates by streptavidin pulldown. Total cell lysates (t-) and surface protein fractions (s-) were subjected to western blot for detection of the indicated proteins.

As an alternative method to inducing ER stress for stimulating cell-surface GRP78 expression, experiments were performed using GRP78 containing plasmids and GRP78 encoding adenoviral particles to increase expression of GRP78. HAECs were transfected with a pcDNA plasmid containing full length GRP78 (pcDNA-GRP) and a GRP78 mutant replacing the KDEL sequence on the C-terminus with a FLAG tag (pcDNA-ΔKDEL-FLAG). Optimization experiments showed transfection ratios 2:1 and 3:1 of the transfection reagent to plasmid DNA were optimal for pcDNA-GRP78 and pcDNA- ΔKDEL-FLAG respectively (Fig. 10A). These conditions were then used along with a 2:1 treatment of the empty control pcDNA vector to examine whether there was an increase in levels of cell-surface GRP78. pcDNA-GRP78 but not the KDEL null vector showed an increase in surface GRP78 levels (Fig. 10B). An obvious caveat is the increased level of surface GRP78 observed in the control transfected cells. This is likely due to cellular and ER stresses caused by the transfection process itself(138), which we have shown is sufficient to induce surface GRP78 expression.

Adenovirus encoding GRP78 was also used as a strategy to increase surface GRP78 expression. Initial optimization experiments treating HUVECs with 1-10 MOI of AdGRP78 or control virus (AdDL) showed no apparent increase in total GRP78 levels and were markedly lower than levels achieved when cells are treated with Tg (Fig. 10C). However, a higher adenoviral load would have likely stressed the cells which lead us to rely on established chemical ER stress

inducers in further experiments which we and others have shown stimulate surface GRP78 expression(92, 139).

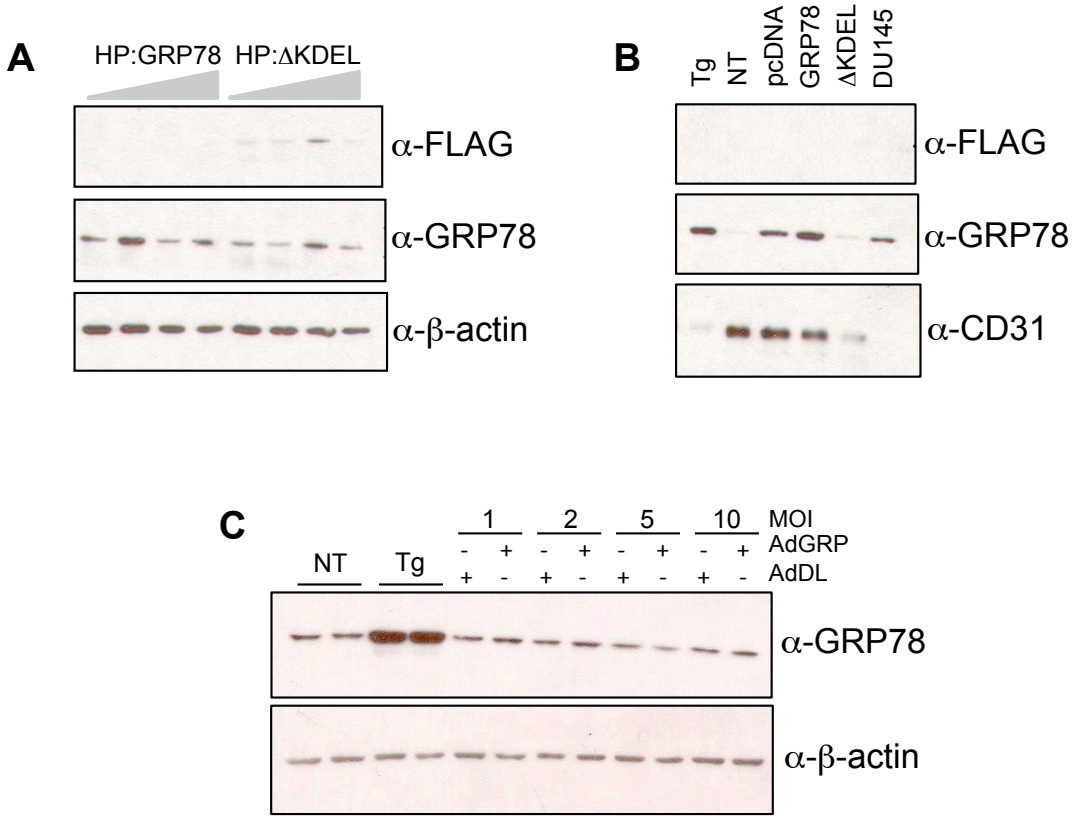

Figure 10. Optimization of GRP78 over-expression in endothelial cells. *(A)* Human aortic endothelial cells (HAECs) were transfected with pcDNA-GRP78 or pcDNA-ΔKDEL-FLAG at increasing ratios of transfection reagent to DNA for 48 hrs. Total cell lysates were subjected to western blot for detection of GRP78 and FLAG. *(B)* HAECs were treated/transfected with the indicated reagent/plasmid for 48 hrs after which surface proteins were biotinylated and separated from total cell lysates by streptavidin pulldown. Surface protein fractions were subjected to western blot for detection of GRP78, the endothelial cell surface marker CD31, and FLAG. Surface proteins isolated from DU145 prostate cancer cells were used as a positive control for the presence of GRP78. *(C)* HAECs (lane 1) or HUVECs (lanes 2-12) were treated for 24 hrs with AdGRP78 or the empty control virus AdDL. Total cell lysates were subjected to western blot for detection of GRP78 and β-actin as a loading control.

3.3.2 *Anti-GRP78 autoantibodies increase adhesion molecule expression and induce leukocyte adhesion.*

GRP78a-Abs have been shown to interact with cell surface GRP78 in cancer cell lines. To investigate the impact of GRP78a-Abs on endothelial cells, HAECs pretreated with Tg or Tm for 24 hours to induce surface GRP78 expression were subsequently exposed to GRP78a-Abs isolated from human cancer patients. Preliminary experiments showed treatment with GRP78a-Abs after Tg or Tm treatment resulted in higher levels of mRNA expression of adhesion molecules *ICAM-1* and *VCAM-1*, which peaked at 8 hrs (Fig. 11A-D). Further experiments demonstrated a significant increase in *ICAM-1* and *VCAM-1* expression compared to Tg or Tm alone and IgG controls (Fig. 11E-H). Importantly, treatment of cells with GRP78a-Abs in the absence of ER stress did not significantly increase *ICAM-1* or *VCAM-1* levels (Fig. 11E-F), indicating the presence of cell surface GRP78 is required for the observed GRP78a-Abs mediated effects on adhesion molecule expression. However, the small peptide WIFPWIQL (WIF), previously shown to interact with surface GRP78(140), did not induce *ICAM-1* or *VCAM-1* expression in cells treated with Tg (Fig. 11E-F), suggesting that adhesion molecule signaling mediated by surface GRP78 in these cells is specific to its interaction with GRP78a-Abs. Moreover, incubation of GRP78a-Abs with the peptide CNVSKDSC (CP), previously shown to block GRP78a-Ab mediated signaling(86), significantly reduced induction of *ICAM-1* and *VCAM-1* expression in Tm treated cells (Fig. 11G-H), again supporting that

the specific interaction with GRP78a-Abs is necessary for cell surface GRP78 mediated induction of adhesion molecule expression in these cells.

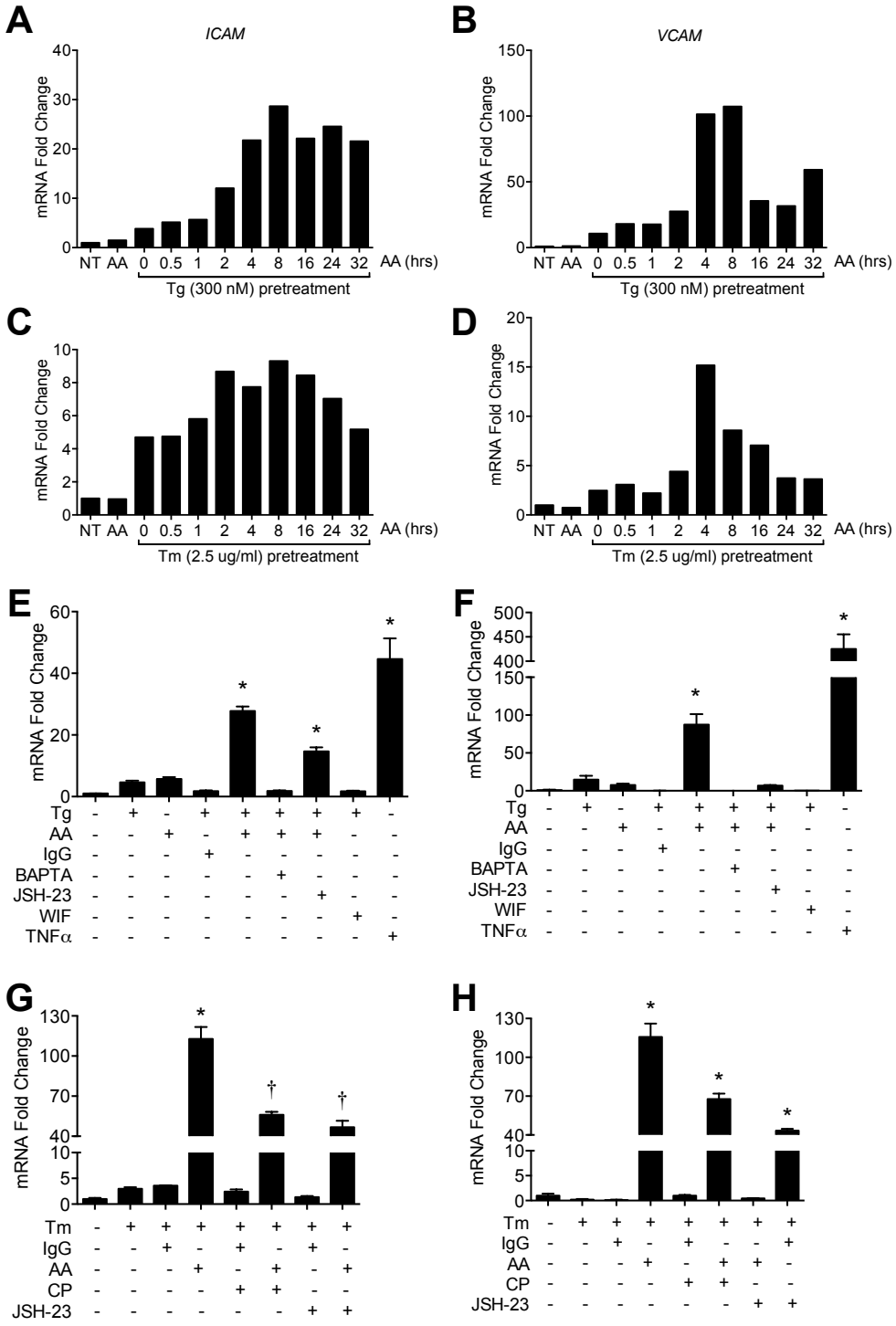

Figure 11. GRP78a-Abs induce adhesion molecule expression in endothelial cells. mRNA levels of *(A,C,E,G) ICAM-1* and *(B,D,F,H*) *VCAM-1* analyzed with quantitative RT-PCR. Total RNA was isolated from HAECs pre-treated without or with (*A-B)* 300 nM thapsigargin (Tg) or *(C-D)* 2.5 μg/mL tunicamycin (Tm) for 24 hrs

followed by purified GRP78a-Abs (AA, 60 μg/mL) for the indicated times. HAECs pre-treated without or with (*E-F)* 300 nM thapsigargin (Tg) or *(G-H)* 2.5 μg/mL tunicamycin (Tm) for 24 hrs followed by purified GRP78a-Abs (AA, 60 μg/mL) or human IgG (60 μg/ml) for 8 hrs combined with the indicated treatments. Data is expressed as fold change relative to untreated cells. **p*<0.05 *versus* all other groups. †*p*<0.05 *versus* all other groups.

3.3.3 *Anti-GRP78 autoantibodies promote proinflammatory gene expression and adhesion molecule expression via the NFκB pathway.*

Adhesion molecule expression has been shown to be regulated by the NFκB signaling pathway(141). To investigate whether the observed GRP78a-Abs mediated cellular responses are regulated by NFκB signaling, expression levels of a panel of cytokines and chemokines known to be regulated by NFκB were measured by NanoString analysis in GRP78a-Abs or IgG stimulated ECs expressing surface GRP78. mRNA levels of cytokines IL-6 and IL-1b, as well as chemokines MCP-1, MIP-1a, and IP-10 were significantly higher in GRP78a-Abs treated cells than in IgG treated cells (Fig. 12A). This suggests that the engagement of GRP78a-Abs with surface GRP78 signals through the NFκB pathway. Importantly, GRP78a-Abs did not increase expression of ER stress signaling/UPR activation markers (Fig. 12B), indicating changes in gene expression are due to signaling through surface GRP78 and not a side effect of additional cellular stresses.

To confirm whether NFκB plays a role in GRP78a-Abs mediated signaling, ECs expressing surface GRP78 were pretreated with an NFκB Activation

Inhibitor (JSH-23) for 2 hours followed by GRP78a-Abs or human IgG. NFκB inhibition significantly reduced GRP78a-Abs mediated induction of *ICAM-1* and *VCAM-1* expression in Tm treated cells (Fig. 11G-H).

Expression of adhesion molecules on endothelial cells is critical for recruitment of monocytes into atherosclerotic lesions(142, 143). However, mRNA expression of these molecules is not proof that adhesion is occurring. Therefore, we examined whether the observed increase of *ICAM-1* and *VCAM-1* expression with GRP78a-Abs induced adhesion of human monocytic cells (U937) to ECs. Treatment of ECs with Tm followed by GRP78a-Abs had significantly increased numbers of attached U937 cells compared to IgG controls (Fig. 12C). Consistent with effects seen on adhesion molecule expression, inhibiting GRP78a-Abs with the CNVSKDSC peptide (CP) reduced U937 attachment. Moreover, treatment with the NFκB inhibitor (JSH-23) reduced monocyte adhesion in GRP78a-Abs stimulated ECs (Fig. 12C), further supporting that GRP78a-Ab mediated surface GRP78 signaling acts through the NFκB pathway in these cells.

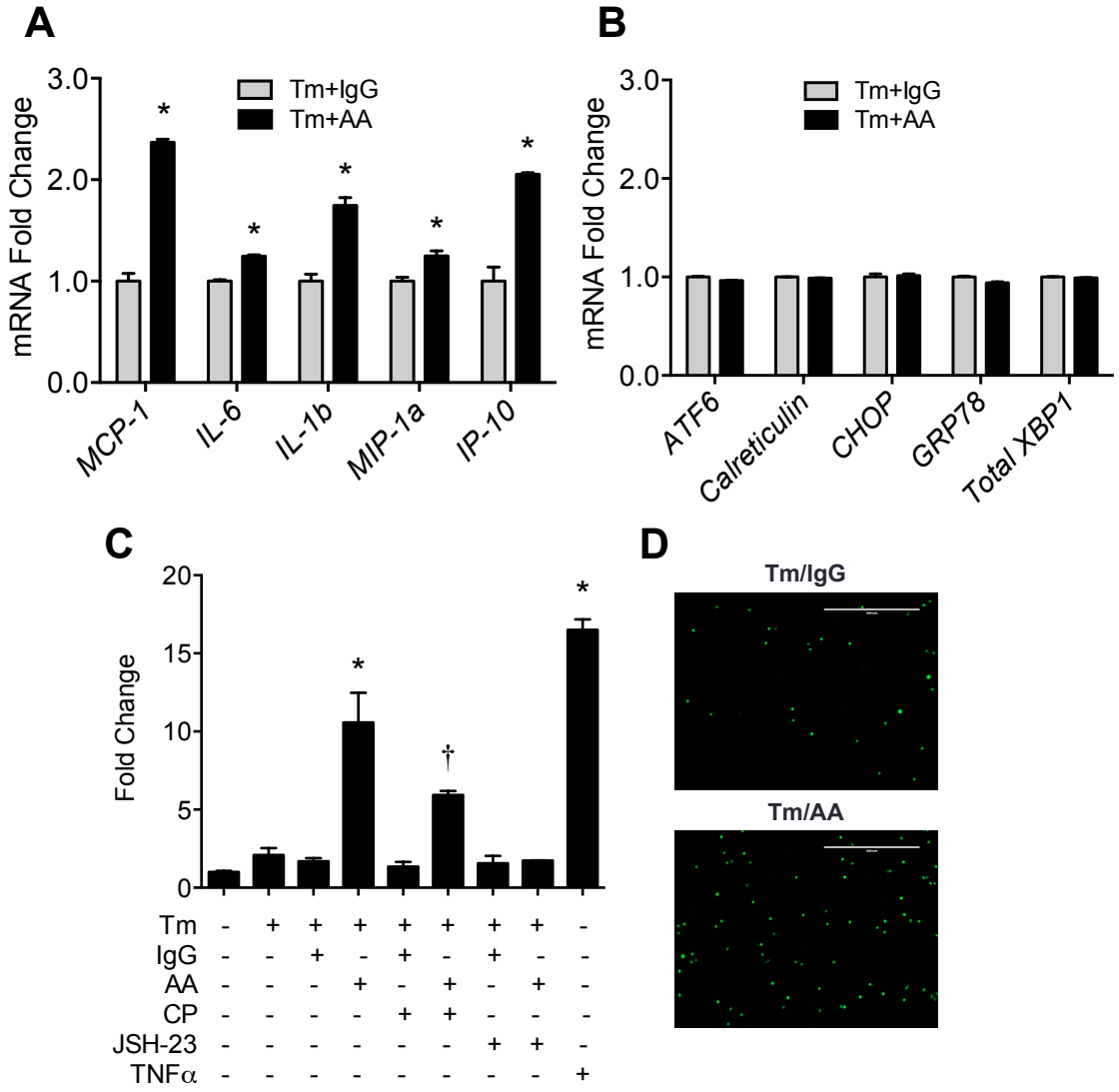

Figure 12. GRP78a-Ab stimulated endothelial cell activation occurs via the NFκB pathway. (*A*) Relative mRNA levels of cytokines and chemokines determined by NanoString analysis of HAECs treated with 2.5μg/mL tunicamycin (Tm, 24hrs) followed by GRP78a-Abs (AA, 60 μg/mL) or human IgG (IgG, 60 μg/mL) for 8 hrs. Data is expressed as fold change relative to tunicamycin with IgG treated cells. **p*<0.05 *versus* Tm+IgG. *(C)* Adhesion of BCECF-AM loaded U937 cells to HAECs treated with 2.5μg/mL tunicamycin (Tm, 24hrs) followed without or with NFκB Activation Inhibitor II (JSH-23, 30nM) for 2hrs. Cells were then exposed to purified GRP78a-Abs (AA, 60 μg/mL) or human IgG (60 μg/ml) for 8 hrs without or with the CNVSKDSC peptide (90 μg/mL). TNFα (100 ng/mL, 8hrs) served as a positive control for adhesion. Data is expressed as percent adhesion relative to untreated cells. **p*<0.05 *versus* all other groups. †*p*<0.05 *versus* all other groups. *(D)*

Representative fluorescent images show adhesion of BCECF-AM loaded U937 cells to HAECs.

3.4 Discussion

Cell surface biotinylation was used to demonstrate the expression of GRP78 on the surface of endothelial cells under conditions of ER stress. This finding is consistent with previous reports that thapsigargin and tunicamycin induced ER stress causes relocalization of GRP78 from the ER lumen to the cell surface in cancer cell lines(137). We have shown previously that markers of ER stress, including GRP78, are upregulated at all stages of atherogenesis in mice(32). Here, we additionally show stimulation of ECs with 7-ketocholesterol, Sin-1, 4HNE, and Peroxynitrite, atherogenic mediators of ER stress in endothelial cells(100, 144), induces surface GRP78 expression.

Although GRP78 has been found on the surface of many cell types, the precise cellular events that allow the evasion of ER retrieval mechanisms and subsequent translocation to the plasma membrane are not well understood. GRP78 contains a C-terminal Lys-Asp-Glu-Leu (KDEL) sequence that is recognized by the KDEL receptor, resulting in selective retrograde transport to the ER (145, 146). One possible explanation is that the retrieval function of the KDEL receptor is compromised as a result of saturation in response to ER stress, allowing proteins containing the KDEL sequence to escape to the cell surface (147, 148). While it was proposed that overexpression of GRP78 lacking a KDEL

sequence would escape the ER retention mechanism, making it available to travel to the cell surface possibly resulting in increased surface GRP78 levels, the lack of surface GRP78 suggests that the sudden increase in production of a KDEL null GRP78 might result in shedding of GRP78 into the media. Similarly, Zhang and colleagues showed expression of GRP78 lacking a KDEL domain or with a small peptide adjacent to the KDEL motif lead to secretion of the protein, suggesting that the KDEL sequence might be required for retention of GRP78 in the cell membrane(92). A clear drawback in the experiments described here was the increased level of surface GRP78 expressed even in control transfected cells. This is likely due to stress induced in cells as a result of the transfection process. Taken together, these findings suggest ER stress contributes to the observed expression of GRP78 on the surface of endothelial cells in atherosclerotic lesions.

GRP78 is classically known as a molecular chaperone involved in protein folding in the ER, however surface GRP78 has been shown to act as a signaling receptor in cancer cells and proliferating endothelial cells(80, 84). Here we demonstrate that GRP78a-Ab activation of surface GRP78 stimulates expression of adhesion molecules ICAM-1 and VCAM-1, as well as cause increased adhesion of monocytic cells to endothelial cells. Additionally, these effects can be reduced by blocking GRP78a-Abs with the peptide CNVSKDSC. Expression of adhesion molecules as well as binding and transmigration of leukocytes into tissue are known to occur during the initial steps of atherosclerotic lesion development, and are considered hallmarks of endothelial cells activation(149).

This suggests GRP78a-Abs contribute to endothelial cell activation and play a role during early events of lesion development.

There is strong evidence suggesting the role of the NFκB signaling pathway in the pathogenesis of atherosclerosis(149). NFκB has been shown to regulate expression of adhesion molecules in ECs, therefore we investigated whether surface GRP78 induction of adhesion molecule expression involved activation of the NFκB pathway. Expression of cytokines and chemokines by the endothelium occurs during endothelial cell activation and has also shown to be regulated by NFκB (149). We observed increased expression of known proinflammatory mediators in cells activated by GRP78a-Abs, further supporting a potential role of NFκB in GRP78a-Ab activated surface GRP78 signaling. Importantly, inhibition of NFκB impaired GRP78a-Ab mediated adhesion molecule expression. NFκB inhibition also suppressed GRP78a-Ab induced leukocyte adhesion.

Further work will need to identify the precise upstream molecular signals that connect NFκB activation to GRP78a-Ab stimulated surface GRP78 receptor signaling in endothelial cells. Some potential pathways are discussed here, however their relevance in endothelial cells remains to be established. Previous findings demonstrated cell surface GRP78 coupled to the G-protein-11 (G-α,B,γ-11) complex in α_2M*-stimulated macrophages(150). It is known that activation of the heterotrimeric G-protein Gαq leads to protein kinase C (PKC) activation,

which in turn results in canonical IKK/NFκB activation in ECs (151, 152). Additionally, work from our group has demonstrated the ability of GRP78a-Abs to activate surface GRP78 in bladder carcinoma cells, resulting in PLC-mediated release of calcium from ER stores(86). Although not completely understood, it is thought that an increase in cytosolic calcium can activate NFκB, possibly through production of mitochondrial ROS generation(153, 154). Finally, recent studies utilizing therapeutically resistant cancer cells showed surface GRP78 complexes with PI3K as well as the ability of GRP78a-Abs to induce surface GRP78 driven PI3K-dependent activation of AKT(94, 137). In endothelial cells, NFκB activation is known to be mediated by PI3K/AKT in response to TNFα stimulation(155).

Chapter 4 – Investigating the Association of Cardiovascular Risk Factors and Anti-GRP78 Autoantibodies in Humans

4.1 Introduction

We have reported that GRP78a-Abs are elevated in atherosclerosis prone ApoE$^{-/-}$ mice, however it is unknown whether GRP78a-Ab levels are elevated in humans with carotid atherosclerosis. It is also unclear whether known risk factors for cardiovascular disease (CVD) influences GRP78a-Ab levels in humans. To investigate the relationship between GRP78a-Abs and CVD, we assessed GRP78a-Abs levels in human plasma samples from three clinical studies spearheaded by researchers at McMaster University: the SHARE, NIATH, and FIN-CAN studies. Below is a brief description and summary of the major findings thus far from each study.

4.1.1 SHARE Study

The Study of Health Assessment and Risk in Ethnic groups (SHARE) was a population-based study to assess cardiovascular disease risk factors in three ethic groups in Canada: Chinese, South Asians, and Europeans(156). The study, lead by Dr. Sonia Anand at McMaster University, sought to examine why rates of cardiovascular disease differed between ethnic groups, having been previously shown to be highest in South Asian Canadians, intermediate in Canadians of European descent, and lowest in Chinese Canadians(157). Participants between 35 and 75 years old were evaluated for cardiovascular disease, subclinical

atherosclerosis, and associated risk factors including levels of circulating cholesterol, triglycerides, glucose, and homocysteine levels. Participants were stratified into two groups as individuals with CVD or without CVD. CVD was defined as participants with: coronary artery disease, defined as angina using the Rose questionnaire; self-reported myocardial infarction; silent myocardial infarction; coronary artery bypass surgery or angioplasty; or stroke, either self-reported or confirmed by a physician(156).

The major findings of the SHARE study included the observation that being of South Asian ethnicity itself was a strong, independent determinant of CVD, although the reasons for this effect are not well understood, and previous conclusions based on European population studies should not be directly applied to other ethnic groups(156). South Asians showed more irregularities in blood lipid, glucose, and homocysteine levels, however Europeans had the highest amount of carotid atherosclerosis(156). It was suggested therefore, that while the South Asians might have smaller atherosclerotic plaques, the higher irregularities in blood lipid and glucose levels might contribute to decreased stability of lesions, resulting in the previously observed higher prevalence of cardiovascular events(156, 157). We sought to investigate whether adults with greater CVD risk using established clinical markers from this study had higher GRP78a-Ab levels.

4.1.2 NIATH Study

The Non-invasive Assessment of Atherosclerosis (NIATH) study was based out of the Pediatric Lipid Clinic at McMaster Children's Hospital and lead by Dr. Katherine Morrison. The intimal medial thickness (IMT) of the carotid artery, measured by carotid B-mode ultrasonography, is a widely accepted and validated surrogate marker of carotid atherosclerosis in adults and is considered a predictor of coronary atherosclerosis(158-160). The aim of the NIATH study was to examine the age at which IMT could reliably predict vascular changes and whether cardiovascular risk factors influence IMT in children(161). Children 5-16 years old were recruited into one of three groups: overweight, elevated LDL-cholesterol (hyperlipidemia), or healthy controls. The overweight and hyperlipidemia groups were determined by a BMI in the 85th centile or higher and fasting LDL-cholesterol levels in the 95th centile or higher respectively. Participants were assessed for family history of coronary heart disease, pubertal stage, fasting blood glucose, insulin, circulating cholesterol and triglycerides, blood pressure, and IMT.

The NIATH study reported that the hyperlipidemia group had increased IMT and that lipid profiles predicted IMT in this group(161). Interestingly, there was no difference in IMT between overweight and control children, regardless of multiple cardiovascular risk factors in the overweight group. Age was reported as the strongest determinant of IMT, although the exact reason for this effect could

not be determined. The authors proposed potential reasons that contributed to the observed effect could include pubertal development, worsening of cardiovascular risk factors with age, or cumulative time of exposure to risk factors(161). Overall, IMT was determined to be a valid, non-invasive surrogate measure of atherosclerosis in children with altered lipid profiles, particularly in children over 10 years of age(161). Given the greater carotid IMT levels in the hyperlipidemic group, we sought to test whether this group had greater circulating GRP78a-Ab levels. Further, this cohort allows us to investigate GRP78a-Abs in a pediatric group, whereas previous clinical assessments of autoantibodies have been limited to adult populations.

4.1.3 FIN-CAN Study

The FIN-CAN project has been an ongoing collaboration between pediatric researchers at McMaster University and Eero Kajantie's group at the University of Helsinki in Finland. This project, lead by Dr. Saroj Saigal, was initiated as one of the first population-based studies following cohorts of extremely low birth weight (ELBW) children from infancy to adulthood. Infants born weighing 500-1000 gm and full term controls were recruited into the study from 1977 to 1982(162). This cohort has been followed through their entire lives and are now in their early thirties. Most of the findings from the study during their childhood and adolescent years were focused on cognitive and psychological outcomes, however it was reported that more ELBW children had deficits in

areas of mobility, self-care, and the ability to see, hear and speak at eight years of age compared to control references(163-166). Additionally, Dr. Katherine Morrison's research team at McMaster University is currently analyzing a thirty-year follow up assessment of these participants. Preliminary data indicate the ELBW group are shorter, have increased percent body fat, higher rates of dysglycemia, higher blood pressure, and generally having a higher predisposition to cardiometabolic disorders compared to their normal birth weight (NBW) counterparts (data not published). Thus, the ELBW cohort represents a population with potentially early developmental adversity that could accelerate athlerosclerotic lesion development and we hypothesized that these individuals may also have elevated GRP78a-Ab levels.

4.1.4 Objective

GRP78a-Abs have been identified in patients with a variety of cancers, and high circulating levels correlate with accelerated cancer progression and reduced survival(93), however whether GRP78a-Abs are associated with CVD in humans is unknown. The objective of this work was to investigate the significance of GRP78a-Abs in humans. These studies allowed us to clarify the relationship between circulating autoantibodies and CVD across three distinct clinical populations at risk for atherosclerosis: adults with known CVD risk factors (SHARE), high circulating lipids in children (NIATH), and early developmental adversity in premature born adults (FIN-CAN).

4.2 Materials & Methods

4.2.1 Subject Samples

Serum samples from study subjects were generously provided from the SHARE study by Dr. Sonia Anand and from the NIATH and FIN-CAN studies by Dr. Katherine Morrison.

4.2.2 Analysis of Anti-GRP78 Autoantibody Titers in Human Serum

Antibodies against GRP78 in human serum were analyzed utilizing an in-house ELISA originally described by Gonzalez-Gronow M. and colleagues(94). The CNVSKDSC peptide was conjugated to keyhole limpet hemocyanin (KLH) using a Sulfo-SMCC linker. KLH (Sigma Aldrich; Cat# H7017) and Sulfo-SMCC (Sigma Aldrich; Cat# M6035) were each dissolved to 10 mg/mL in activation buffer (0.1M $NaHCO_3$, 0.9M NaCl, ph 8.0), after which 100 μL Sulfo-SMCC solution was added to each 1 mL of KLH solution and incubated for one hour at room temperature. Excess Sulfo-SMCC was removed by size exclusion chromatography on a pre-packed PD-10 Sephadex G25-M (GE Healthcare Lifesciences) column equilibrated with conjugation buffer (0.1M $NaHCO_3$, 0.9M NaCl, 0.1M EDTA, ph 8.0). KLH-Sulfo-SMCC was eluted in conjugation buffer by collecting 0.25 mL fractions. Elution fractions containing KLH-Sulfo-SMCC were determined with the DC Protein Assay (Bio-Rad Laboratories) and pooled. The CNVSKDSC peptide was dissolved to 10 mg/mL in conjugation buffer, mixed

with the KLH-Sulfo-SMCC solution at an equivalent mass ratio (1 mg peptide per 1 mg KLH-Sulfo-SMCC) and incubated for two hours at room temperature. 96-well plates were coated with the CNVSKDSC-KLH conjugate (5 μg/mL) diluted in coating buffer (0.1M $NaHCO_3$, 0.5M NaCl, pH 9.6), washed with PBST (1x PBS; 0.1% Tween-20), and blocked with coating buffer containing normal goat serum (R&D Systems) at a 1:20 dilution for 1 hour at 37°C. After washing plates two times with PBST, 50 μL per well of samples diluted 1:500 in PBST were added in triplicate and incubated overnight at room temperature. Following three washes with PBST, 100 μL biotinylated goat anti-human IgG (Vector Laboratories) diluted 1:500 in PBST was added per well and incubated 1-2 hours at room temperature. Plates were washed three times with PBST and incubated with 100 μL per well streptavidin conjugated to horseradish peroxidase (R&D Systems) diluted 1:200 in PBST for 30 min at room temperature while covered. Following three washes with PBST, plates were developed with 200 μL per well of prepared TMB solution (Sigma Aldrich) for 15 minutes, after which the reaction was stopped with 50 μL per well Stop Solution (R&D Systems). Absorbance was read at 450 nm and background signal from wells without sample added was subtracted. All assays were performed in triplicate and the data expressed relative to a common sample used on every plate to control for plate-to-plate variation.

4.2.3 Statistical Analysis

Data represent the mean ± SD when normally distributed. Categorical variables are described as number (%). Data was analyzed for normality using a D'Agostino-Pearson omnibus normality test. When data were not normally distributed, data was log-transformed. If the transformed data then did not meet criteria for normality, non-parametric statistical analyses were used. Statistical analysis of GRP78a-Ab levels were performed using an unpaired *t*-test when normally distributed and a Mann-Whitney non-parametric rank test when non-normally distributed. Significance was defined as $p<0.05$. Multiple comparisons were performed using a one-way ANOVA for normally distributed variables and a Kruskal Wallis non-parametric difference test for non-normally distributed variables. In the FINCAN and NIATH studies, the determinants of GRP78a-Abs were first assessed with univariate analysis (Pearson or Spearman regression as per conditions of normality). Further multivariate regression analysis was performed for GRP78a-Abs including all variables that were determined to be of interest ($p<0.10$) in the univariate analysis. Significance was defined as $p<0.05$.

4.3 Results

4.3.1 *SHARE Study: Anti-GRP78 autoantibody titres in serum from adult participants with cardiovascular disease*

To determine whether levels of GRP78a-Abs were altered in patients with CVD, we analyzed a subset of SHARE study blood samples from participants

with defined CVD and without CVD matched for age, gender, and ethnicity. Baseline participant characteristics are outlined in Table 2. Serum GRP78a-Ab levels were assessed by enzyme-linked immunosorbent assay. No significant difference in GRP78a-Ab titre levels was observed between participants with CVD and those without CVD (Fig. 13A).

Table 2. SHARE Study
Characteristics of the study population, by group.

	Control (n = 68)	CVD (n = 69)
Age (years)	60.9 (9.3)	60.7 (9.2)
Male	34 (50.0)	32 (46.4)
Diabetes	25 (36.8)	8 (11.6)
Hypertension	28 (41.2)	13 (18.8)
Impaired GT	8 (11.7)	11 (15.9)
High Cholesterol	23 (33.8)	5 (7.2)
Elevated LDL-cholesterol	44 (64.7)	36 (52.2)
Low HDL-cholesterol	23 (33.8)	14 (20.3)
Smoking	10 (14.7)	17 (24.6)

Values are mean ± SD or n (%). LDL = low-density lipoprotein; HDL = high-density lipoprotein; GT = glucose tolerance.

It is not known how risk factors for CVD impact GRP78a-Abs levels. To reduce the effect of these confounding factors on our analysis, all participants with diabetes, impaired glucose tolerance, high blood pressure, high cholesterol, high LDL levels, or that habitually smoked tobacco were excluded from the control group sample set. The remaining samples were matched for age, gender, and ethnicity to samples from the CVD group. Although not statistically significant, there was a tendancy toward increased GRP78a-Abs in the CVD group (p=0.074, Fig. 13B). There were also no differences in titers observed

when samples from each group were compared based on the total number of risk factors reported for each participant (Fig. 13C-D). The control and CVD groups were also compared after separation by gender, however no differences were seen between men or women with and without CVD respectively (Fig. 13E-F). While these data suggest that middle-aged adults with CVD tend to have higher GRP78a-Ab levels compared to healthy controls, the data is not conclusive as to how common risk factors for CVD might influence GRP78a-Abs. Further work involving circulating GRP78a-Ab levels should be performed in a larger sample set to minimize the effects of confounding variables related to CVD.

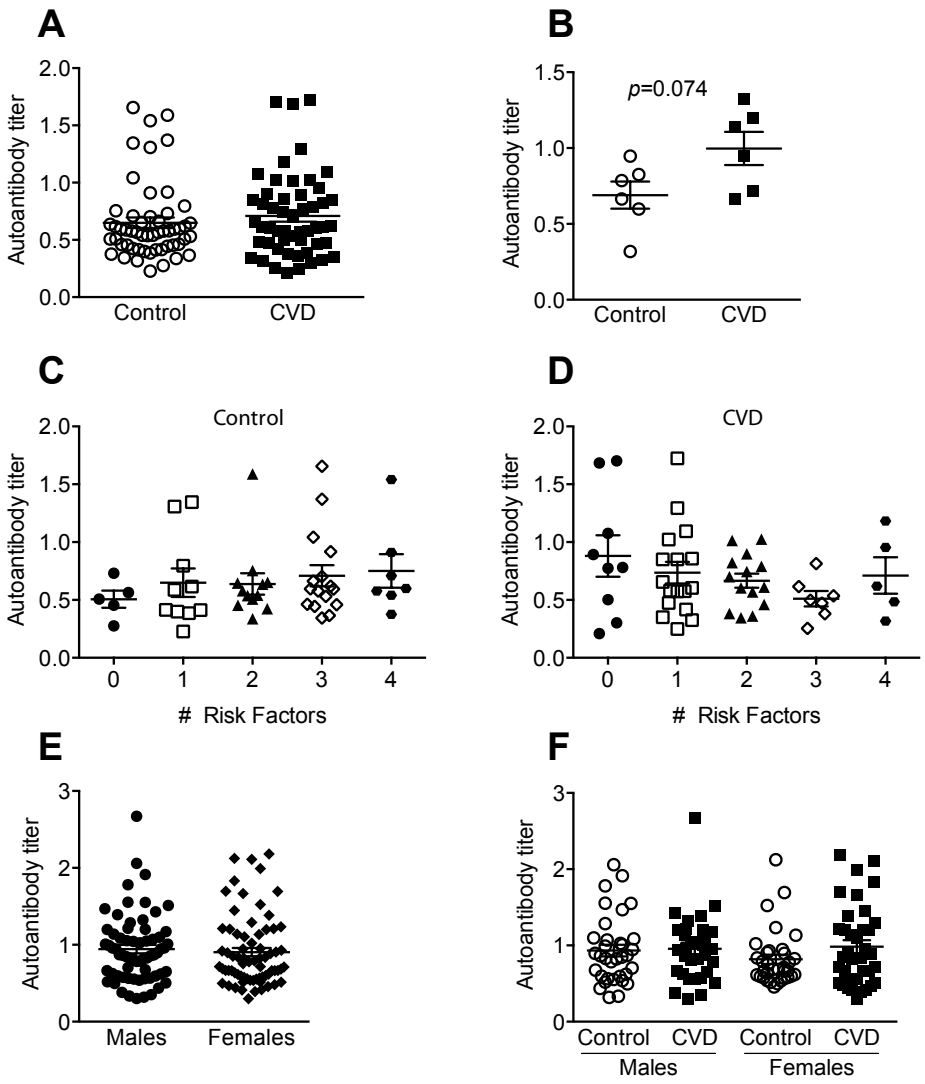

Figure 13. GRP78a-Ab titers from participants in the SHARE study. Levels of GRP78a-Abs were measured by ELISA from *(A)* age, gender, and ethnicity matched participants with defined cardiovascular disease (CVD) or without (Control). *(B)* Control participants with no risk factors for cardiovascular disease matched for age, gender, and ethnicity to participants with CVD (n=6 per group). *S*amples from the *(C)* control and *(D)* CVD groups were divided based on the number of risk factors for cardiovascular disease each participant displayed. Samples were divided by gender into males and females *(E)* from the entire cohort or *(F)* by group. Data is expressed as absorbance values at 450nm relative to a common sample.

4.3.2 *NIATH Study: Anti-GRP78 autoantibody titres in serum from hyperlipidemic or overweight children*

To examine GRP78a-Ab levels in children, serum from overweight, hyperlipidemic, or healthy control children 5-16 years of age were analyzed for GRP78a-Abs by enzyme-linked immunosorbent assay. Baseline participant characteristics are outlined in Table 3. GRP78a-Ab titre levels were significantly higher in the hyperlipidemic group compared to the overweight group, however neither were statistically different from the control group (Fig. 14). Similar findings were seen in results adjusted for age. Covariate analysis performed adjusting for age and body fat showed no differences between groups, suggesting the difference in GRP78a-Ab levels between the hyperlipidemic and overweight groups is due to the difference in body fat between the groups.

Table 3. NIATH Study
Characteristics of the study population, by group.

	Control (n = 38)	Hyperlipidemia (n = 39)	Overweight (n = 36)
Male n (%)	20 (52.6)	20 (51.3)	23 (63.8)
Age (years)	11.5 (2.7)	11.9 (3.1)	10.3 (2.5)
% Body Fat	19.7 (8.9)	22.6 (3.8)	38.9 (6.5)
BMI-Z	0.08 (1.2)	0.48 (1.1)	2.3 (0.4)
Systolic BP (mmHg)	100 (9.1)	101 (6.8)	110 (11.3)
Diastolic BP (mmHg)	64 (6.5)	65 (7.02)	66 (7.5)
Total Cholesterol (mmol/L)	4.0 (0.6)	6.6 (1.4)	4.5 (0.9)
LDL-cholesterol (mmol/L)	2.05 (0.5)	4.6 (1.4)	2.6 (0.8)
HDL-cholesterol (mmol/L)	1.5 (0.3)	1.4 (0.3)	1.3 (0.3)
Triglyceride (mmol/L)	0.87 (0.51)	1.27 (0.71)	1.36 (0.97)
Glucose (mmol/L)	4.7 (0.35)	4.8 (0.44)	4.7 (0.34)
Average maximum IMT (mm)	0.386 (0.027)	0.399 (0.039)	0.392 (0.034)
Average mean IMT (mm)	0.385 (0.026)	0.398 (0.039)	0.391 (0.033)

Values are mean ± SD or n (%). BP = blood pressure; LDL = low-density lipoprotein; HDL = high-density lipoprotein.

The main predictors of GRP78a-Ab levels were examined using univariate and multivariate regression analysis of the entire cohort. GRP78a-Ab levels inversely correlated with body fat, BMI-Z score, waist/height ratio, and systolic blood pressure in univariate analysis (Table 4). There was no relationship between GRP78a-Abs and carotid IMT, blood lipids, or fasting glucose levels. However, the multivariate linear regression model showed body fat was a predictor of GRP78a-Ab levels (Table 5). The model explained 13.5% of the variability in GRP78a-Abs. These data suggest that greater body fat in children may reduce GRP78a-Abs.

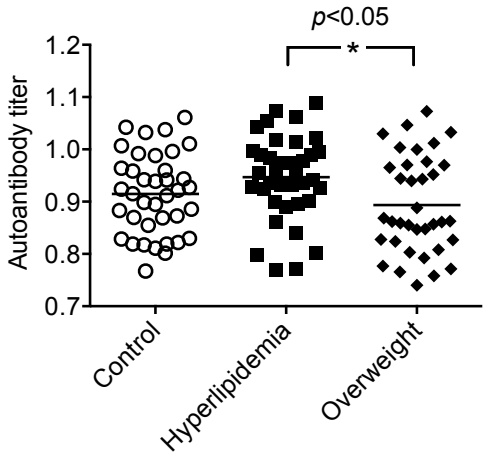

Figure 14. GRP78a-Ab titers from participants in the NIATH study. Levels of GRP78a-Abs were measured by ELISA from healthy control, hyperlipidemic, or overweight children 5-16 years of age. Data is expressed as absorbance values at 450nm relative to a common sample. *Indicates a significant difference (p<0.05) from the indicated group.

Table 4. NIATH Study
Univariate regression analysis of GRP78a-Ab.

Variable	GRP78a-Ab	
	R^2	*p*
BMI-Z	-0.329	0.002
Waist-Z	-0.356	0.0001
Total Cholesterol	0.123	0.22
LDL-cholesterol	0.141	0.16
HDL-cholesterol	0.007	0.95
Triglyceride	-0.076	0.46
Fasting GL	0.002	0.98
Systolic BP	-0.189	0.062
Diastolic BP	-0.080	0.43
Average Max IMT	-0.001	0.989
Average Mean IMT	-0.003	0.975

Table 5. NIATH Study
Determinants of GRP78a-Ab in multivariate analysis.

Dependent Variable	Independent variables	$\beta \pm$ SE	*p*
R^2 – 0.13			
GRP78a-Ab	Age	0.092 ± 0.002	0.401
	Gender	-0.118 ± 0.009	0.277
	Group	0.180 ± 0.005	0.229
	% Body Fat	-0.375 ± 0.001	0.017
	Systolic BP	-0.098 ± 0.0001	0.373

4.3.3 *FIN-CAN Study: Anti-GRP78 autoantibody titres in serum from individuals born at extremely low birth weight*

Premature birth with low birth weight predisposes individuals to dysglycemia, hypertension and obesity in adulthood. To examine whether GRP78a-Ab levels are affected by prematurity and birth weight, GRP78a-Abs were analyzed in serum from individuals born premature with extremely low birth weight (ELBW) and compared to term, normal birth weight (NBW) subjects. The samples were acquired from adults in their early 30s. Baseline participant characteristics are outlined in Table 6. In contrast to our hypothesis that prematurity would enhance levels of GRP78a-Abs and thus be related to the enhanced CVD risk typically seen in this population, GRP78a-Ab levels were significantly lower in the ELBW group than in the NBW comparison group (Fig. 15A). Additionally, GRP78a-Ab levels were significantly higher in females than in males in the entire cohort (Fig. 15B). These data suggest that prematurity is associated with reduced circulating GRP78a-Abs.

Table 6. FIN-CAN Study
Characteristics of the study population, by group.

	NBW (n=80)	ELBW (n=89)
Male n(%)	(40)	(38.2)
Age (years)	31.6 (2.5)	31.6 (1.6)
Gestational Age (weeks)	40.0 (0)	27.2 (2.5)
% Body Fat	30.09 (10.4)	35.7 (11.02)
BMI	26.2 (5.1)	27.1 (6.4)
Systolic BP (mmHg)	109 (10.6)	114 (11.8)
Diastolic BP (mmHg)	70 (8.3)	74 (10.1)
Total Cholesterol (mmol/L)	4.7 (0.86)	4.8 (0.97)
LDL-cholesterol (mmol/L)	2.7 (0.76)	2.7 (0.87)
HDL-cholesterol (mmol/L)	1.5 (0.40)	1.5 (0.45)
Triglyceride (mmol/L)	1.25 (1.03)	1.40 (0.73)
Glucose (mmol/L)	4.9 (0.60)	5.2 (0.69)
Average maximum IMT (mm)	0.644 (0.11)	0.627 (0.103)
Average mean IMT (mm)	0.606 (0.106)	0.587 (0.095)

Values are mean ± SD or n (%). BP = blood pressure; LDL = low-density lipoprotein; HDL = high-density lipoprotein.

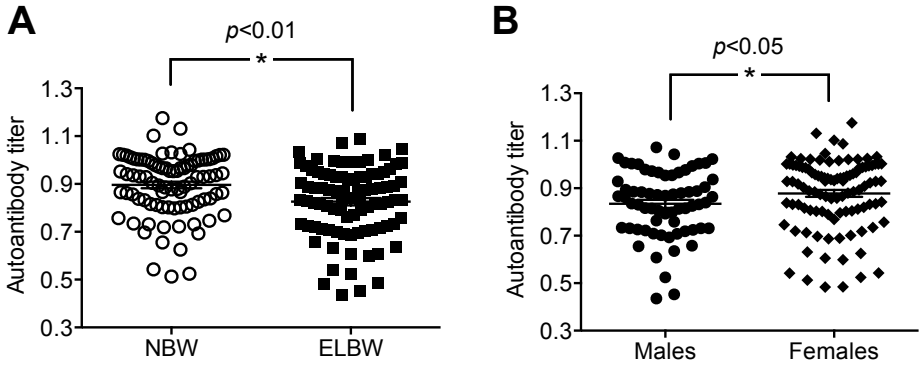

Figure 15. GRP78a-Ab titers from participants in the FIN-CAN study. Levels of GRP78a-Abs were measured by ELISA from *(A)* adults born at normal birth weight (NBW) or pre-term at extremely low birth weight (ELBW). *(B)* Levels of GRP78a-Abs in males and females from the entire cohort. Data is expressed as absorbance values at 450nm relative to a common sample. *Indicates a significant difference (p<0.05) from the indicated group.

4.4 Discussion

Overall, the human cohort data do not support the idea that GRP78a-Abs are elevated in groups at risk for atherosclerosis. However, there are notable caveats to the current data that should serve as a guideline for future studies in this area.

There was no significant difference in levels of GRP78a-Abs between controls and participants with CVD as defined based on parameters of the SHARE study. However, this study may have not been an ideal cohort to examine a new biomarker of atherosclerotic lesion development. Firstly, in this study the control group contained individuals with potentially confounding factors including current and former smokers, diabetics, and those being treated for hypertension and/or high cholesterol. It is unknown whether these risk factors are associated with GRP78a-Abs and could therefore be independently influencing GRP78a-Abs in the control group. Although the control group was formed based on the lack of a CVD qualifying event, control subjects were not required to lack other heath problems or diseases. However, the purpose of the SHARE study was to assess risk factors in three different ethnic groups, not compare characteristics of truly healthy people to those with CVD. In an effort to address this problem in the current GRP78a-Ab analysis, participants with reported risk factors for CVD were excluded from the control group in order to better represent a cohort of “healthy” individuals. It was thought that using more stringent exclusion criteria would allow for a more accurate evaluation of whether

there was a correlation between GRP78a-Abs and the occurrence of CVD. However, eliminating participants with risk factors for CVD severely reduced the sample size of the control group. Therefore the lack of statistical significance in comparing GRP78a-Abs between the redefined control group and those with CVD was likely due to reduced statistical power. Although not statistically significant, it is interesting to note the slight increase of GRP78a-Abs in control group samples with greater numbers of risk factors for CVD. This classification was not based on one specific risk factor however, so it remains to be determined whether the type of risk factor differentially influences GRP78a-Abs and to what extent. Another caveat to analysis was the lack of absolute values for the individual test characteristics. The information provided for each sample included a “yes” or “no” indicator for the described characteristic rather than a quantitative measurement. This prevented additional univariate or multivariate analysis on the continuous variables and limited analysis to categorical variables. Furthermore, while participants classified as having CVD presented with a symptomatic event, this does not necessarily correlate with the prevalence and extent of atherosclerosis. Indeed, the original study found that although South Asians had the highest rates of CVD, they had less carotid atherosclerosis than Europeans(156).

In the pediatric cohort from the NIATH study, children with hyperlipidemia had significantly higher GRP78a-Abs levels than obese children. Similarly, GRP78a-Abs were inversely related to body fat and BMI-Z score in univariate

regression and body fat significantly contributed to GRP78a-Abs levels in the multivariate model, suggesting body fat is a determinant of GRP78a-Abs in children. Additional work will be required to determine how body fat might be involved in modulating GRP78a-Abs, whether this relationship is also relevant in adults, and to identify other factors that modulate GRP78a-Ab levels.

Adults born with extremely low birth weights had lower GRP78a-Abs than their normal birth weight counterpart controls in the FIN-CAN study. Birth weight group classification was related to GRP78a-Ab levels in univariate analysis, but not age or gender, suggesting there is a relationship between prematurity and lower GRP78a-Ab levels.

In order to more directly relate measures of atherogenesis to GRP78a-Abs, we compared carotid IMT to plasma autoantibody levels. No relationship was seen between IMT and GRP78a-Abs. Age has been shown to be an important determinant of IMT in children, adolescents and adults, regardless of contributing CVD risk factors, therefore it was controlled for when analysis were performed(161, 167). Although the NIATH study showed children with hyperlipidemia had greater IMT, overweight children did not have higher IMT even though they had multiple cardiovascular risk factors(161). It is important to consider that children, even those with hyperlipidemia, have only very early atherosclerotic change consisting of fatty streaks, but not more advanced, complicated lesions(168). For this reason, it may be too early in the progression

of lesion development in these subjects for us to observe a difference in GRP78a-Abs levels.

There was no relationship between GRP78a-Abs and IMT in the FIN-CAN study, regardless of group. However, there was also no difference in IMT between groups, suggesting that premature birth does not strongly influence atherosclerosis at this age. Additionally, the IMT values, lack of large unstable plaques and good CVD health suggests that these subjects do not have high risk for atherosclerotic CVD based on established guidelines(169). This again suggests that in these subjects in their early 30s, it may be too early in life to detect a rise in GRP78a-Ab levels.

While the above data relating GRP78a-Abs to human atherosclerosis markers in primarily younger (<35 year old) subjects appears underwhelming, atherosclerosis is known to develop and increase with advanced age. Carotid IMT, shown to be a marker of risk for coronary heart disease and atherosclerosis as well as ischemic events and stroke, increases at an average rate of ≤0.03mm per year(158, 160) and aortic plaques are most prevalent in individuals over 50 years of age(170). The data presented here does support this in that only the oldest adult population analyzed (SHARE study) showed an increase in GRP78a-Ab levels in participants with CVD when compared to healthy controls. Future work should be focused on middle-aged to elderly adults using more in-depth clinical phenotyping of CVD risk factors and carotid IMT analysis to truly

tease out whether GRP78a-Abs are related to human atherosclerosis. The timing and progression of GRP78a-Ab formation and accumulation is not known in humans, and particularly unclear in relation to the development of atherosclerosis. It is possible that there is a temporal lag between the onset of ER stress and endothelial activation and the point in which GRP78a-Abs accumulate in circulation to levels divergent enough to detect significant differences between population groups using our current methods of analysis.

Chapter 5 - Discussion and Conclusions

5.1 Concluding Remarks

In this study, we investigated whether activation of surface GRP78 by GRP78a-Abs modulates endothelial cell function, the effects of circulating GRP78a-Abs on atherosclerotic lesion development in ApoE$^{-/-}$ mice, and whether GRP78a-Abs were associated with CVD in humans.

Overall this thesis supports our hypothesis that signaling through cell surface GRP78 on endothelial cells promotes endothelial cell activation and augments the progression of lesion development. We showed levels of GRP78a-Abs correspond to lesion progression in ApoE$^{-/-}$ mice and demonstrated an interaction of GRP78a-Abs with resident endothelial cells on the surface of lesions. Furthermore, we demonstrated increasing GRP78a-Abs accelerated lesion development in ApoE$^{-/-}$ mice. Additionally, work here suggests blocking of circulating GRP78a-Abs is a viable strategy towards attenuating lesion progression. We also established that ER stress leads to surface GRP78 expression in endothelial cells, and that activation of surface GRP78 by GRP78a-Abs induces endothelial cell activation through the NFkB pathway. Finally we present initial analysis of GRP78a-Abs in humans that suggest GRP78a-Abs levels are increased in middle aged to elderly adults at risk for cardiovascular disease. Collectively, these results demonstrate a novel role for GRP78a-Abs and surface GRP78 receptor activity in endothelial cell activation and the early stages of atherosclerotic lesion development, as well as set a framework for

further investigation into the mechanism by which surface GRP78 signaling aggravates lesion development.

5.2 Future Directions

Since the above data suggest that reducing circulating GRP78a-Abs can mitigate lesion development, there are several possible ways to manage these autoantibodies therapeutically. The first may be by blocking cell surface GRP78 signaling, possibly through direct binding neutralization of circulating GRP78a-Abs in order to attenuate atherosclerotic lesion development. Also, discovery of novel ligands with greater affinity for GRP78a-Abs than surface GRP78 are promising avenues for atherosclerosis therapy. Finally, antibodies interacting with different epitopes on surface GRP78, specifically those that recognize the C-terminus, have shown contrasting signaling effects to GRP78a-Abs in cancer cells and would be interesting to test on endothelial cells and in rodent models of atherosclerosis(171).

While the current work provides evidence that GRP78a-Abs work to enhance atherogenesis via endothelial cell activation, it remains unclear how this signal is being transmitted from binding on the surface of the cell. The work presented here indicates signaling of surface GRP78 initiated by GRP78a-Abs involves the NFκB pathway in endothelial cells, however further work is required to delineate the precise pathway linking surface GRP78 to NFκB in these cells. Previous work suggests surface GRP78 signals through G proteins, activating PLC which increases IP_3 and results in Ca^{2+} release from the ER(86, 150).

Increased cytosolic [Ca^{2+}] activates NFκB, therefore continued experiments should include blocking these potential pathway components, using a PLC inhibitor (i.e. U73122)(172), an IP_3 receptor inhibitor (i.e. xestospongin C)(173), or a calcium chelator (i.e. BAPTA), to examine their effects on GRP78a-Ab stimulated endothelial cell activation.

Another avenue to continue and strengthen the work presented here should be to examine the endothelial-specific role of NFκB in GRP78a-Ab mediated effects on lesion growth *in vivo*. $ApoE^{-/-}$ mice expressing an endothelial-specific dominant-negative IκBα show inhibition of NFκB activity and NFκB-dependent gene expression exclusively in the vascular endothelium resulting in reduced plaque formation compared to $ApoE^{-/-}$ littermate controls (174). Experiments modulating GRP78a-Abs in these mice would provide further insight into whether GRP78a-Ab mediated lesion progression is primarily occurring due to signaling via the endothelial cell NFκB cascade.

It is possible and likely that GRP78a-Abs also act as receptor agonists for surface GRP78 on other cell types involved in atherosclerosis. In addition to endothelial cells, surface GRP78 is expressed on macrophage foam cells within atherosclerotic plaques(135) as well as on the surface of platelets(175). Current evidence suggests surface GRP78 directly interacts with tissue factor (TF) on both macrophages and platelets, inhibiting TF function and resulting in reduced procoagulant activity and platelet adhesion (135, 175). Future studies to determine whether GRP78a-Abs influence surface GRP78 activity in these cell

types may provide support for a multifaceted role of GRP78a-Abs and surface GRP78 in atherosclerosis.

Chapter 6 – References

1. I. Tabas, G. García-Cardeña, G.K. Owens, Recent insights into the cellular biology of atherosclerosis. J Cell Biol 209, (13-22) 2015.
2. A.J. Lusis, Atherosclerosis. Nature 407, (233-41) 2000.
3. E. Braunwald, Shattuck lecture--cardiovascular medicine at the turn of the millennium: triumphs, concerns, and opportunities. N Engl J Med 337, (1360-9) 1997.
4. A.C. Luca, C. Iordache, Obesity--a risk factor for cardiovascular diseases. Rev Med Chir Soc Med Nat Iasi 117, (65-71) 2013.
5. J.C. Wang, M. Bennett, Aging and atherosclerosis: mechanisms, functional consequences, and potential therapeutics for cellular senescence. Circ Res 111, (245-59) 2012.
6. S. Barquera, A. Pedroza-Tobías, C. Medina, L. Hernández-Barrera, K. Bibbins-Domingo, R. Lozano, A.E. Moran, Global Overview of the Epidemiology of Atherosclerotic Cardiovascular Disease. Arch Med Res 46, (328-38) 2015.
7. K.J. Williams, I. Tabas, The response-to-retention hypothesis of early atherogenesis. Arterioscler Thromb Vasc Biol 15, (551-61) 1995.
8. R. Ross, Atherosclerosis is an inflammatory disease. Am Heart J 138, (S419-20) 1999.
9. M.A. Crowther, Pathogenesis of atherosclerosis. Hematology Am Soc Hematol Educ Program, (436-41) 2005.
10. A. Janoudi, F.E. Shamoun, J.K. Kalavakunta, G.S. Abela, Cholesterol crystal induced arterial inflammation and destabilization of atherosclerotic plaque. Eur Heart J 2015.
11. G.K. Hansson, P. Libby, I. Tabas, Inflammation and plaque vulnerability. J Intern Med 278, (483-93) 2015.
12. A.D. Blann, Assessment of endothelial dysfunction: focus on atherothrombotic disease. Pathophysiol Haemost Thromb 33, (256-61) 2003.
13. P.E. Szmitko, C.-H. Wang, R.D. Weisel, J.R. de Almeida, T.J. Anderson, S. Verma, New markers of inflammation and endothelial cell activation: Part I. Circulation 108, (1917-23) 2003.
14. P.O. Bonetti, L.O. Lerman, A. Lerman, Endothelial dysfunction: a marker of atherosclerotic risk. Arterioscler Thromb Vasc Biol 23, (168-75) 2003.
15. R.J. Esper, R.A. Nordaby, J.O. Vilariño, A. Paragano, J.L. Cacharrón, R.A. Machado, Endothelial dysfunction: a comprehensive appraisal. Cardiovasc Diabetol 5, (4) 2006.
16. M. Bijl, Endothelial activation, endothelial dysfunction and premature atherosclerosis in systemic autoimmune diseases. Neth J Med 61, (273-7) 2003.
17. S.P. Alom-Ruiz, N. Anilkumar, A.M. Shah, Reactive oxygen species and endothelial activation. Antioxid Redox Signal 10, (1089-100) 2008.

18. W. Durante, A.K. Sen, F.A. Sunahara, Impairment of endothelium-dependent relaxation in aortae from spontaneously diabetic rats. Br J Pharmacol 94, (463-8) 1988.
19. W. Lockette, Y. Otsuka, O. Carretero, The loss of endothelium-dependent vascular relaxation in hypertension. Hypertension 8, (II61-6) 1986.
20. T.F. Lüscher, Y. Dohi, F.C. Tanner, C. Boulanger, Endothelium-dependent control of vascular tone: effects of age, hypertension and lipids. Basic Res Cardiol 86 Suppl 2, (143-58) 1991.
21. P.F. Davies, M. Civelek, Y. Fang, I. Fleming, The atherosusceptible endothelium: endothelial phenotypes in complex haemodynamic shear stress regions in vivo. Cardiovasc Res 99, (315-27) 2013.
22. P. Davies, M. Civelek, Y. Fang, M. Guerraty, A. Passerini, Endothelial Heterogeneity Associated with Regional Athero-Susceptibility and Adaptation to Disturbed Blood Flow in Vivo Seminars in Thrombosis and Hemostasis 36, (265-275) 2010.
23. P.F. Davies, Flow-mediated endothelial mechanotransduction. Physiol Rev 75, (519-60) 1995.
24. G. Dai, M.R. Kaazempur-Mofrad, S. Natarajan, Y. Zhang, S. Vaughn, B.R. Blackman, R.D. Kamm, G. García-Cardeña, M.A. Gimbrone, Distinct endothelial phenotypes evoked by arterial waveforms derived from atherosclerosis-susceptible and -resistant regions of human vasculature. Proc Natl Acad Sci U S A 101, (14871-6) 2004.
25. B.R. Kwak, F. Mulhaupt, N. Veillard, D.B. Gros, F. Mach, Altered pattern of vascular connexin expression in atherosclerotic plaques. Arterioscler Thromb Vasc Biol 22, (225-30) 2002.
26. P.A. VanderLaan, C.A. Reardon, G.S. Getz, Site specificity of atherosclerosis: site-selective responses to atherosclerotic modulators. Arterioscler Thromb Vasc Biol 24, (12-22) 2004.
27. A.R. Brooks, P.I. Lelkes, G.M. Rubanyi, Gene expression profiling of human aortic endothelial cells exposed to disturbed flow and steady laminar flow. Physiol Genomics 9, (27-41) 2002.
28. A.G. Passerini, D.C. Polacek, C. Shi, N.M. Francesco, E. Manduchi, G.R. Grant, W.F. Pritchard, S. Powell, G.Y. Chang, C.J. Stoeckert, P.F. Davies, Coexisting proinflammatory and antioxidative endothelial transcription profiles in a disturbed flow region of the adult porcine aorta. Proc Natl Acad Sci U S A 101, (2482-7) 2004.
29. L. Hajra, A.I. Evans, M. Chen, S.J. Hyduk, T. Collins, M.I. Cybulsky, The NF-kappa B signal transduction pathway in aortic endothelial cells is primed for activation in regions predisposed to atherosclerotic lesion formation. Proc Natl Acad Sci U S A 97, (9052-7) 2000.
30. Austin RC (2009) Antioxid Redox Signal. Antioxid Redox Signal 11:2279-87.
31. J. Zhou, G.H. Werstuck, S. Lhoták, A.B.L. de Koning, S.K. Sood, G.S. Hossain, J. Møller, M. Ritskes-Hoitinga, E. Falk, S. Dayal, S.R. Lentz, R.C. Austin, Association of multiple cellular stress pathways with accelerated atherosclerosis in

hyperhomocysteinemic apolipoprotein E-deficient mice. Circulation 110, (207-13) 2004.
32. J. Zhou, S. Lhoták, B.A. Hilditch, R.C. Austin, Activation of the unfolded protein response occurs at all stages of atherosclerotic lesion development in apolipoprotein E-deficient mice. Circulation 111, (1814-21) 2005.
33. M. Civelek, E. Manduchi, R.J. Riley, C.J. Stoeckert, P.F. Davies, Chronic endoplasmic reticulum stress activates unfolded protein response in arterial endothelium in regions of susceptibility to atherosclerosis. Circ Res 105, (453-61) 2009.
34. R.E. Feaver, N.E. Hastings, A. Pryor, B.R. Blackman, GRP78 upregulation by atheroprone shear stress via p38-, alpha2beta1-dependent mechanism in endothelial cells. Arterioscler Thromb Vasc Biol 28, (1534-41) 2008.
35. L. Zeng, A. Zampetaki, A. Margariti, A.E. Pepe, S. Alam, D. Martin, Q. Xiao, W. Wang, Z.-G. Jin, G. Cockerill, K. Mori, Y.-S.J. Li, Y. Hu, S. Chien, Q. Xu, Sustained activation of XBP1 splicing leads to endothelial apoptosis and atherosclerosis development in response to disturbed flow. Proc Natl Acad Sci U S A 106, (8326-31) 2009.
36. R. Sitia, I. Braakman, Quality control in the endoplasmic reticulum protein factory. Nature 426, (891-4) 2003.
37. Y. Ma, L.M. Hendershot, ER chaperone functions during normal and stress conditions. J Chem Neuroanat 28, (51-65) 2004.
38. E.F. Corbett, K. Oikawa, P. Francois, D.C. Tessier, C. Kay, J.J. Bergeron, D.Y. Thomas, K.H. Krause, M. Michalak, Ca2+ regulation of interactions between endoplasmic reticulum chaperones. J Biol Chem 274, (6203-11) 1999.
39. S.M. Jethmalani, K.J. Henle, Calreticulin associates with stress proteins: implications for chaperone function during heat stress. J Cell Biochem 69, (30-43) 1998.
40. H.F. Lodish, N. Kong, Perturbation of cellular calcium blocks exit of secretory proteins from the rough endoplasmic reticulum. J Biol Chem 265, (10893-9) 1990.
41. A.J. Dorner, D.G. Bole, R.J. Kaufman, The relationship of N-linked glycosylation and heavy chain-binding protein association with the secretion of glycoproteins. J Cell Biol 105, (2665-74) 1987.
42. L. Ellgaard, A. Helenius, Quality control in the endoplasmic reticulum. Nat Rev Mol Cell Biol 4, (181-91) 2003.
43. E.J. Wiertz, D. Tortorella, M. Bogyo, J. Yu, W. Mothes, T.R. Jones, T.A. Rapoport, H.L. Ploegh, Sec61-mediated transfer of a membrane protein from the endoplasmic reticulum to the proteasome for destruction. Nature 384, (432-8) 1996.
44. K. Meerovitch, S. Wing, D. Goltzman, Proparathyroid hormone-related protein is associated with the chaperone protein BiP and undergoes proteasome-mediated degradation. J Biol Chem 273, (21025-30) 1998.
45. D. Ron, P. Walter, Signal integration in the endoplasmic reticulum unfolded protein response. Nat Rev Mol Cell Biol 8, (519-29) 2007.
46. J.D. Malhotra, R.J. Kaufman, The endoplasmic reticulum and the unfolded protein response Seminars in Cell & Developmental Biology 18, (716-731) 2007.

47. H.P. Harding, M. Calfon, F. Urano, I. Novoa, D. Ron, Transcriptional and translational control in the Mammalian unfolded protein response. Annu Rev Cell Dev Biol 18, (575-99) 2002.
48. C.Y. Liu, R.J. Kaufman, The unfolded protein response. J Cell Sci 116, (1861-2) 2003.
49. R.J. Kaufman, Stress signaling from the lumen of the endoplasmic reticulum: coordination of gene transcriptional and translational controls. Genes Dev 13, (1211-33) 1999.
50. J.S. Cox, P. Walter, A novel mechanism for regulating activity of a transcription factor that controls the unfolded protein response. Cell 87, (391-404) 1996.
51. K. Mori, W. Ma, M.J. Gething, J. Sambrook, A transmembrane protein with a cdc2+/CDC28-related kinase activity is required for signaling from the ER to the nucleus. Cell 74, (743-56) 1993.
52. K. Mori, N. Ogawa, T. Kawahara, H. Yanagi, T. Yura, MRNA splicing-mediated C-terminal replacement of transcription factor Hac1p is required for efficient activation of the unfolded protein response. Proc Natl Acad Sci U S A 97, (4660-5) 2000.
53. Y. Kimata, Y.I. Kimata, Y. Shimizu, H. Abe, I.C. Farcasanu, M. Takeuchi, M.D. Rose, K. Kohno, Genetic evidence for a role of BiP/Kar2 that regulates Ire1 in response to accumulation of unfolded proteins. Mol Biol Cell 14, (2559-69) 2003.
54. A. Bertolotti, Y. Zhang, L.M. Hendershot, H.P. Harding, D. Ron, Dynamic interaction of BiP and ER stress transducers in the unfolded-protein response. Nat Cell Biol 2, (326-32) 2000.
55. F.R. Papa, C. Zhang, K. Shokat, P. Walter, Bypassing a kinase activity with an ATP-competitive drug. Science 302, (1533-7) 2003.
56. J.J. Credle, J.S. Finer-Moore, F.R. Papa, R.M. Stroud, P. Walter, On the mechanism of sensing unfolded protein in the endoplasmic reticulum. Proc Natl Acad Sci U S A 102, (18773-84) 2005.
57. H. Yoshida, T. Matsui, N. Hosokawa, R.J. Kaufman, K. Nagata, K. Mori, A time-dependent phase shift in the mammalian unfolded protein response. Dev Cell 4, (265-71) 2003.
58. H. Yoshida, M. Oku, M. Suzuki, K. Mori, PXBP1(U) encoded in XBP1 pre-mRNA negatively regulates unfolded protein response activator pXBP1(S) in mammalian ER stress response. J Cell Biol 172, (565-75) 2006.
59. U. Ozcan, Q. Cao, E. Yilmaz, A.-H. Lee, N.N. Iwakoshi, E. Ozdelen, G. Tuncman, C. Görgün, L.H. Glimcher, G.S. Hotamisligil, Endoplasmic reticulum stress links obesity, insulin action, and type 2 diabetes. Science 306, (457-61) 2004.
60. A.M. Reimold, N.N. Iwakoshi, J. Manis, P. Vallabhajosyula, E. Szomolanyi-Tsuda, E.M. Gravallese, D. Friend, M.J. Grusby, F. Alt, L.H. Glimcher, Plasma cell differentiation requires the transcription factor XBP-1. Nature 412, (300-7) 2001.
61. K. Haze, H. Yoshida, H. Yanagi, T. Yura, K. Mori, Mammalian transcription factor ATF6 is synthesized as a transmembrane protein and activated by proteolysis in response to endoplasmic reticulum stress. Mol Biol Cell 10, (3787-99) 1999.

62. J. Ye, R.B. Rawson, R. Komuro, X. Chen, U.P. Davé, R. Prywes, M.S. Brown, J.L. Goldstein, ER stress induces cleavage of membrane-bound ATF6 by the same proteases that process SREBPs. Mol Cell 6, (1355-64) 2000.
63. J. Shen, X. Chen, L. Hendershot, R. Prywes, ER stress regulation of ATF6 localization by dissociation of BiP/GRP78 binding and unmasking of Golgi localization signals. Dev Cell 3, (99-111) 2002.
64. G.H. Werstuck, S.R. Lentz, S. Dayal, G.S. Hossain, S.K. Sood, Y.Y. Shi, J. Zhou, N. Maeda, S.K. Krisans, M.R. Malinow, R.C. Austin, Homocysteine-induced endoplasmic reticulum stress causes dysregulation of the cholesterol and triglyceride biosynthetic pathways. J Clin Invest 107, (1263-73) 2001.
65. S.M. Colgan, D. Tang, G.H. Werstuck, R.C. Austin, Endoplasmic reticulum stress causes the activation of sterol regulatory element binding protein-2. Int J Biochem Cell Biol 39, (1843-51) 2007.
66. H.L. Kammoun, H. Chabanon, I. Hainault, S. Luquet, C. Magnan, T. Koike, P. Ferré, F. Foufelle, GRP78 expression inhibits insulin and ER stress-induced SREBP-1c activation and reduces hepatic steatosis in mice. J Clin Invest 119, (1201-15) 2009.
67. R.J. Kaufman, Regulation of mRNA translation by protein folding in the endoplasmic reticulum. Trends Biochem Sci 29, (152-8) 2004.
68. D. Scheuner, B. Song, E. McEwen, C. Liu, R. Laybutt, P. Gillespie, T. Saunders, S. Bonner-Weir, R.J. Kaufman, Translational control is required for the unfolded protein response and in vivo glucose homeostasis. Mol Cell 7, (1165-76) 2001.
69. H.P. Harding, Y. Zhang, A. Bertolotti, H. Zeng, D. Ron, Perk is essential for translational regulation and cell survival during the unfolded protein response. Mol Cell 5, (897-904) 2000.
70. T.W. Fawcett, J.L. Martindale, K.Z. Guyton, T. Hai, N.J. Holbrook, Complexes containing activating transcription factor (ATF)/cAMP-responsive-element-binding protein (CREB) interact with the CCAAT/enhancer-binding protein (C/EBP)-ATF composite site to regulate Gadd153 expression during the stress response. Biochem J 339 (Pt 1), (135-41) 1999.
71. K.D. McCullough, J.L. Martindale, L.O. Klotz, T.Y. Aw, N.J. Holbrook, Gadd153 sensitizes cells to endoplasmic reticulum stress by down-regulating Bcl2 and perturbing the cellular redox state. Mol Cell Biol 21, (1249-59) 2001.
72. Y. Ma, L.M. Hendershot, Delineation of a negative feedback regulatory loop that controls protein translation during endoplasmic reticulum stress. J Biol Chem 278, (34864-73) 2003.
73. I. Novoa, H. Zeng, H.P. Harding, D. Ron, Feedback inhibition of the unfolded protein response by GADD34-mediated dephosphorylation of eIF2alpha. J Cell Biol 153, (1011-22) 2001.
74. C. Jousse, S. Oyadomari, I. Novoa, P. Lu, Y. Zhang, H.P. Harding, D. Ron, Inhibition of a constitutive translation initiation factor 2alpha phosphatase, CReP, promotes survival of stressed cells. J Cell Biol 163, (767-75) 2003.
75. I.G. Haas, BiP (GRP78), an essential hsp70 resident protein in the endoplasmic reticulum. Experientia 50, (1012-20) 1994.

76. R.J. Deshaies, B.D. Koch, M. Werner-Washburne, E.A. Craig, R. Schekman, A subfamily of stress proteins facilitates translocation of secretory and mitochondrial precursor polypeptides. Nature 332, (800-5) 1988.
77. G.C. Flynn, J. Pohl, M.T. Flocco, J.E. Rothman, Peptide-binding specificity of the molecular chaperone BiP. Nature 353, (726-30) 1991.
78. M.J. Gething, Role and regulation of the ER chaperone BiP. Semin Cell Dev Biol 10, (465-72) 1999.
79. S. Luo, C. Mao, B. Lee, A.S. Lee, GRP78/BiP is required for cell proliferation and protecting the inner cell mass from apoptosis during early mouse embryonic development Molecular and cellular biology 26, (5688-5697) 2006.
80. M. Ni, Y. Zhang, A.S. Lee, Beyond the endoplasmic reticulum: atypical GRP78 in cell viability, signalling and therapeutic targeting. Biochem J 434, (181-8) 2011.
81. D.T. Rutkowski, S.-W. Kang, A.G. Goodman, J.L. Garrison, J. Taunton, M.G. Katze, R.J. Kaufman, R.S. Hegde, The role of p58IPK in protecting the stressed endoplasmic reticulum. Mol Biol Cell 18, (3681-91) 2007.
82. R. Ye, D.Y. Jung, J.Y. Jun, J. Li, S. Luo, H.J. Ko, J.K. Kim, A.S. Lee, Grp78 heterozygosity promotes adaptive unfolded protein response and attenuates diet-induced obesity and insulin resistance. Diabetes 59, (6-16) 2010.
83. Y.-B. Ouyang, L.-J. Xu, J.F. Emery, A.S. Lee, R.G. Giffard, Overexpressing GRP78 influences Ca2+ handling and function of mitochondria in astrocytes after ischemia-like stress. Mitochondrion 11, (279-86) 2011.
84. M. Gonzalez-Gronow, M.A. Selim, J. Papalas, S.V. Pizzo, GRP78: a multifunctional receptor on the cell surface. Antioxid Redox Signal 11, (2299-306) 2009.
85. C.L. Berger, Z. Dong, D. Hanlon, E. Bisaccia, R.L. Edelson, A lymphocyte cell surface heat shock protein homologous to the endoplasmic reticulum chaperone, immunoglobulin heavy chain binding protein BIP. Int J Cancer 71, (1077-85) 1997.
86. A.A. Al-Hashimi, J. Caldwell, M. Gonzalez-Gronow, S.V. Pizzo, D. Aboumrad, L. Pozza, H. Al-Bayati, J.I. Weitz, A. Stafford, H. Chan, A. Kapoor, D.W. Jacobsen, J.G. Dickhout, R.C. Austin, Binding of anti-GRP78 autoantibodies to cell surface GRP78 increases tissue factor procoagulant activity via the release of calcium from endoplasmic reticulum stores. J Biol Chem 285, (28912-23) 2010.
87. U.K. Misra, R. Deedwania, S.V. Pizzo, Activation and cross-talk between Akt, NF-kappaB, and unfolded protein response signaling in 1-LN prostate cancer cells consequent to ligation of cell surface-associated GRP78. J Biol Chem 281, (13694-707) 2006.
88. B. Hardy, A. Battler, C. Weiss, O. Kudasi, A. Raiter, Therapeutic angiogenesis of mouse hind limb ischemia by novel peptide activating GRP78 receptor on endothelial cells. Biochem Pharmacol 75, (891-9) 2008.
89. U.K. Misra, Y. Mowery, S. Kaczowka, S.V. Pizzo, Ligation of cancer cell surface GRP78 with antibodies directed against its COOH-terminal domain up-regulates p53 activity and promotes apoptosis. Mol Cancer Ther 8, (1350-62) 2009.
90. D.J. Davidson, C. Haskell, S. Majest, A. Kherzai, D.A. Egan, K.A. Walter, A. Schneider, E.F. Gubbins, L. Solomon, Z. Chen, R. Lesniewski, J. Henkin, Kringle 5 of

human plasminogen induces apoptosis of endothelial and tumor cells through surface-expressed glucose-regulated protein 78. Cancer Res 65, (4663-72) 2005.
91. C. Liu, G. Bhattacharjee, W. Boisvert, R. Dilley, T. Edgington, In vivo interrogation of the molecular display of atherosclerotic lesion surfaces. Am J Pathol 163, (1859-71) 2003.
92. Y. Zhang, R. Liu, M. Ni, P. Gill, A.S. Lee, Cell surface relocalization of the endoplasmic reticulum chaperone and unfolded protein response regulator GRP78/BiP. J Biol Chem 285, (15065-75) 2010.
93. P.J. Mintz, J. Kim, K.-A. Do, X. Wang, R.G. Zinner, M. Cristofanilli, M.A. Arap, W.K. Hong, P. Troncoso, C.J. Logothetis, R. Pasqualini, W. Arap, Fingerprinting the circulating repertoire of antibodies from cancer patients. Nat Biotechnol 21, (57-63) 2003.
94. M. Gonzalez-Gronow, M. Cuchacovich, C. Llanos, C. Urzua, G. Gawdi, S.V. Pizzo, Prostate Cancer Cell Proliferation In vitro Is Modulated by Antibodies against Glucose-Regulated Protein 78 Isolated from Patient Serum Cancer Research 66, (11424-11431) 2006.
95. C. Blasi, The autoimmune origin of atherosclerosis. Atherosclerosis 201, (17-32) 2008.
96. C.J. Binder, P.X. Shaw, M.-K. Chang, A. Boullier, K. Hartvigsen, S. Hörkkö, Y.I. Miller, D.A. Woelkers, M. Corr, J.L. Witztum, The role of natural antibodies in atherogenesis. J Lipid Res 46, (1353-63) 2005.
97. W. Palinski, M.E. Rosenfeld, S. Ylä-Herttuala, G.C. Gurtner, S.S. Socher, S.W. Butler, S. Parthasarathy, T.E. Carew, D. Steinberg, J.L. Witztum, Low density lipoprotein undergoes oxidative modification in vivo. Proc Natl Acad Sci U S A 86, (1372-6) 1989.
98. C.K. Glass, J.L. Witztum, Atherosclerosis. the road ahead. Cell 104, (503-16) 2001.
99. A. Mertens, P. Holvoet, Oxidized LDL and HDL: antagonists in atherothrombosis. FASEB J 15, (2073-84) 2001.
100. M. Sanson, N. Augé, C. Vindis, C. Muller, Y. Bando, J.-C. Thiers, M.-A. Marachet, K. Zarkovic, Y. Sawa, R. Salvayre, A. Nègre-Salvayre, Oxidized low-density lipoproteins trigger endoplasmic reticulum stress in vascular cells: prevention by oxygen-regulated protein 150 expression. Circ Res 104, (328-36) 2009.
101. J.A. Berliner, G. Subbanagounder, N. Leitinger, A.D. Watson, D. Vora, Evidence for a role of phospholipid oxidation products in atherogenesis. Trends Cardiovasc Med 11, (142-7) 2001.
102. J.L. Witztum, D. Steinberg, The oxidative modification hypothesis of atherosclerosis: does it hold for humans? Trends Cardiovasc Med 11, (93-102) 2001.
103. W. Palinski, S. Ylä-Herttuala, M.E. Rosenfeld, S.W. Butler, S.A. Socher, S. Parthasarathy, L.K. Curtiss, J.L. Witztum, Antisera and monoclonal antibodies specific for epitopes generated during oxidative modification of low density lipoprotein. Arteriosclerosis 10, (325-35) 1990.

104. S. Ylä-Herttuala, W. Palinski, S.W. Butler, S. Picard, D. Steinberg, J.L. Witztum, Rabbit and human atherosclerotic lesions contain IgG that recognizes epitopes of oxidized LDL. Arterioscler Thromb 14, (32-40) 1994.
105. S. Tsimikas, W. Palinski, J.L. Witztum, Circulating autoantibodies to oxidized LDL correlate with arterial accumulation and depletion of oxidized LDL in LDL receptor-deficient mice. Arterioscler Thromb Vasc Biol 21, (95-100) 2001.
106. W. Palinski, E. Miller, J.L. Witztum, Immunization of low density lipoprotein (LDL) receptor-deficient rabbits with homologous malondialdehyde-modified LDL reduces atherogenesis. Proc Natl Acad Sci U S A 92, (821-5) 1995.
107. C.A. Reardon, E.R. Miller, L. Blachowicz, J. Lukens, C.J. Binder, J.L. Witztum, G.S. Getz, Autoantibodies to OxLDL fail to alter the clearance of injected OxLDL in apolipoprotein E-deficient mice. J Lipid Res 45, (1347-54) 2004.
108. C.J. Binder, Natural IgM antibodies against oxidation-specific epitopes. J Clin Immunol 30 Suppl 1, (S56-60) 2010.
109. K.S. Meir, E. Leitersdorf, Atherosclerosis in the apolipoprotein-E-deficient mouse: a decade of progress. Arterioscler Thromb Vasc Biol 24, (1006-14) 2004.
110. A. Daugherty, Mouse models of atherosclerosis. Am J Med Sci 323, (3-10) 2002.
111. S.H. Zhang, R.L. Reddick, J.A. Piedrahita, N. Maeda, Spontaneous hypercholesterolemia and arterial lesions in mice lacking apolipoprotein E. Science 258, (468-71) 1992.
112. A.S. Plump, J.D. Smith, T. Hayek, K. Aalto-Setälä, A. Walsh, J.G. Verstuyft, E.M. Rubin, J.L. Breslow, Severe hypercholesterolemia and atherosclerosis in apolipoprotein E-deficient mice created by homologous recombination in ES cells. Cell 71, (343-53) 1992.
113. S. Ishibashi, M.S. Brown, J.L. Goldstein, R.D. Gerard, R.E. Hammer, J. Herz, Hypercholesterolemia in low density lipoprotein receptor knockout mice and its reversal by adenovirus-mediated gene delivery. J Clin Invest 92, (883-93) 1993.
114. S. Ishibashi, J.L. Goldstein, M.S. Brown, J. Herz, D.K. Burns, Massive xanthomatosis and atherosclerosis in cholesterol-fed low density lipoprotein receptor-negative mice. J Clin Invest 93, (1885-93) 1994.
115. W.P. Sheffield, T.R. McCurdy, V. Bhakta, Fusion to albumin as a means to slow the clearance of small therapeutic proteins using the Pichia pastoris expression system: a case study. Methods Mol Biol 308, (145-54) 2005.
116. W.P. Sheffield, B. Wilson, L.J. Eltringham-Smith, S. Gataiance, V. Bhakta, Recombinant albumins containing additional peptide sequences smaller than barbourin retain the ability of barbourin-albumin to inhibit platelet aggregation. Thromb Haemost 93, (914-21) 2005.
117. J.C. Mavropoulos, M. Cuchacovich, C. Llanos, J.C. Aguillón, H. Gatica, S.V. Pizzo, M. Gonzalez-Gronow, Anti-tumor necrosis factor-alpha therapy augments dipeptidyl peptidase IV activity and decreases autoantibodies to GRP78/BIP and phosphoglucose isomerase in patients with rheumatoid arthritis. J Rheumatol 32, (2116-24) 2005.

118. S. Lhoták, J. Zhou, R.C. Austin, Immunohistochemical detection of the unfolded protein response in atherosclerotic plaques. Methods Enzymol 489, (23-46) 2011.
119. T.A. Seimon, Y. Wang, S. Han, T. Senokuchi, D.M. Schrijvers, G. Kuriakose, A.R. Tall, I.A. Tabas, Macrophage deficiency of p38alpha MAPK promotes apoptosis and plaque necrosis in advanced atherosclerotic lesions in mice. J Clin Invest 119, (886-98) 2009.
120. K. Iiyama, L. Hajra, M. Iiyama, H. Li, M. DiChiara, B.D. Medoff, M.I. Cybulsky, Patterns of vascular cell adhesion molecule-1 and intercellular adhesion molecule-1 expression in rabbit and mouse atherosclerotic lesions and at sites predisposed to lesion formation. Circ Res 85, (199-207) 1999.
121. Y. Nakashima, A.S. Plump, E.W. Raines, J.L. Breslow, R. Ross, ApoE-deficient mice develop lesions of all phases of atherosclerosis throughout the arterial tree. Arterioscler Thromb 14, (133-40) 1994.
122. J. Wei, L.M. Hendershot, Characterization of the nucleotide binding properties and ATPase activity of recombinant hamster BiP purified from bacteria. J Biol Chem 270, (26670-6) 1995.
123. W.P. Sheffield, L.J. Eltringham-Smith, S. Gataiance, V. Bhakta, Addition of a sequence from alpha2-antiplasmin transforms human serum albumin into a blood clot component that speeds clot lysis. BMC Biotechnol 9, (15) 2009.
124. W.P. Sheffield, L.J. Eltringham-Smith, S. Gataiance, V. Bhakta, A long-lasting, plasmin-activatable thrombin inhibitor aids clot lysis in vitro and does not promote bleeding in vivo Thromb Haemost 2009.
125. G.S. Abela, K. Aziz, A. Vedre, D.R. Pathak, J.D. Talbott, J. Dejong, Effect of cholesterol crystals on plaques and intima in arteries of patients with acute coronary and cerebrovascular syndromes. Am J Cardiol 103, (959-68) 2009.
126. P.D.R.N.W.D.R.K.J.M. M J Davies, Risk of thrombosis in human atherosclerotic plaques: role of extracellular lipid, macrophage, and smooth muscle cell content. British Heart Journal 69, (377) 1993.
127. P.L. Kastritis, A.M.J.J. Bonvin, On the binding affinity of macromolecular interactions: daring to ask why proteins interact. J R Soc Interface 10, (20120835) 2013.
128. O. Pelkonen, H. Raunio, In vitro screening of drug metabolism during drug development: can we trust the predictions? Expert Opin Drug Metab Toxicol 1, (49-59) 2005.
129. M. Werle, A. Bernkop-Schnürch, Strategies to improve plasma half life time of peptide and protein drugs. Amino Acids 30, (351-67) 2006.
130. Y. Fu, A.S. Lee, Glucose regulated proteins in cancer progression, drug resistance and immunotherapy. Cancer Biol Ther 5, (741-4) 2006.
131. U.K. Misra, R. Deedwania, S.V. Pizzo, Binding of activated alpha2-macroglobulin to its cell surface receptor GRP78 in 1-LN prostate cancer cells regulates PAK-2-dependent activation of LIMK. J Biol Chem 280, (26278-86) 2005.

132. R. Burikhanov, Y. Zhao, A. Goswami, S. Qiu, S.R. Schwarze, V.M. Rangnekar, The tumor suppressor Par-4 activates an extrinsic pathway for apoptosis. Cell 138, (377-88) 2009.
133. M. Philippova, D. Ivanov, M.B. Joshi, E. Kyriakakis, K. Rupp, T. Afonyushkin, V. Bochkov, P. Erne, T.J. Resink, Identification of proteins associating with glycosylphosphatidylinositol- anchored T-cadherin on the surface of vascular endothelial cells: role for Grp78/BiP in T-cadherin-dependent cell survival. Mol Cell Biol 28, (4004-17) 2008.
134. A. Nakatsuka, J. Wada, I. Iseda, S. Teshigawara, K. Higashio, K. Murakami, M. Kanzaki, K. Inoue, T. Terami, A. Katayama, K. Hida, J. Eguchi, D. Ogawa, Y. Matsuki, R. Hiramatsu, H. Yagita, S. Kakuta, Y. Iwakura, H. Makino, Visceral adipose tissue-derived serine proteinase inhibitor inhibits apoptosis of endothelial cells as a ligand for the cell-surface GRP78/voltage-dependent anion channel complex. Circ Res 112, (771-80) 2013.
135. G. Bhattacharjee, J. Ahamed, B. Pedersen, A. El-Sheikh, N. Mackman, W. Ruf, C. Liu, T.S. Edgington, Regulation of tissue factor--mediated initiation of the coagulation cascade by cell surface grp78. Arterioscler Thromb Vasc Biol 25, (1737-43) 2005.
136. D. Bouïs, G.A. Hospers, C. Meijer, G. Molema, N.H. Mulder, Endothelium in vitro: a review of human vascular endothelial cell lines for blood vessel-related research. Angiogenesis 4, (91-102) 2001.
137. Y. Zhang, C.-C. Tseng, Y.-L. Tsai, X. Fu, R. Schiff, A.S. Lee, Cancer cells resistant to therapy promote cell surface relocalization of GRP78 which complexes with PI3K and enhances PI(3,4,5)P3 production. PLoS One 8, (e80071) 2013.
138. A. Fiszer-Kierzkowska, N. Vydra, A. Wysocka-Wycisk, Z. Kronekova, M. Jarząb, K.M. Lisowska, Z. Krawczyk, Liposome-based DNA carriers may induce cellular stress response and change gene expression pattern in transfected cells. BMC Mol Biol 12, (27) 2011.
139. Y.-L. Tsai, Y. Zhang, C.-C. Tseng, R. Stanciauskas, F. Pinaud, A.S. Lee, Characterization and Mechanism of Stress-induced Translocation of 78-kilodalton Glucose Regulated Protein (GRP78) to the Cell Surface. J Biol Chem 290, (8049-64) 2015.
140. M.A. Arap, J. Lahdenranta, P.J. Mintz, A. Hajitou, A.S. Sarkis, W. Arap, R. Pasqualini, Cell surface expression of the stress response chaperone GRP78 enables tumor targeting by circulating ligands. Cancer Cell 6, (275-84) 2004.
141. Z. Zhou, M.C. Connell, D.J. MacEwan, TNFR1-induced NF-kappaB, but not ERK, p38MAPK or JNK activation, mediates TNF-induced ICAM-1 and VCAM-1 expression on endothelial cells. Cell Signal 19, (1238-48) 2007.
142. V.V.N.V.G.M.J.H.L.C.A.L.B. Rizwan, P-Selectin or Intercellular Adhesion Molecule (Icam)-1 Deficiency Substantially Protects against Atherosclerosis in Apolipoprotein E–Deficient Mice The Journal of Experimental Medicine 191, (189) 2000.

143. M.I. Cybulsky, K. Iiyama, H. Li, S. Zhu, M. Chen, M. Iiyama, V. Davis, J.C. Gutierrez-Ramos, P.W. Connelly, D.S. Milstone, A major role for VCAM-1, but not ICAM-1, in early atherosclerosis. J Clin Invest 107, (1255-62) 2001.
144. J.G. Dickhout, G.S. Hossain, L.M. Pozza, J. Zhou, S. Lhoták, R.C. Austin, Peroxynitrite causes endoplasmic reticulum stress and apoptosis in human vascular endothelium: implications in atherogenesis. Arterioscler Thromb Vasc Biol 25, (2623-9) 2005.
145. M.J. Lewis, H.R. Pelham, Ligand-induced redistribution of a human KDEL receptor from the Golgi complex to the endoplasmic reticulum. Cell 68, (353-64) 1992.
146. L. Orci, M. Stamnes, M. Ravazzola, M. Amherdt, A. Perrelet, T.H. Söllner, J.E. Rothman, Bidirectional Transport by Distinct Populations of COPI-Coated Vesicles Cell 90, (335-349) 1997.
147. D.H. Llewellyn, H.L. Roderick, S. Rose, KDEL receptor expression is not coordinatedly up-regulated with ER stress-induced reticuloplasmin expression in HeLa cells. Biochem Biophys Res Commun 240, (36-40) 1997.
148. K. Yamamoto, R. Fujii, Y. Toyofuku, T. Saito, H. Koseki, V.W. Hsu, T. Aoe, The KDEL receptor mediates a retrieval mechanism that contributes to quality control at the endoplasmic reticulum. EMBO J 20, (3082-91) 2001.
149. M.P.J. de Winther, E. Kanters, G. Kraal, M.H. Hofker, Nuclear factor kappaB signaling in atherogenesis. Arterioscler Thromb Vasc Biol 25, (904-14) 2005.
150. U.K. Misra, S.V. Pizzo, Heterotrimeric Galphaq11 co-immunoprecipitates with surface-anchored GRP78 from plasma membranes of alpha2M*-stimulated macrophages. J Cell Biochem 104, (96-104) 2008.
151. A.M. Bair, P.B. Thippegowda, M. Freichel, N. Cheng, R.D. Ye, S.M. Vogel, Y. Yu, V. Flockerzi, A.B. Malik, C. Tiruppathi, Ca2+ entry via TRPC channels is necessary for thrombin-induced NF-kappaB activation in endothelial cells through AMP-activated protein kinase and protein kinase Cdelta. J Biol Chem 284, (563-74) 2009.
152. A. Rahman, F. Fazal, Blocking NF-κB: an inflammatory issue. Proc Am Thorac Soc 8, (497-503) 2011.
153. H.L. Pahl, P.A. Baeuerle, A novel signal transduction pathway from the endoplasmic reticulum to the nucleus is mediated by transcription factor NF-kappa B. EMBO J 14, (2580-8) 1995.
154. B.J. Hawkins, L.A. Solt, I. Chowdhury, A.S. Kazi, M.R. Abid, W.C. Aird, M.J. May, J.K. Foskett, M. Madesh, G protein-coupled receptor Ca2+-linked mitochondrial reactive oxygen species are essential for endothelial/leukocyte adherence. Mol Cell Biol 27, (7582-93) 2007.
155. R.S. Frey, X. Gao, K. Javaid, S.S. Siddiqui, A. Rahman, A.B. Malik, Phosphatidylinositol 3-kinase gamma signaling through protein kinase Czeta induces NADPH oxidase-mediated oxidant generation and NF-kappaB activation in endothelial cells. J Biol Chem 281, (16128-38) 2006.
156. S.S. Anand, S. Yusuf, V. Vuksan, S. Devanesen, K.K. Teo, P.A. Montague, L. Kelemen, C. Yi, E. Lonn, H. Gerstein, R.A. Hegele, M. McQueen, Differences in risk

factors, atherosclerosis, and cardiovascular disease between ethnic groups in Canada: the Study of Health Assessment and Risk in Ethnic groups (SHARE) Lancet 356, (279-84) 2000.
157. T. Sheth, C. Nair, M. Nargundkar, S. Anand, S. Yusuf, Cardiovascular and cancer mortality among Canadians of European, south Asian and Chinese origin from 1979 to 1993: an analysis of 1.2 million deaths. CMAJ 161, (132-8) 1999.
158. L.E. Chambless, G. Heiss, A.R. Folsom, W. Rosamond, M. Szklo, A.R. Sharrett, L.X. Clegg, Association of coronary heart disease incidence with carotid arterial wall thickness and major risk factors: the Atherosclerosis Risk in Communities (ARIC) Study, 1987-1993. Am J Epidemiol 146, (483-94) 1997.
159. D.H. O'Leary, J.F. Polak, R.A. Kronmal, T.A. Manolio, G.L. Burke, S.K. Wolfson, Carotid-artery intima and media thickness as a risk factor for myocardial infarction and stroke in older adults. Cardiovascular Health Study Collaborative Research Group. N Engl J Med 340, (14-22) 1999.
160. H.N. Hodis, W.J. Mack, L. LaBree, R.H. Selzer, C.R. Liu, C.H. Liu, S.P. Azen, The role of carotid arterial intima-media thickness in predicting clinical coronary events. Ann Intern Med 128, (262-9) 1998.
161. K.M. Morrison, L. Dyal, W. Conner, E. Helden, L. Newkirk, S. Yusuf, E. Lonn, Cardiovascular risk factors and non-invasive assessment of subclinical atherosclerosis in youth. Atherosclerosis 208, (501-5) 2010.
162. S. Saigal, P. Rosenbaum, B. Stoskopf, J.C. Sinclair, Outcome in infants 501 to 1000 gm birth weight delivered to residents of the McMaster Health Region. J Pediatr 105, (969-76) 1984.
163. S. Saigal, P. Rosenbaum, P. Szatmari, L. Hoult, Non-right handedness among ELBW and term children at eight years in relation to cognitive function and school performance. Dev Med Child Neurol 34, (425-33) 1992.
164. S. Saigal, M. Lambert, C. Russ, L. Hoult, Self-esteem of adolescents who were born prematurely. Pediatrics 109, (429-33) 2002.
165. S. Saigal, J. Pinelli, L. Hoult, M.M. Kim, M. Boyle, Psychopathology and social competencies of adolescents who were extremely low birth weight. Pediatrics 111, (969-75) 2003.
166. S. Saigal, P. Rosenbaum, B. Stoskopf, L. Hoult, W. Furlong, D. Feeny, E. Burrows, G. Torrance, Comprehensive assessment of the health status of extremely low birth weight children at eight years of age: Comparison with a reference group The Journal of Pediatrics 125, (411-417) 1994.
167. A. Wiegman, E. de Groot, B.A. Hutten, J. Rodenburg, J. Gort, H.D. Bakker, E.J.G. Sijbrands, J.J.P. Kastelein, Arterial intima-media thickness in children heterozygous for familial hypercholesterolaemia. Lancet 363, (369-70) 2004.
168. G.S. Berenson, S.R. Srinivasan, W. Bao, W.P. Newman, R.E. Tracy, W.A. Wattigney, Association between multiple cardiovascular risk factors and atherosclerosis in children and young adults. The Bogalusa Heart Study. N Engl J Med 338, (1650-6) 1998.

169. P. Greenland, J.S. Alpert, G.A. Beller, E.J. Benjamin, M.J. Budoff, Z.A. Fayad, E. Foster, M.A. Hlatky, J.M. Hodgson, F.G. Kushner, M.S. Lauer, L.J. Shaw, S.C. Smith, A.J. Taylor, W.S. Weintraub, N.K. Wenger, A.K. Jacobs, J.L. Anderson, N. Albert, C.E. Buller, M.A. Creager, S.M. Ettinger, R.A. Guyton, J.L. Halperin, J.S. Hochman, R. Nishimura, E.M. Ohman, R.L. Page, W.G. Stevenson, L.G. Tarkington, C.W. Yancy, American Heart Association, 2010 ACCF/AHA guideline for assessment of cardiovascular risk in asymptomatic adults: a report of the American College of Cardiology Foundation/American Heart Association Task Force on Practice Guidelines. J Am Coll Cardiol 56, (e50-103) 2010.
170. M.W. Lorenz, S. von Kegler, H. Steinmetz, H.S. Markus, M. Sitzer, Carotid intima-media thickening indicates a higher vascular risk across a wide age range: prospective data from the Carotid Atherosclerosis Progression Study (CAPS). Stroke 37, (87-92) 2006.
171. U.K. Misra, S. Kaczowka, S.V. Pizzo, Inhibition of NF-kappaB1 and NF-kappaB2 activation in prostate cancer cells treated with antibody against the carboxyl terminal domain of GRP78: effect of p53 upregulation. Biochem Biophys Res Commun 392, (538-42) 2010.
172. J.E. Bleasdale, N.R. Thakur, R.S. Gremban, G.L. Bundy, F.A. Fitzpatrick, R.J. Smith, S. Bunting, Selective inhibition of receptor-coupled phospholipase C-dependent processes in human platelets and polymorphonuclear neutrophils. J Pharmacol Exp Ther 255, (756-68) 1990.
173. J. Gafni, J.A. Munsch, T.H. Lam, M.C. Catlin, L.G. Costa, T.F. Molinski, I.N. Pessah, Xestospongins: potent membrane permeable blockers of the inositol 1,4,5-trisphosphate receptor. Neuron 19, (723-33) 1997.
174. R. Gareus, E. Kotsaki, S. Xanthoulea, I. van der Made, M.J.J. Gijbels, R. Kardakaris, A. Polykratis, G. Kollias, M.P.J. de Winther, M. Pasparakis, Endothelial cell-specific NF-kappaB inhibition protects mice from atherosclerosis. Cell Metab 8, (372-83) 2008.
175. B. Molins, E. Peña, T. Padro, L. Casani, C. Mendieta, L. Badimon, Glucose-Regulated Protein 78 and Platelet Deposition Arteriosclerosis, Thrombosis, and Vascular Biology 30, (1246-1252) 2010.